Doctoral theses at NTNU, 2021:411

Ingrid Nyhus Moen

Pharmaceutical targeting of RIPK1-signaling

Characterization of cell death in human macrophage systems and therapeutic potential in multiple myeloma

Doctoral thesis

NTNU
Norwegian University of Science and Technology
Thesis for the Degree of
Philosophiae Doctor
Faculty of Medicine and Health Sciences
Department of Clinical and Molecular Medicine

NTNU
Norwegian University of
Science and Technology

Ingrid Nyhus Moen

Pharmaceutical targeting of RIPK1-signaling

Characterization of cell death in human macrophage systems and therapeutic potential in multiple myeloma

Thesis for the Degree of Philosophiae Doctor

Trondheim, December 2021

Norwegian University of Science and Technology
Faculty of Medicine and Health Sciences
Department of Clinical and Molecular Medicine

NTNU
Norwegian University of
Science and Technology

NTNU
Norwegian University of Science and Technology

Thesis for the Degree of Philosophiae Doctor

Faculty of Medicine and Health Sciences
Department of Clinical and Molecular Medicine

ISBN 978-82-326-5280-8 (printed ver.)
ISBN 978-82-326-6757-4 (electronic ver.)
ISSN 1503-8181 (printed ver.)
ISSN 2703-8084 (online ver.)

Doctoral theses at NTNU, 2021:411

Printed by NTNU Grafisk senter

Farmasøytisk behandling rettet mot RIPK1-signalisering:

Karakterisering av celledød i humane makrofager og terapeutisk potensiale i myelomatose

Receptor-interacting protein kinase 1(RIPK1)-signalveien er viktig for respons og aktivering av makrofagtyper og regulerer både inflammasjon og celledød. RIPK1-avhengig celledød som en respons på patogeninfeksjon har blitt godt studert i immunceller i mus, men mer kunnskap om hvordan celledød kan bli farmasøytisk indusert i humane celler er nødvendig. Farmasøytisk behandling rettet mot RIPK1-signalisering inkluderer smac-mimetics (SM) og TGF-β activated kinase 1 (TAK1)-inhibitorer. Disse inhibitorene har blitt studert som terapeutiske alternativer i behandling av kreft og kroniske sykdommer, men studier av effekten på humane immunceller slik som osteoklaster og makrofager har vært begrenset. SM er under klinisk utprøving i ulike kreftformer inkludert myelomatose. Overaktivering av osteoklaster bidrar til beinsykdom hos myelomatosepasienter og effekten av SM på disse cellene bør derfor også undersøkes. I tillegg har TAK1 blitt funnet til å være en driver av myelomatose og nødvendig for differensiering av osteoklaster. Behandling med TAK1-inhibitorer kan derfor være et nytt terapeutisk alternativ ved å både fungere som en anti-tumor agent og også redusere osteoklastaktivitet i myelompasienter.

Målet med prosjektet har vært å bidra til en bedre forståelse av farmasøytisk indusering av RIPK1-avhengig celledød i humane osteoklaster og andre makrofagtyper. Håpet er dette kan bidra til økt forståelse av i hvilke patologiske settinger behandlinger med SM og TAK1-inhibitorer kan ha en mulig effekt. Prosjektet har brukt humane osteoklaster, pro- og anti-inflammatoriske makrofager og myelomceller og studert effekten av behandling med SM og TAK1-inhibitorer på blant annet viabilitet, deres evne til å indusere celledød og celledødsmekanisme.

I første del av arbeidet ønsket vi å studere effekten av SM-behandling på humane osteoklaster og dets potensiale i å redusere beinsykdom i myelomatose. Vi fant at behandlingen med SM induserte celledød i humane osteoklaster. SM blokkerte også dannelsen av nye osteoklaster, dette også i en setting ved patologisk økning av osteoklaster. Behandling med SM kan derfor mulig gi en ekstra fordel ved å redusere beinsykdom i myelompasienter. I andre del av arbeidet ønsket vi å undersøke om pro- og anti-inflammatorisk stimuli hadde noen effekt på SM-indusert celledød i humane makrofager. Vi fant at makrofager behandlet med pro- og anti-inflammatorisk stimuli hadde ulik sensitivitet til SM og induserte ulike former for celledød. Pro-inflammatoriske makrofager var spesielt sensitive til behandling med SM som kan ha et terapeutisk potensialt i sykdommer hvor denne makrofagtypen er oppregulert. I den siste delen av arbeidet fokuserte vi på å studere effekten av behandling med TAK1-inhibitorer på myelomceller og osteoklaster. Vi fant at behandling med TAK1-inhibitorer var cytotoksisk for myelomceller og blokkerte dannelsen av nye osteoklaster. TAK1-inhibitorer kan derfor være en ny interessant kandidat for behandling av myelomatose.

Kandidat: Ingrid Nyhus Moen

Institutt: Institutt for klinisk og molekylærmedisin (IKOM), NTNU

Veiledere: Forsker Kristian K. Starheim og Professor Geir Bjørkøy

Finansieringskilder: Kreftforeningen og Samarbeidsorganet, Helse Midt-Norge

Overnevnte avhandling er funnet verdig for å forsvares offentlig
for graden PhD i medisin og helsevitenskap.
Disputas finner sted onsdag 1. desember og vil bli avviklet digitalt.

Table of Contents

Acknowledgements I
List of Papers III
Abbreviations V
Abstract IX
1 Introduction 1
1.1. The monocytic lineage 1
1.1.1. Monocytes 1
1.1.2 Macrophages 1
1.1.3 Macrophage polarization 4
1.1.4 Osteoclasts 5
1.2 NF-κB and MAPK-signaling promotes inflammation and survival 8
1.2.1 NF-κB-signaling 8
1.2.2 MAPK signaling 11
1.2.3. TAK1 is a key activator of NF-κB1 and MAPKs 11
1.3. RIPK1 is a regulator of inflammation and cell death 12
1.3.1. RIPK1-recruitment to the TNF-TNFR1 complex 13
1.3.2. Inhibitor of apoptosis proteins 15
1.3.3. RIPK1-recruitment to the LPS-TLR4 complex 16
1.4. RIPK1 regulates the activation of apoptosis, necroptosis and pyroptosis 19
1.4.1. Redirection of RIPK1-signaling to cell death: the early and late cell death checkpoints 19
1.4.2. Caspase 8-dependent apoptosis 22
1.4.3. RIPK1-dependent necroptosis 25
1.4.4. The inflammasome and pyroptosis 26
1.5. Pharmaceutical targeting of the RIPK1 pathway 29
1.5.1. Inhibiting RIPK1-dependent cell death 29
1.5.2. Smac-mimetics 29
1.5.3. TAK1-inhibitors 30

1.6. Multiple myeloma 30
1.6.1. Myeloma bone disease 31
1.6.2. Current treatment strategies of MM 33
2 Aims of study 35
3 Summary of papers 37
4 Discussion 41
4.1. Differential response to SM on macrophage subtypes and implications in inflammatory disease settings 41
4.2. SM and TAK1-inhibitors reduce human OC activity 42
4.3. SM-treatment display RIPK1-dependent cell death plasticity 43
4.4. Targeting the RIPK1-pathway in human versus mice systems 47
4.5. Pharmacological inhibitors versus genetic approach in inhibiting TAK1 48
4.6. TAK1-inhibitors and SM as possible treatment options in MM 48
5 Future perspectives 51
6 Conclusions 53
7 References 55

Acknowledgements

This work was carried out at the Centre of Molecular Inflammation Research (CEMIR), at the Department of Clinical and Molecular Medicine (IKOM) at the Faculty of Medicine and Health Sciences, Norwegian University of Science and Technology (NTNU), Trondheim. I am truly grateful for the funding from Samarbeidsorganet, Helse Midt-Norge-RHF that made the work on this PhD thesis possible.

First and foremost, I would like to give my sincere gratitude to my main supervisor Kristian Starheim. Your view on research and your engagement in this project has been a great inspiration to me. Thank you for your endless support and encouragement, and for always having an open door. I truly appreciate the close cooperation we have had over the last four years and for letting me be a part of building up this project. I would also like to thank my co-supervisor Geir Bjørkøy. Your train of thoughts and your vault of knowledge have been truly inspiring.

To all present and past members of the Myeloma group: thank you for creating a fun and inspiring working environment. Kristin, Oddrun, Pegah, Marita, Esten, Siv, Hanne, Berit, Vlado, Qianli, Tonje, thank you for making long hours in the lab something I look forward to. To all present and past members of the Autophagy group: Camilla, Sonja, Kristine, Apsana, Ansooya, Miriam, Ulrike, Ida, Unni, I really appreciate being a part of your group and for exchanging ideas across research projects. I would also like to give a huge thanks to the people I have shared an office with over the last years. Ragnhild, Erlend, Kristin, Hany, Vlado, Pia, Sindre and Tone, the support you have showed me through highs and lows both academically but also through personal matters have meant so much to me. Thank you, Camilla, for being my go-to-person, work related or not, and for answering my long list of questions in the process of writing this thesis. Ragnhild, thank you for lighting up even the darkest days, for forcing me to take breaks and for your continuous motivation and encouragement.

To all my colleagues at CEMIR, thank you for letting me be a part of such and inspiring and warm research environment that is truly unique. I would also like to give a huge thanks to all co-authors for contributions to the papers included in this thesis.

Lastly to my family and friends both near and far: thank you for always cheering me on. Thank you for always being there for me not only for the fun parts but also when things are though. Thank you for taking my mind of things when I needed to and for always believing in me. I could not have done this without you.

Ingrid Nyhus Moen

Trondheim, June 2021

List of Papers

Paper I

Ingrid Nyhus Moen, Marita Westhrin, Erling Håland, Markus Haug, Unni Nonstad, Merisa Klaharn, Therese Standal & Kristian K. Starheim

Smac-mimetics reduce numbers and viability of human osteoclasts. *Cell Death Discov.* **7,** 36 (2021). https://doi.org/10.1038/s41420-021-00415-1

Paper II

Ingrid Nyhus Moen, Merisa Klaharn, Marie Holter-Sørensen, Animesh Sharma & Kristian K. Starheim

Pro- and anti-inflammatory treatment dictates Smac-mimetic cytotoxicity in human macrophages

Manuscript

Paper III

Erling Håland, **Ingrid Nyhus Moen**, Elias Veidal, Hanne Hella, Kristine Misund, Tobias S. Slørdahl & Kristian K. Starheim

TAK1-inhibitors are cytotoxic for multiple myeloma cells alone and in combination with melphalan

In press, Oncotarget

Abbreviations

ALR	Absent in melanoma 2-like receptor
AP-1	Activator protein-1
ASC	Apoptosis-associated speck-like protein containing a CARD
ASCT	Autologous stem cell transplantation
ATM	Ataxia-telangiectasia mutated
BAFF	B cell activator of the TNF family
BIR	Baculoviral IAP repeat
BIRC	BIR containing protein
BM	Bone marrow
BRUCE	BIR repeat-containing ubiquitin-conjugating enzyme
CARD	Caspase activation and recruitment domain
CAII	Carbonic anhydrase II
CCL2	C-C motif chemokine ligand
CD	Cluster of differentiation
cFLIP	cellular FLICE-like inhibitory protein (also named CFLAR)
cIAP	Cellular inhibitor of apoptosis protein
Cl^-	Chloride
CREB	Cyclic AMP responsive-element binding protein
CSF-1	Colony-stimulating factor 1
CSFR1	Colony-stimulating factor receptor 1
CYLD	Cylindromatosis
DAMP	Danger-associated molecular pattern
DC	Dendritic cell
DC-STAMP	Dendritic cell-specific transmembrane protein
DED	Death effector domain
DIABLO	Direct IAP binding proteins with low pI (also known as SMAC)
E1	Ubiquitin-activating enzyme
E2	Ubiquitin-conjugating enzyme
E3	Ubiquitin-ligating enzyme
ERK	Extracellular signal-regulated kinase
FADD	FAS-associated death domain

FAS	First apoptosis signal
FcγR	Fc-gamma receptor
GSDMD	Gasdermin D
H^+	Proton
HMGB1	High mobility group box 1
IBM	IAP-binding motif
IFN	Interferon
IkBα	Inhibitor of NF-κB-α
IKK	IκB kinase
IL	Interleukin
IRF	Interferon-regulatory factor
ITAM	Immunoreceptor tyrosine-based activation motif
JNK	c-Jun N-terminal kinase
K	Lysine
LBP	Lipopolysaccharide binding protein
LPS	Lipopolysaccharide
LUBAC	Linear ubiquitin chain assembly complex
M	Methionine
MAPK	Mitogen-activated protein kinase
MBD	Myeloma bone disease
MD-2	Myeloid differentiation factor-2
MGUS	Monoclonal gammopathy of undetermined significance
MHC-II	Major histocompatibility complex class II
MITF	Microphthalmia-associated transcription factor
MLKL	Mixed lineage kinase domain like pseudokinase
MM	Multiple myeloma
MRD	Minimal residual disease
MyD88	Myeloid differentiation factor 88
Mϕ	Macrophage
NAIP	Neuronal apoptosis inhibitory protein
NEMO	NF-κB essential modulator
NFATc1	Nuclear factor of activated T cells cytoplasmic 1

NF-κB	Nuclear factor kappa-light-chain-enhancer of activated B cells
NIK	NF-κB-inducing kinase
NLR	Nucleotide-binding leucine-rich repeat receptor
NLRP3	NLR pyrin 3
NSA	Necrosulfonamide
OAF	Osteoclast activating factor
OB	Osteoblast
OBIF	Osteoblast inhibitory factor
OC	Osteoclast
OPG	Osteoprotegerin
PAMP	Pathogen-associated molecular pattern
Poly I:C	Polyinosinic:polycytidylic acid
Pre-OC	Precursor osteoclasts
PRR	Pattern recognition receptor
RANKL	Receptor activator of NF-κB ligand
RHIM	RIP homotypic interaction motif
RING	Really Interesting New Gene
RIPK	Receptor interacting protein kinase
RNF11	RING finger 11
SMAC	Second mitochondrial activator of caspases (also known as DIABLO)
SM	Smac-mimetics
SMM	Smoldering multiple myeloma
STAT	Signal transducers and activators of transcription
TAB	TAK1-binding protein
TAK1	TGF-β-activated kinase 1 (also known as MAP3K7)
TAM	Tumor-associated macrophage
TAX1BP1	TAX1-binding protein 1
TGF-β	Transforming growth factor-β
TIR	Toll/IL-1 receptor
TIRAP	Toll/IL-1 receptor domain-containing adaptor protein
TLR	Toll-like receptor
TNF	Tumor necrosis factor

TNFR	Tumor necrosis factor receptor
TRADD	TNFR1-associated death domain protein
TRAF	TNFR-associated factor
TRAIL	TNF-related apoptosis-inducing ligand
TRAILR	TNF-related apoptosis-inducing ligand receptor
TRAM	TRIF-related adaptor molecule
TRAP	Tartrate-resistant acid phosphatase
TRIF	Toll/IL-1 receptor domain-containing adaptor-inducing IFN-β
Ub	Ubiquitin
UBA	Ub-associated
XIAP	X-linked inhibitor of apoptosis protein
YopJ	*Yersinia* outer protein J
ZBP1	Z-DNA binding protein 1

Abstract

The receptor-interacting protein kinase 1 (RIPK1)-pathway is a key regulator of inflammation and cell death. RIPK1-dependent cell death has been well studied in murine macrophages but as it is context dependent and differently regulated in humans, more knowledge on pharmaceutically induced cell death in human macrophages are needed. Our aim for this thesis was thus to contribute to a better understanding of pharmaceutical induction of RIPK1-dependent cell death in a context of human osteoclasts (OC) and other macrophage subtypes. Pharmaceutical targeting of RIPK1-signaling by drugs like Smac-mimetics (SM) and TGF-β-activated kinase 1 (TAK1)-inhibitors has been extensively studied as therapeutic options in both cancer and other chronic diseases like psoriasis and inflammatory bowel disease, but studies on primary human immune cells have been warranted. Currently, SM are in clinical trials in cancers such as multiple myeloma (MM) and as OC contribute to the disease pathology, the effect of SM on these cells should be investigated. In addition, TAK1 has been found to be a driver of MM and necessary for osteoclastogenesis in mice. TAK1-inhibitors could thus be a novel therapeutic option as an antitumorigenic agent and in reducing bone disease in MM-patients.

In paper I we sought to investigate the effect of SM-treatment on human OC and the possible beneficial role in MM therapy. We demonstrated that the SM birinapant and LCL-161 restrained osteoclastogenesis and induced TNF-dependent cytotoxicity in primary human OC. Birinapant induced apoptosis, and also necroptosis in some donors. In addition, we discovered that both SM blocked osteoclastogenesis induced by myeloma patient bone-marrow aspirates, proposing an additional benefit by reducing bone degradation in patients.

The objective of paper II was to investigate the effect of pro- and anti-inflammatory pretreatment on SM-induced cell death in human macrophages. We found that pro- and anti-inflammatory treatment dictated the sensitivity and cell death mechanism induced by the SM birinapant and LCL-161. LPS pretreated macrophages were considerably more susceptible to cell death compared to the other tested subtypes, which was caused by a potentiation of apoptosis. In contrast, the other tested subtypes depended on the necroptotic machinery for full birinapant cytotoxicity, an intriguing observation as necroptosis could be induced in a setting were caspase activity was functional. Birinapant-induced apoptosis in LPS pretreated macrophages was accompanied by IL-1β release independent of caspase 1. Taken together, our findings suggest a therapeutic potential of SM in a disease setting where inflammatory up-regulation of macrophages is involved.

Paper III focuses on the effect of TAK1-inhibitor treatment on MM cells and the possible beneficial effect on human OC. We demonstrated that the TAK1-inhibitors NG25 and 5Z-7-oxozeaenol (5Z-7) were cytotoxic to MM cell lines and patient cells both alone and in combination with the DNA-damaging drug melphalan. In addition, NG25 and 5Z-7 reduced differentiation and viability of human OC, suggesting a double beneficial effect for patients by reducing bone disease.

Altogether, this work contributes to the understanding of pharmaceutical targeting of RIPK1-signaling in human macrophage systems and points out potential therapy candidates for treatment of inflammatory conditions and cancers such as MM.

1 Introduction

1.1. The monocytic lineage

1.1.1. Monocytes

Monocytes are a group of leukocytes that are essential players in the innate immune system. They continuously enter the blood circulation and constitute around 10 % of the total amount of leukocytes in humans (1, 2). They are part of the myeloid lineage as they originate from hematopoietic stem cells in the bone marrow (BM) and develop to monocytes through a series of sequential differentiation steps (3-5). Human peripheral monocytes are a heterogenous population and are divided into three subsets based on the composition of surface expression markers Cluster of Differentiation (CD) 14 and 16. CD14 is a lipopolysaccharide (LPS)-binding protein that functions as an endotoxin receptor (6). CD16, also known as Fc-gamma receptor III (FcγRIII), binds immunoglobulins and induce cellular cytotoxicity against antibody-coated cells such as transformed or virus-infected cells (7). Classical monocytes are the major population that express CD14 and not CD16 (1, 8). Monocytes are part of the innate immune system as they play a role in immune surveillance and mediate host defense against pathogens by differentiating into macrophages (Mϕ) and dendritic cells (DCs) upon exposure to microbial molecules or stimulation by cytokines (9). Their function is less defined during homeostasis, but they are believed to be part of the neutralization of toxic molecules, phagocytosis of dead cells and to replenish resident macrophages and DCs in different organs (10).

1.1.2 Macrophages

Macrophages originate from monocytes and are a heterogenous group of mononuclear phagocytes of the myeloid lineage (Figure 1.1). They are located in most tissues in the body and involved in tissue development and repair, immune surveillance and clearing of apoptotic cells (11, 12). Macrophages are an important part of the innate immune system as they express pattern recognition receptors (PRRs) and are thus able to recognize different danger-associated molecular patterns (DAMPs) and pathogen-associated molecular patterns (PAMPs). As a response, they produce a variety of pro- and anti-inflammatory cytokines. In addition, macrophages are important cells bridging the innate and adaptive immune system as they express major histocompatibility complex class II (MHC-II) molecules under inflammatory settings and are thus able to present antigens to T-cells (13).

Based on their origin, macrophages can both be tissue-resident and recruited. Tissue-resident macrophages originate from fetal liver, the yolk sac, and hematopoietic stem cells in the BM during embryonic development. For instance, the tissue-resident macrophage microglia in the brain and spinal cord are involved in the development of the central nervous system by producing neurotrophic factors. Recruited macrophages are on the other hand differentiated from monocytes in the circulation. They are short-lived effector cells that are recruited to different tissues and differentiate to perform different tasks (14-16).

The key factor in influencing homeostatic control of monocyte and macrophage development is colony-stimulating factor 1 (CSF-1, previously known as M-CSF) (Figure 1.1) (17). CSF-1 is a hematopoietic growth factor that promotes proliferation, differentiation, and survival of cells from the monocytic lineage. CSF-1 is produced by stromal cells and binds to CSF-1 receptor (CSF-1R), a transmembrane tyrosine kinase receptor expressed on most mononuclear phagocytic cells. *CSF-1* knockout mice display a wide range of developmental defects including skeletal, growth and neurological abnormalities underpinning its importance for proper macrophage development (18, 19).

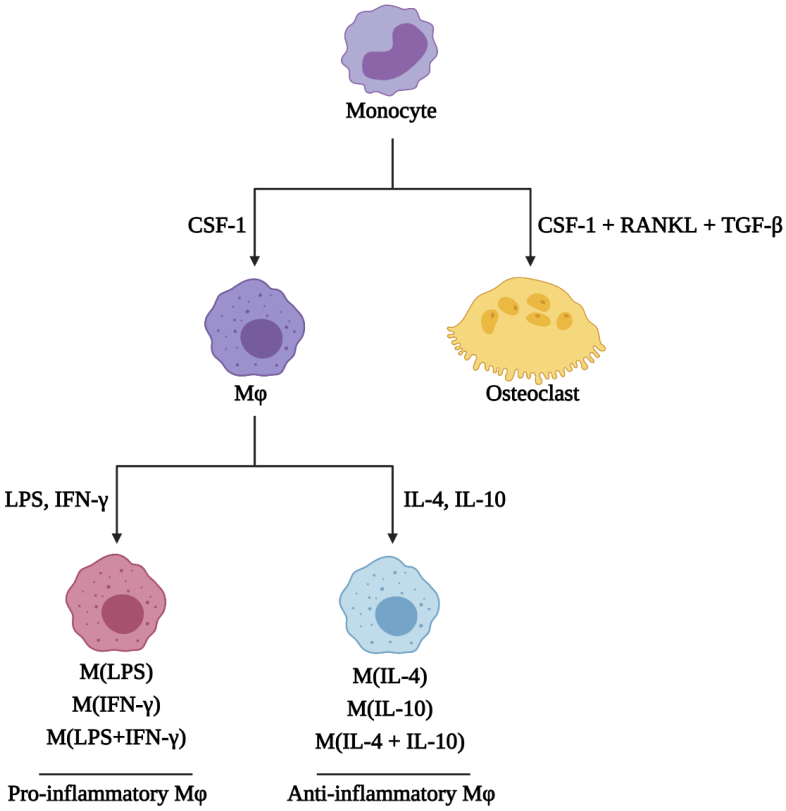

Figure 1.1: Macrophages and osteoclasts differentiate from monocytes. Monocytes require stimuli from CSF-1 to differentiate into macrophages (Mϕ) while stimuli with CSF-1, RANKL and TGF-β give rise to osteoclasts. Mϕ differentiate into pro-inflammatory macrophages when treated with stimulants like LPS and IFN-γ. Polarization towards anti-inflammatory macrophages are promoted by cytokines like IL-4 and IL-10. CSF-1, colony-stimulating factor-1; RANKL, receptor activator of NF-κB ligand; TGF-β, transforming growth factor-β; IL, interleukin; LPS, lipopolysaccharide; IFN, interferon. Modified from (20). The figure is created with biorender.com.

The phenotype of macrophages is determined by the polarization in response to different stimuli (12). CSF-1 stimulation is necessary for monocytes to differentiate into Mϕ (Figure 1.1). In addition, other stimuli from the surrounding environment influence macrophage function and expression of specific surface markers (10, 12). This process is known as polarization. Previously, the categorization of macrophages followed the M1-M2 nomenclature, where M1 includes pro-inflammatory macrophages and M2 anti-inflammatory.

Critique of this categorization is based on the fact that macrophage polarization is highly dynamic, and their gene expression and response is adaptable depending on the environmental stimuli (21, 22). The M1/M2 nomenclature does therefore not represent the actual situation *in vivo* as macrophages are not stable and clearly defined subtypes. In this thesis, the nomenclature of macrophages is rather based on which cytokines or other modulators they are subjected to such as M(LPS+IFN-γ) and M(IL-4) (Figure 1.1) (21).

1.1.3 Macrophage polarization

Pro-inflammatory macrophages are implicated in host defense upon infection. They are activated by toll-like receptor (TLR) ligands like LPS and polyinosinic:polycytidylic acid (poly I:C), and inflammatory cytokines like tumor necrosis factor (TNF) or interferon gamma (IFN-γ) (Figure 1.1) (21, 23). Pro-inflammatory macrophages support inflammation, pathogen response, and resistance against tumor cells through the secretion of pro-inflammatory cytokines like TNF, interleukin (IL)-6, IL-12, and IL-23 activated through nuclear factor kappa-light-chain-enhancer of activated B cells (NF-κB) and signal transducers and activators of transcription 1 (STAT1) signaling (1, 24). Additional characteristics include increased antigen presentation, phagocytosis of pathogens and production of reactive oxygen and nitrogen species (25). Prolonged or chronic activation of pro-inflammatory macrophages can result in host-tissue damage and inflammatory or autoimmune diseases (10, 12).

To counteract the inflammatory response, pro-inflammatory macrophages either die or polarize to the anti-inflammatory phenotype (26). The resolution of inflammation involves macrophage-mediated efferocytosis of apoptotic cells which reduces the expression of inflammatory cytokines in the microenvironment (27). Efferocytosis and other factors like the secretion of anti-inflammatory cytokines from regulatory T-cells directs polarization towards anti-inflammatory macrophages (28). Anti-inflammatory macrophages are activated by cytokines such as IL-4, IL-10, and IL-13 and secrete immunosuppressive cytokines to support tissue-repair processes (Figure 1.1) (29). These cytokines activate signaling through STAT3/6 resulting in the release of transforming growth factor (TGF)-β and IL-10 which additionally institute a positive feedback loop enhancing polarization of anti-inflammatory macrophages (10, 24, 30).

Besides promoting tissue healing and growth, anti-inflammatory macrophages are also involved in inducing tumor growth, facilitating angiogenesis, and accumulate in the tumor

microenvironment (10, 31, 32). At the early stages of cancer, pro-inflammatory macrophages are activated as a response to tissue damage and participate in tumor destruction (33). As a response, regulatory T-cells and tumor cells themselves secrete factors skewing the polarization towards anti-inflammatory macrophages. These factors include IL-4, IL-10, and C-C motif chemokine ligand (CCL2) that stimulate and recruit tumor-associated macrophages (TAMs) that share several characteristics with anti-inflammatory macrophages (34). TAMs secrete growth factors and cytokines that promote tumor-cell migration and invasion and increase angiogenesis that facilitate the escape of tumor cells into vascular and lymphatic tissue to metastasize (35, 36). They also dampen anti-tumor responses through the secretion of immunosuppressive agents. TAMs also promote immune evasion of the tumor through the production of chemokines that downregulate cytotoxic T-cell activity (37).

Macrophage polarization is a dynamic process as it depends on factors present in the given environment. Therefore, it is not surprising that crosstalk exists between pro- and anti-inflammatory macrophages which is mediated by STAT1 and STAT3/6 activation (24). In sepsis for instance, the first line of inflammatory response is NF-κB mediated activation of pro-inflammatory macrophages. To resolve this inflammatory response, pro-inflammatory macrophages subsequently polarize to the anti-inflammatory phenotype through NF-κB inhibition to exhibit immunosuppressive features. In different disease settings, macrophages can also have mixed phenotypes depending on the stimulants present. The switch controlling this balance in polarization and the signaling networks involved are not fully understood but is a key interest in research (24). For instance, research has been focused on the reprogramming of TAMs to pro-inflammatory macrophages for anti-tumor immunity (38-40).

1.1.4 Osteoclasts

Osteoclasts (OC) are multinucleated specialized forms of macrophages that degrade bone (41, 42). They originate from hematopoietic stem cells and differentiate from monocytes into precursor osteoclasts (pre-OC) upon stimuli with osteoclastogenic cytokines (Figure 1.1). In the late stage of differentiation, pre-OC fuse together, giving rise to multinucleated mature OC (43). Pre-OC fusion is mediated by Rho GTPases that reorganize the cytoskeleton to reduce the distance to neighboring precursors. Additionally, cytoskeleton reorganization increase the fusion-probability by mediating the formation of membrane protrusions (43). OC are highly migratory cells and display phenotypic characteristics like pleomorphic vacuoles, lysosomes and mitochondria (41, 44).

Function, differentiation and survival of OC are regulated by several cytokines and hormones (45, 46). The master cytokine driving osteoclastogenesis is receptor activator of NF-κB ligand (RANKL). RANKL is secreted by osteocytes, osteoblasts (OB), and stromal cells and stimulate the differentiation from pre-OC to mature OC (42, 47). In mature OC, RANKL additionally mediates activation and survival (48). RANKL is a member of the TNF superfamily and binds to its receptor RANK expressed on pre-OC (41). Another key regulator of osteoclastogenesis is osteoprotegerin (OPG) produced by OB, stromal cells, and fibroblasts. OPG is a soluble competitive binding partner for RANKL inhibiting osteoclastogenesis though blocking the RANK-RANKL interaction (42, 49).

Binding of RANKL to RANK leads to the engagement of TNF receptor-associated factors (TRAFs) which ultimately results in the activation of several kinase cascades. These cascades include NF-κB and the mitogen-activated protein kinases (MAPKs) p38, extracellular signal-regulated kinase (ERK) 1/2 and c-Jun N-terminal kinase (JNK) (50). This leads to the activation of transcription factors like NF-κB, activator protein-1 (AP-1) and nuclear factor of activated T cells cytoplasmic 1 (NFATc1) (51). Activated RANK also induce the phosphorylation of immunoglobulin-like receptor associated adaptor proteins like immunoreceptor tyrosine-based activation motif (ITAM) and FcγR subunit (52). In the nucleus, NFATc1 in combination with other transcription factors like AP-1, PU.1, microphthalmia-associated transcription factor (MITF), and cyclic AMP responsive-element binding protein (CREB) bind cis regulatory DNA elements, leading to the induction of OC-specific genes. These include genes coding for OC specific markers like calcitonin receptor, dendritic cell-specific transmembrane protein (DC-STAMP), cathepsin K and tartrate resistant acid phosphatase (TRAP), resulting in differentiation and proliferation of OC (46, 52). Calcitonin receptors are involved in the maintenance of calcium homeostasis while DC-STAMP is crucial for the fusion of pre-OC (42).

Other osteoclastogenic cytokines include CSF-1 and TGF-β. In addition to stimulating macrophage differentiation, CSF-1 promotes OC proliferation and inhibits apoptosis, resulting in increased osteoclastogenesis (42). CSF-1 additionally influence the expression of genes that are important for the RANKL- and IL-signaling responses (45). TGF-β is a multifunctional growth factor that is produced by many cells in the bone and is abundant in the bone matrix. TGF-β regulate OC formation and bone resorption induced by RANKL (53, 54). The

inflammatory cytokines IL-1β, IL-6 and TNF are key components of acute and chronic inflammation. They are in addition regarded as osteoclastic cytokines that are strong inducers of bone resorption through lowering the threshold for RANKL-induced osteoclastogenesis, as well as inducing of stromal cells to increase RANKL-production (52, 55). Besides cytokine stimuli, osteoclastogenesis is dependent on cellular contact between pre-OC, OB, and stromal cells. Given their monocytic origin and their dependency on inflammatory cytokines for differentiation, osteoclastogenesis and aberrant bone degradation can be viewed as inflammatory processes.

The definition of mature OC are TRAP positive cells with three or more nuclei that are capable to resorb bone (56). The first step in the bone-resorption process is the attachment of OC to the bone matrix through specialized $\alpha_v\beta_3$ integrins, making up the sealing zone (Figure 1.2) (42). A crucial step in the degradation of bone matrix is the acidification of the bone-resorption area mediated by transport of protons (H^+) and chloride (Cl^-). H^+ are generated by the enzyme carbonic anhydrase II (CAII) and HCO_3^-/Cl^- exchangers increase the intracellular concentration of Cl^- (43). Proton pumps and chloride channels subsequently transports H^+ and Cl^- across the ruffled border, a special membrane structure in contact with the bone matrix at the site of bone-resorption. The acidified environment in the resorption area results in solubilization of the mineral phase of the bone and activation of secreted enzymes (57). This includes lysosomal enzymes like the protease cathepsin K and the phosphatase TRAP which cleave and degrade organic bone matrix (41, 43). Bone-degradation products are then removed through endocytosis, trafficked through the OC by transcytosis, and released into the extracellular space (42). The sealing zone subsequently disassembles, a new adhesion sites are formed next to the former resorption area, and the OC repolarizes. This oscillation between resorption and polarization phases results in trails of resorption pits along the bone surface (43).

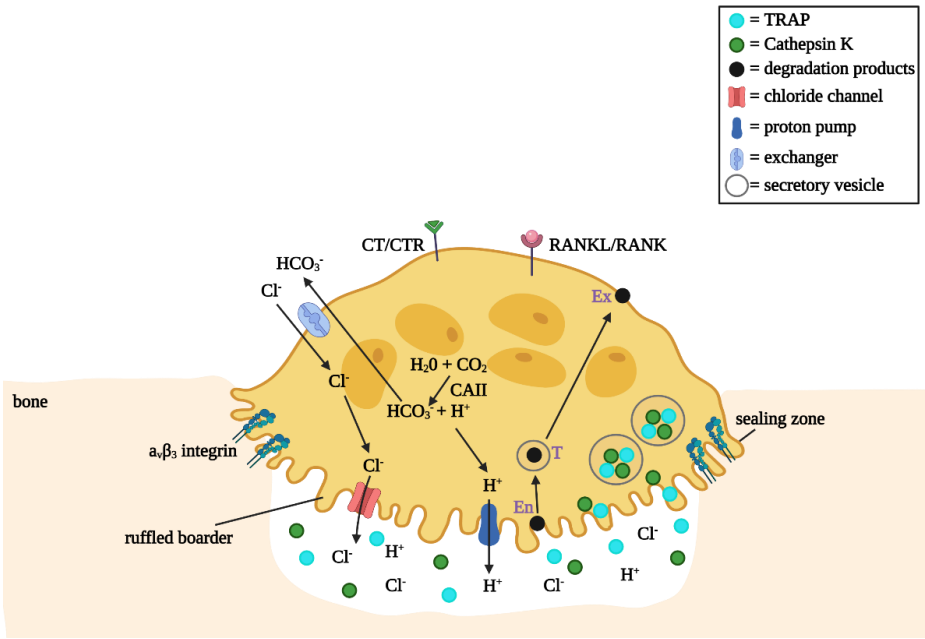

Figure 1.2 Osteoclast-mediated resorption of bone matrix. The sealing zone makes up the area where osteoclasts attach to the bone, mediated by $\alpha_v\beta_3$ integrins. Generation of H^+ is generated by CAII while the concentration of Cl^- increases by the exchange of HCO_3^-/Cl^-. Within the sealing zone, chloride channels and proton pumps exports H^+ and Cl^- acidifying the surface that is in contact with the ruffled border. This results in the dissolution of the mineral matrix of the bone in the resorption pit mediated by phosphatases and proteolytic enzymes like TRAP and cathepsin K. Degradation products are endocytosed (En), transported by transcytosis (T) and released by exocytosis (Ex). CAII, Carbonic anhydrase II; CT, Calcitonin; CTR, calcitonin receptor; RANK, receptor activator of NF-κB; RANKL, RANK ligand; TRAP, Tartrate resistant acid phosphatase. Modified from (43). The figure is created with biorender.com.

1.2 NF-κB and MAPK-signaling promotes inflammation and survival

1.2.1 NF-κB-signaling

NF-κB is a family of transcription factors that regulates a wide array of cellular functions, including immune cell homeostasis and inflammation. Activation of NF-κB occurs in most cells upon stimulation with a wide range of stimuli including TNF, LPS, RANKL, viral and bacterial antigens, free radicals and genotoxic stress (55). The main function of NF-κB is to initiate and maintain inflammatory activation through its involvement in adaptive and innate immunity responses against pathogens and autoimmune stimuli (58). The transcription factor

promotes the expression of numerous genes, including cytokines like IL-6 and TNF. Other examples include regulators of apoptosis as cellular inhibitor of apoptosis (cIAP) and cellular FLICE-like inhibitory protein (cFLIP, also named CFLAR) and growth factors like CSF-1 (59). The family of NF-κB consists of five members named RelA (p65), RelB, c-Rel, NF-κB1 p52 and NF-κB2 p50, which form complexes as either homodimers or heterodimers (60). NF-κB is a target in anti-inflammatory drugs as dysregulation of NF-κB signaling is involved in several inflammatory diseases including multiple sclerosis and rheumatoid arthritis (61).

The most commonly found heterodimer in NF-κB1 signaling is RelA/p50 (Figure 1.3 A) (62, 63). Several receptors activate NF-κB1 signaling, including TNF receptor (TNFR) and TLR4 (63, 64). Activation engage TRAFs to the receptors which initiates complex formation with TGF-β activated kinase 1 (TAK1) and TAK1-binding protein 2 (TAB2) (Figure 1.3 A). Complex formation activates TAK1 which phosphorylate the inhibitor of κB (IκB) kinase (IKK). IKK is composed of two catalytic subunits IKKα and IKKβ, and a regulatory subunit NF-κB essential modulator (NEMO) (58). When IKK is inactive, NF-κB inhibitor-α (IκBα) is bound to NF-κB, preventing its activation. Once activated by TAK1, IKK phosphorylates IκBα which targets the inhibitor for ubiquitylation and proteasomal degradation, releasing its hold on RelA/p50. RelA/p50 subsequently translocate to the nucleus to induce transcription of target genes like *TNF*, *IL6* and *IL1A* (60, 65).

In OC, the NF-κB2 pathway is also activated upon RANKL-stimuli (Figure 1.3 B). Alternative activators include other members of the TNF family like CD40 ligand and lymphotoxin and B cell activator of the TNF family (BAFF) (64). While the NF-κB1 pathway can be activated within minutes, NF-κB2 signaling display a slower time dynamic requiring several hours for its activation (58). RelB/p52 is the most common dimer in NF-κB2 signaling. RANK-induced signaling targets the activation of NF-κB-inducing kinase (NIK), which in turn activate IKKα through phosphorylation (58). In unstimulated cells, NIK is targeted for ubiquitin-dependent degradation by TRAF3 in complex with TRAF2 and cIAP1/2 (66). During stimulation by RANKL, cIAP1/2 ubiquitinate TRAF3 resulting in its degradation and ultimately release of NIK from the complex (Figure 1.3 B). NIK is then free to phosphorylate IKKα, inducing the processing of p100 to p52. RelB/p52 then translocate to the nucleus to promote target gene expression like *TNF*, *CXCL12* and *CCL19*. In contrast to NF-κB1-signaling, the NF-κB2 pathway does not rely on the degradation of IκBα. It is instead dependent on the proteolytic

cleavage of RelB from p100 to the active p52 form (60). A consequence of low cIAP activity, either through low protein levels or by chemical inhibition, is the stabilization of NIK. This leads to increased NF-κB2-signaling (66, 67).

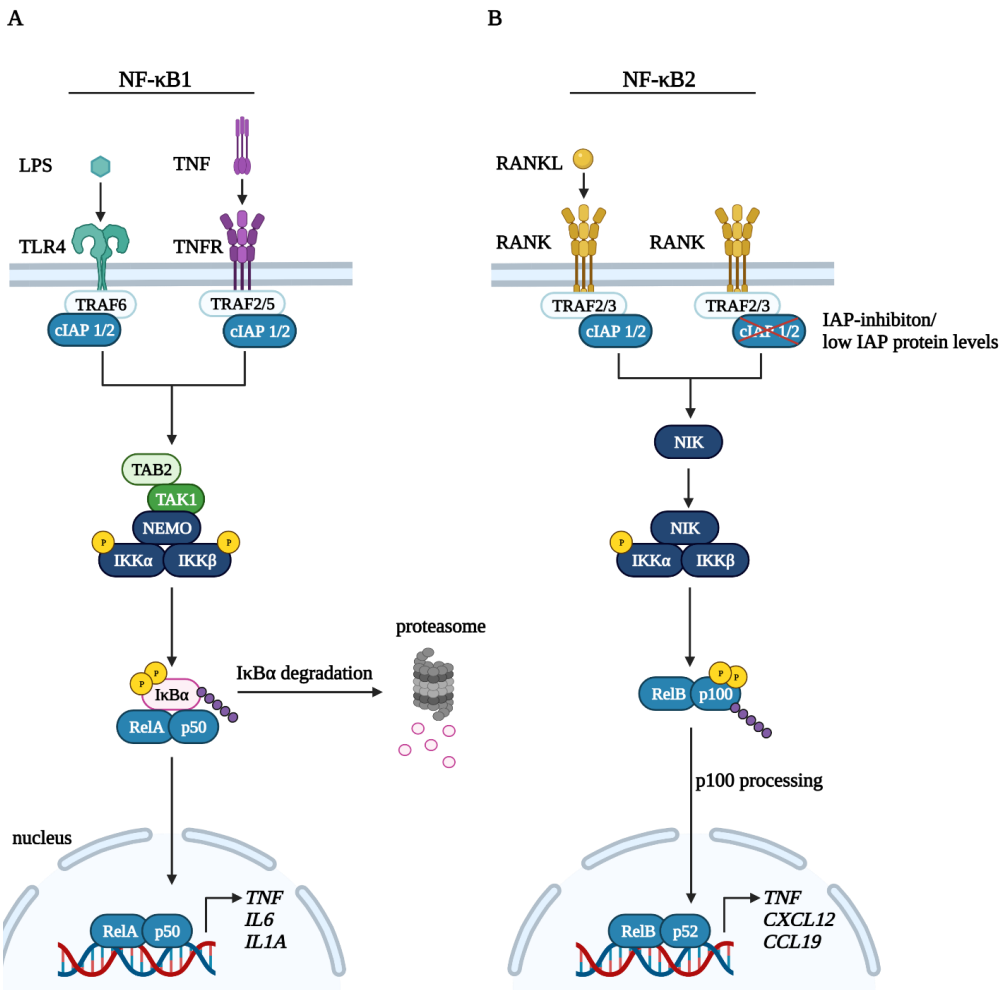

Figure 1.3 NF-κB1 and NF-κB2 signaling. A. The NF-κB1 pathway is induced by different types of cytokine stimuli including LPS and TNF. Signaling involves the activation of the IKK-complex by TAK1 and the phosphorylation and subsequent degradation of IκBα mediated by IKK. This results in a rapid translocation of RelA/p50 into the nucleus. **B.** The NF-κB2 pathway is activated by stimuli from different TNF superfamily members, including RANKL. NF-κB2-signaling activates NIK and IKKα mediating the processing of p100 to p52. This results the activation of the RelB/p52 dimer and its subsequent translocation to the nucleus. NIK, NF-κB inducing kinase. Modified from (58, 60). The figure is created with biorender.com.

1.2.2 MAPK signaling

MAPKs are a family of serine/threonine kinases involved in proliferation, differentiation, survival, and cell death. Activation of a MAPK pathway involves at least three core kinases, MAP3K, MAP2K and MAPK (68). The signal is transduced through kinase cascades resulting in transcriptional activation or direct activation of regulatory proteins. The MAPK family include p38, ERKs and JNK.

Upon stimulation by TNF or LPS, TRAF mediates the recruitment of TAB-TAK1 as described for NF-κB1. TAK1 phosphorylates and activates a downstream MAP2K which in turn activates p38, ERK and JNK (69, 70). In this context the MAPKs are often activated together with NF-κB1 downstream of TNFR1, TLR4 and TAK1 and exert some of the same responses. ERK, JNK and p38 are all involved in cell proliferation through regulation of the cell cycle. The ERK pathway is central for the control of proliferation by for instance activation of the transcription factor Elk-1 that leads to the subsequent activation of AP-1. AP-1 is necessary for cyclin D expression that is involved in the G_1/S transition and cell cycle progression (71, 72). Similar to ERK, JNK is also involved in AP-1 and cyclin D expression but here mainly through the activation of the target protein c-Jun (71). The p38 module is important in inflammatory responses by the induction of proinflammatory cytokines. p38 is additionally involved in cell cycle regulation for instance by activating MYC proto-oncogene protein. MYC regulates survival as well as cell cycle control through E2F, a family of transcription factors that are critical for G_1/S transition and entry into the S-phase (73).

1.2.3. TAK1 is a key activator of NF-κB1 and MAPKs

TAK1 (also known as MAP3K7) is a serine/threonine kinase that is a key regulator of proinflammatory signaling. It is a member of the MAP3K family and promote survival and inflammation by activation of the NF-κB1 and MAPK signaling pathways, as previously described. As the name implies, TAK1 was first discovered to be activated by TGF-β (74). TAK1 was subsequently identified as a mediator of inflammatory responses as it is also activated by TNF and LPS. A variety of other factors including RANKL and genotoxic stress have later been discovered to induce TAK1 activation (75).

TNF-TNFR1 and LPS-TLR4 signaling recruit the E3 ubiquitin ligases TRAF2 and TRAF6 respectively to the receptors. Through their ubiquitin ligase activities, TRAF2 and TRAF6 generate a lysine-linked polyubiquitin chain that recruit the adaptor proteins TAB1 and TAB2.

TAB1/2 is constitutively bound to TAK1 and initiate complex formation by linking TRAF2/6 to TAK1 (48, 60). This triggers a conformational change in TAK1 leading to its autophosphorylation and subsequent phosphorylation of downstream targets.

Genotoxic stress such as DNA-damaging agents and ionizing radiation induce DNA lesions (76-78). This triggers the recruitment and subsequent activation of the kinase ataxia-telangiectasia mutated (ATM) (79). ATM recruits and phosphorylates NEMO which results in their translocation from the nucleus into the cytosol. This leads to the formation of a cytosolic complex containing ATM, NEMO, TAK1 and either receptor-interacting protein kinase 1 (RIPK1) or ELKS (80, 81). Complex formation results in the activation of TAK1 and subsequent downstream activation of MAPKs and NF-κB1. NF-κB and MAPK signaling promote tumor progression and increase the resistance of tumor cells to anticancer therapy. For instance, these pathways support tumor survival through cell cycle regulation, producing factors inhibiting apoptosis and senescence (75, 82).

Knockout of *TAK1* is embryonically lethal in mice demonstrating that TAK1 is necessary for proper embryonic development (75). Inducible knockout of *TAK1* leads to development of liver injury, psoriasis and inflammatory bowel disease (70). TAK1 is necessary for OC activity and osteoclastogenesis in mice. TAK1-deficient mice display reduced osteoclastogenesis and osteopetrosis (50, 83). The consequence of TAK1 inhibition on osteoclastogenesis in humans is however less described.

1.3. RIPK1 is a regulator of inflammation and cell death

RIPK1 is a serine/threonine kinase that is recruited to a wide range of receptor-ligand complexes, including TNF, LPS, IL-1β, IL-6, IFN-α/β and IFN-γ. RIPK1 is a key regulator of distinct cellular processes functioning both as a scaffold promoting cell survival, and as an inducer of cell death either dependent or independent of its enzymatic activity (84, 85). By being placed at crossroad of contrasting signaling outputs, RIPK1 requires tight regulation to be able to control normal tissue homeostasis as mutations or inadequate regulation of RIPK1 or other factors in the pathway lead to overexpression of inflammatory cytokines or cell death (86, 87). Overproduction of inflammatory cytokines can result in hyperinflammation, and autoinflammatory diseases like polyarthritis, rheumatoid arthritis and multiple sclerosis (88-90).

The scaffolding role of RIPK1 contributes to the activation of NF-κB and MAPK signaling, resulting in the expression of inflammatory and pro-survival molecules. In addition, this scaffolding function of RIPK1 protects the cell from regulated cell death, termed apoptosis and necroptosis. In contrast, the enzymatic kinase activity of RIPK1 contributes to the context-dependent induction of either apoptosis, necroptosis or pyroptosis (84, 85, 91). The scaffolding role of RIPK1, and not it's enzymatic activity, has been demonstrated to be indispensable for the viability and homeostasis in mice. *RIPK1* knockout cause systemic inflammation and cell death in several tissues and death short time after birth while mice expressing catalytically inactive RIPK1 are viable and protected from cell death(92-97). A rare homozygous *RIPK1* loss-of-function mutation in humans results in immunodeficiency with lymphopenia and recurrent infections, gut inflammation, progressive polyarthritis, and death during adolescence (88, 90). This suggests that *RIPK1* is an essential gene in humans as well as in mice and that the scaffolding function of RIPK1 is evolutionary conserved.

1.3.1. RIPK1-recruitment to the TNF-TNFR1 complex

RIPK1 is necessary for TNF-TNFR1 activation of NF-κB and MAPKs. TNF is an inflammatory cytokine involved in systemic inflammation that binds two receptors, TNFR1 and TNFR2 (98). TNFR1 has an intracellular death domain (DD) which enables the recruitment of TNFR1-associated death domain protein (TRADD) (99). TNFR2 lacks this death domain and signals instead through TRAF1 and TRAF2 (99). Signaling through both receptors promote activation of the canonical NF-κB-pathway, but only signaling through TNFR1-TRADD induce cell death (100).

Upon TNF stimulation, poly-ubiquitin chains coordinate the assembly of the membrane bound TNFR1 complex (also known as complex I or TNFR1-signaling complex (TNFR1-SC)) and subsequent NF-κB and MAPK activation. Ubiquitin (Ub) is an 8 kDa protein that is covalently linked to lysine (K) or methionine (M) residues on target proteins, forming poly-ubiquitinylated conjugates (101). This process is named ubiquitylation and is a three-step process involving Ub-activating (E1), Ub-conjugating (E2) and Ub-ligating (E3) enzymes. The ubiquitin system is best known for its role in labelling proteins and cellular constituents for degradation by the proteasome or autophagy system. Covalent ligation of ubiquitin targets the protein for degradation, usually performed by the 26S proteasome complex (102). Ub-mediated degradation of regulatory proteins serves important roles in processes such as transcriptional regulation and receptor down-regulation. In addition, Ub conjugates are important in other

cellular processes independent of proteolytic degradation. In many inflammatory pathways, Ub is crucial for gathering and structuring signal complexes (103). Poly-Ub chains can be formed by elongation at different residues. For example, if Ub-units are linked through lysine at position 48 it is designated K48-polyubiquitination. Proteins attached to K48-linked poly-Ub chains are targeted for degradation, while K63- and M1-linkages reinforce protein scaffolding (100).

TNF-signaling recruits TRADD and RIPK1 to TNFR1 via homotypic DD interactions. TRADD subsequently engage TRAF2 which bind and recruit cIAP1/2, making up the membrane bound TNFR1-signaling complex (Figure 1.4) (104). RIPK1 is polyubiquitylated upon receptor binding. Ubiquitylation is mediated by the E3 ligases cIAP1/2 and TRAF2 and the linear ubiquitin chain assembly complex (LUBAC) which add poly-Ub chains to RIPK1 through K63- and M1-linkages, respectively (Figure 1.4) (86). The poly-Ub chains on RIPK1 serve as docking sites for TAK1-TAB2/3 and NEMO, recruiting them to the TNFR1 signaling core. The binding of NEMO to these poly-Ub chains subsequently recruits IKKα/β to the membrane bound complex. Both TAB2/3 and NEMO link to the ubiquitin chains via their ubiquitin-binding domains where TAB2/3 binds K63-linkages and NEMO to M1-linked chains (105-109). The K63-linkages are proposed to serve as substrates for the M1 poly-Ub chains, where the K63/M1-chains facilitates proximity between TAB2/3-TAK1 and NEMO-IKK α/β (109, 110). This leads to the subsequent TAK1-mediated activation of NF-κB, p38 and JNK promoting cell survival. As previously mentioned, NF-κB and MAPK activation is independent of the kinase activity of RIPK1, and RIPK1 functions instead as an ubiquitylated and enzymatically inactive scaffold in this context.

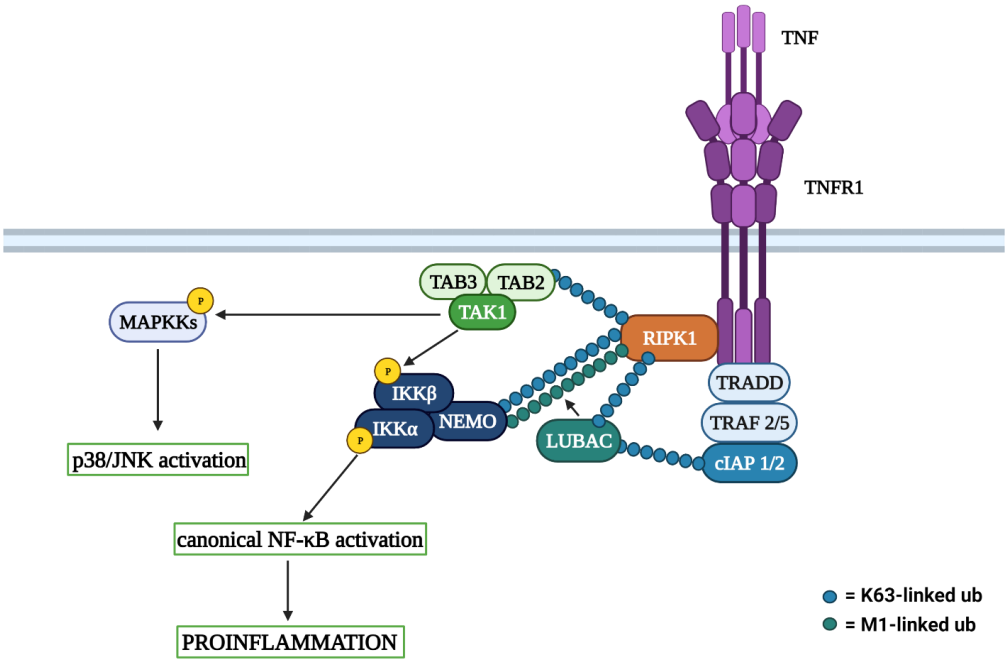

Figure 1.4 The TNFR1 membrane bound complex activates NF-κB and MAPK signaling to promote proinflammatory signaling. Upon binding of TNF to TNR1, the receptor binds TRADD which leads to recruitment of RIPK1, TRAF2/5 and cIAP1/2 forming the membrane bound signaling complex. Polyubiquitylation of RIPK1 mediated by cIAP1/2 and LUBAC recruits TAB2, TAB3 and TAK1. This leads to the activation of NF-κB and the MAPKs p38, JNK promoting cell survival. Modified from (100). The figure is created with biorender.com.

1.3.2. Inhibitor of apoptosis proteins

IAPs (also named Baculoviral IAP repeat containing protein (BIRC)) are a group of ubiquitin E3 ligases that function in restricting both intrinsic and extrinsic cell death (111). There are at least eight human IAP proteins, including neuronal apoptosis inhibitory protein (NAIP/BIRC1), cIAP1 (BIRC2), cIAP2 (BIRC3),), X-linked inhibitor of apoptosis protein (XIAP/BIRC4), survivin (BIRC5), and Baculoviral IAP repeat (BIR) repeat-containing ubiquitin-conjugating enzyme (BRUCE/BIRC6), melanoma-IAP (ML-IAP/BIRC7) and IAP-like protein 2 (ILP2/BIRC8) (112, 113). The cIAP proteins are characterized by the presence of one or several BIR domains which are required for the restriction of apoptosis for some of the IAP-members (114-117). cIAP1, cIAP2 and XIAP contains three BIR domains, and the

structure is also comprised of a Really Interesting New Gene (RING)-finger domain that has E3 ligase activity, and a Ub-associated (UBA) domain that enables interaction with ubiquitylated proteins (118, 119). In addition, cIAP1 and cIAP2 have a caspase recruitment domain (CARD) that can inhibit their E3 ligase activity (120, 121).

cIAP1 and cIAP2 are paralogue proteins that function in a partly redundant manner (122). They are present both at the mitochondria where they restrain intrinsic cell death, and at inflammatory receptors where they are involved in inflammatory responses and extrinsic cell death regulation. This includes recruitment to the TNF-TNFR1 complex and the regulation of NF-κB2 signaling by triggering the proteasomal degradation of NIK and restricting extrinsic cell death through the ubiquitylation of RIPK1. Of note, XIAP is most likely the only IAP-family member that directly inhibit caspase-3, -7, and -9 as cIAP1/2 does not share the crucial residues in their BIR domains necessary for direct inhibition (123, 124). cIAP1/2 are instead believed to indirectly interfere with caspase-3 and -7 through K48-ubiquitylation, promoting their proteasomal degradation (125).

The anti-apoptotic activity of IAPs can be neutralized by the mitochondrial protein second mitochondrial activator of caspases (Smac, also known as direct IAP binding proteins with low pI (Diablo)). Smac is released from the mitochondria into the cytoplasm in response to pro-apoptotic stimuli (114). Once cytosolic, Smac binds the BIR domains of cIAPs via their IAP-binding motif (IBM). Interaction with Smac antagonizes the XIAP-mediated inhibition of caspases and promote the auto-ubiquitination and degradation of cIAP1 and cIAP2 (126-129).

1.3.3. RIPK1-recruitment to the LPS-TLR4 complex

LPS is an integral component of the outer membrane in gram-negative bacteria (130). LPS is known to protect the bacteria from various forms of stress. Upon infection however, it is recognized as a PAMP by the innate immune system which triggers inflammatory responses (131). LPS is recognized by TLR4, a PRR belonging to the TLR family expressed on immune cells including monocytes and macrophages.

Detection of LPS by TLR4 is not a straightforward process as it requires the conversion of LPS aggregates from bacteria into monomers that needs to be in close proximity to TLR4 at the cell surface (130). This involves three other proteins: LPS binding protein (LBP), CD14 and myeloid differentiation factor-2 (MD-2) (Figure 1.5). LBP is an acute phase response

protein that is upregulated upon an innate immune response and extracts LPS aggregates from the lipid bilayer of gram-negative bacteria (132). CD14 then functions as a lipid transferase that accepts extracted LPS monomers from LBP. CD14 is expressed on macrophages and other immune cells and can either be surface GPI-linked (mCD14) or soluble (sCD14) (133). LPS can either be bound directly to mCD14 or be transferred from sCD14 to mCD14. CD14 has no internal signaling domain and thus cannot signal by itself. The final step of LPS recognition involves the small, soluble extracellular protein MD-2. MD-2 non-covalently associates with TLR4 and is essential for LPS signaling (130, 133).

Binding of LPS to TLR4 triggers signaling via two different adaptors: myeloid differentiation factor 88 (MyD88) and Toll/IL-1 receptor (TIR) domain-containing adaptor inducing IFN-γ (TRIF) (Figure 1.5). When TLR4 is located at the plasma membrane, TIR domain-containing adapter protein (TIRAP) recruits MyD88 (134). This in turn recruits TRAF6 which triggers a signaling cascade involving TAK1 that results in activation of NF-κB and MAPK (130). TLR4-MyD88 signaling also results in signaling through type I PI_3 kinase which activates Akt (135). The collective outcome of the TLR4-MyD88 signaling pathway results in the expression of genes encoding pro-inflammatory mediators like IL-6, TNF, and type III IFNs.

LPS signaling additionally induce the internalization of TLR4. TIRAP and MyD88 then dissociate from the membrane and TLR4 binds the endosome with a second adaptor pair: TRIF and TRIF-related adaptor molecule (TRAM). TRAM bridges TRIF to TLR4 which leads to the activation of TRAF3. Signaling through TRAF3 ultimately results in the activation of interferon regulatory factor 3 (IRF3) and 7, which induces the expression of type I IFNs (136). TRIF-dependent signaling can also lead to the recruitment of other signaling complexes. Active TRIF can recruit TRADD, TRAF6, cIAP1/2 and RIPK1 (137, 138) (Figure 1.5). cIAP1/2 then polyubiquitinates RIPK1 which in turn recruits TAK1 and the activation of NF-κB and MAPK signaling cascades. The deubiquitylation of RIPK1 will in turn shift the signaling towards cell death.

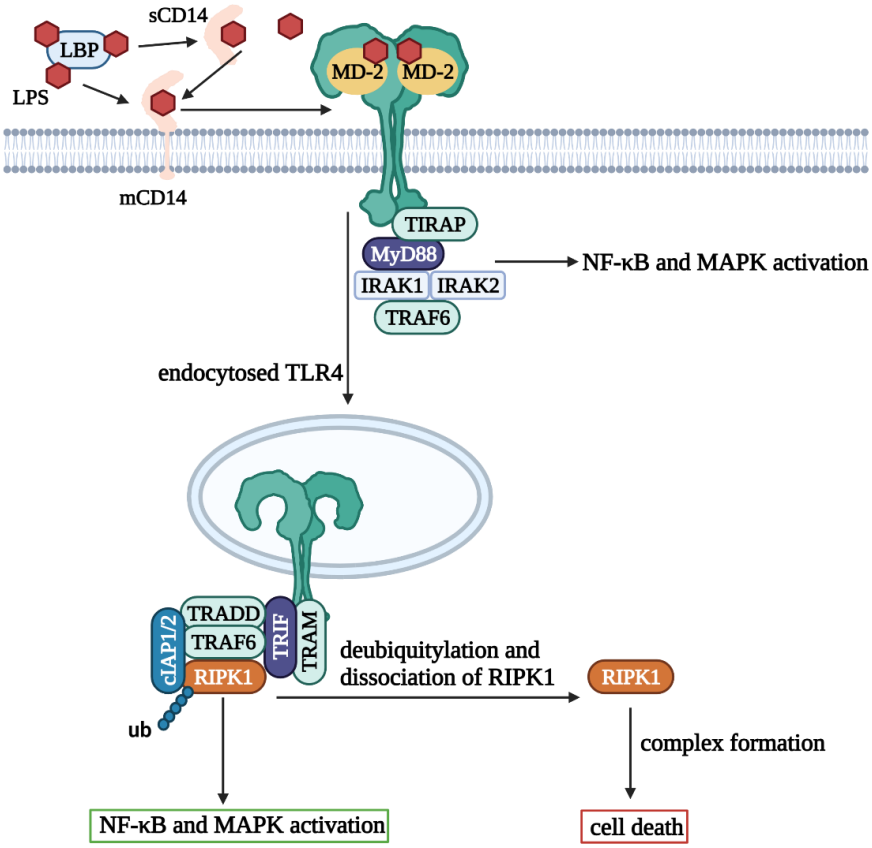

Figure 1.5 LPS-TLR4 activates RIPK1-dependent cell death via TRIF-TRAM. LPS bound to LBP is transferred to CD14 before being recognized by TLR4-MD-2. Binding of LPS to TLR4 triggers two distinct signaling pathways: MyD88- and TRIF-dependent signaling. MyD88 bind the intracellular domain of TLR4 through the adaptor protein TIRAP. This subsequently recruits TRAF6 and cumulates in the activation of NF-κB and MAPK signaling pathways. When TLR4 is internalized in the endosome, TRIF binds the receptor through its adaptor protein TRAM. TRADD, TRAF6, cIAP1/2 and RIPK1 can be recruited to this complex. Polyubiquitylated RIPK1 leads to NF-κB and MAPK activation. Deubiquitylation of RIPK1 results in its dissociation from the TLR4-bound complex and the induction of cell death. Modified from (130, 137). The figure is created with biorender.com.

1.4. RIPK1 regulates the activation of apoptosis, necroptosis and pyroptosis

1.4.1. Redirection of RIPK1-signaling to cell death: the early and late cell death checkpoints

Signaling through TNF-TNFR1-RIPK1 predominantly promotes inflammatory signaling through NF-κB and MAPK. However, this pathway is also able to induce cell death under circumstances where protective cell death checkpoints are turned off (110, 139). One checkpoint is the NF-κB dependent transcription of pro-survival factors and have thus been termed the late NF-κB dependent cell death checkpoint (110, 140, 141) (Figure 1.6). These pro-survival molecules include cFLIP, a caspase-8 homolog that will be further described in chapter 1.4.2 (142, 143). Other NF-κB-induced gene products include members of the BCL2 family which block intrinsic apoptosis and members of the TNFR1 complex like cIAP1/2, TRAF2 and A20 (144-147).

To ensure a transient and controlled response, NF-κB-signaling requires active repression. Deubiquitylating enzymes are partly responsible for this negative regulation of NF-κB by releasing the tight ubiquitin network associated with the membrane bound complex. A20 is a ubiquitin-editing enzyme that acts on RIPK1 and is an inducible NF-κB target-gene expressed upon TNF, LPS and IL-1β stimuli. The ubiquitylation on RIPK1 by A20 is regulated by A20-bining proteins. These include the E3 ligases ITCH and RING finger 11 (RNF11), and the Ub-binding protein TAX1-binding protein 1 (TAX1BP1) (86). A20 is a dual ubiquitin-editing enzyme being proposed to both remove K63-linked polyubiquitin chains on RIPK1 and subsequently add K48-linkages promoting its proteasomal degradation(148). This proposed function of A20 have however been debated by recent literature (149-152). Another regulator of RIPK1 is the constitutively active deubiquitylating enzyme cylindromatosis (CYLD) (153). CYLD interacts with the membrane bound complex via TRAF2 and removes K63- and M1-linked polyubiquitin chains from RIPK1 thereby dismantling the polyubiquitin scaffold for TAB2/3-TAK1 and NEMO-IKKα/β necessary for their recruitment and subsequent activation (149, 154-157).

In addition to the late NF-κB dependent checkpoint, a second NF-κB independent checkpoint regulating TNFR1 signaling exists (158). The two cell death checkpoints function sequentially in the TNFR1 pathway, and the second checkpoint has thus been termed the early NF-κB

independent cell death checkpoint (110, 159, 160) (Figure 1.6). The off- switch of this early checkpoint are dependent on the non-degradative ubiquitylation of RIPK1, as demonstrated by depletion of cIAP1/2, mutating the ubiquitin acceptor site K377 of RIPK1 or the deletion of NEMO (158, 161, 162).

Recent evidence have however demonstrated that there are additional modifications of RIPK1 repressing its enzymatic activity and enhancing the early checkpoint (163). This was demonstrated by the fact that inactivation of both cIAP1/2 and TAK1 triggered apoptosis, but that inhibition of TAK1 induced cell death without altering the ubiquitylation of RIPK1(164, 165). IKKα/β have subsequently been identified to phosphorylate the serine 25 residue of ubiquitylated RIPK1 to further suppress its cytotoxic capacity (166, 167). In other words, the early checkpoint inactivates RIPK1 via a two-step mechanism that depends firstly on the ubiquitylation and secondly on the phosphorylation of RIPK1(163). This checkpoint are additionally strengthened in a positive feedback loop by the expression pro-survival factors of the late NF-κB-dependent checkpoint such as cIAP1/2 (168).

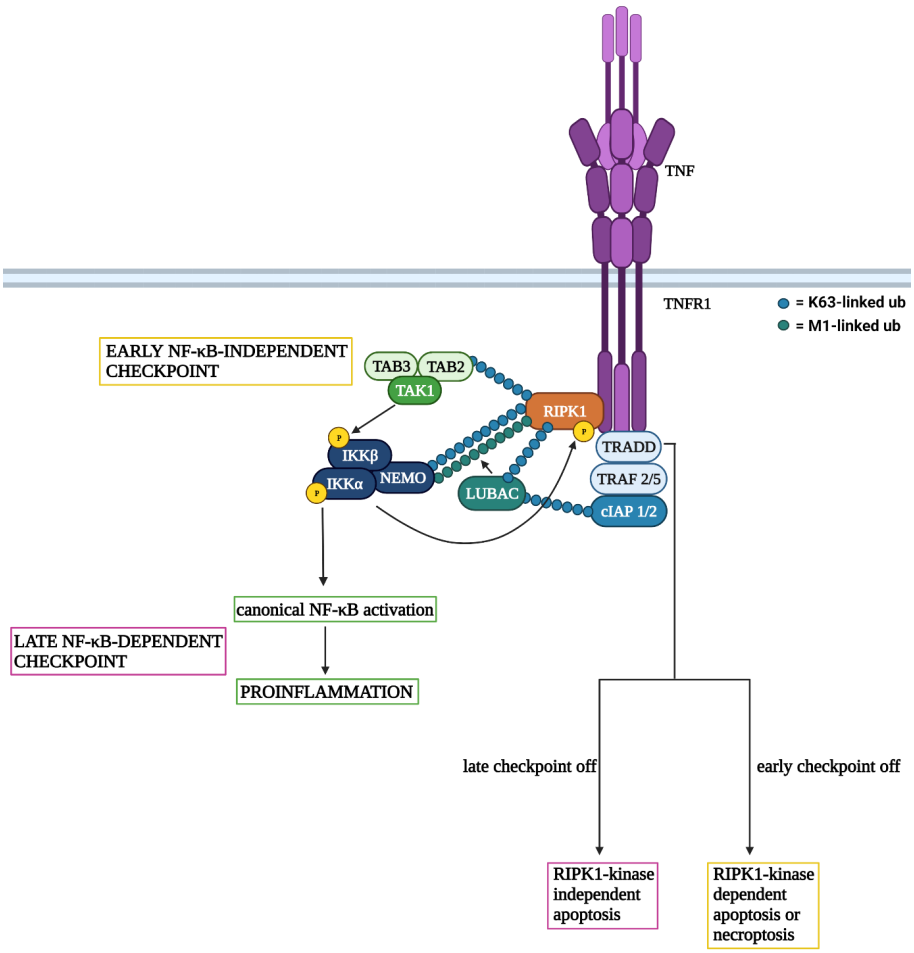

Figure 1.6 The early and late cell death checkpoints in the TNFR1 pathway. The early NF-κB independent cell death checkpoint is initiated by the ubiquitylation of RIPK1 by the E3 ligases including cIAP1/2. Ubiquitylated RIPK1 in turn recruits TAB2/3-TAK1 and NEMO-IKKα/β and the subsequent activation of IKKα/β. IKKα/β subsequently phosphorylates RIPK1 which restricts RIPK1 to form death-inducing complexes. Active IKKα/β additionally results in activation of NF-κB and pro-survival molecules which serves as the late cell death checkpoint. Inhibition of NF-κB signaling turns off this late checkpoint and results in the induction of RIPK1-kinase independent apoptosis. Blocking the early checkpoint by for instance cIAP1/2 depletion in turn induces RIPK1-kinase dependent apoptosis or necroptosis. Modified from (100, 110). The figure is created with biorender.com.

1.4.2. Caspase 8-dependent apoptosis

Apoptosis is a non-inflammatory form of programmed cell death. It is a natural process in the body during development and aging, and a mechanism to control homeostasis of cell populations in different tissues (169). Apoptosis is also important in the resolution of acute inflammatory responses through clearance of immune cells, and it is the immunoregulatory function of apoptosis that is the focus of this thesis (170). An apoptotic cell exhibit plasma membrane blebbing, cytoplasmic shrinkage, nuclear fragmentation and chromatin condensation (171, 172). This leads to the formation of small vesicles named apoptotic bodies that are phagocytosed and degraded by macrophages and neighboring cells (169).

Apoptosis can be extrinsically and intrinsically triggered. While intrinsic apoptosis is induced by intracellular stressors like DNA damage, nutrient deprivation and free radicals, the extrinsic apoptosis cascade is activated by cell-surface receptors. Both pathways are dependent on activation of caspases. Caspases are a family of cysteine proteases that cleave proteins at aspartic acid residues and regulate apoptosis and inflammatory processes (169). Mammalian caspases are categorized into apoptotic initiators (caspase-2, -8, -9, -10), apoptotic executioners (caspase-3, -6, -7) and inflammatory caspases (caspase-1, -4, -5, -11, -12) (173). Of note, caspase-4 and caspase-5 are only present in humans, and caspase-11 is the murine ortholog of caspase-4 (174, 175).

Upon apoptotic activation, monomers of initiator caspases are activated when their death-effector domains (DEDs) interacts with DEDs or CARDs on adaptor proteins of both the intrinsic and extrinsic pathway (114). This interaction results in the dimerization of the initiator pro-caspases that facilitates autocatalytic cleavage into one large and small subunit, resulting in its activation (175). Active initiator caspases subsequently activate executioner caspases by mediating their cleavage and conformational rearrangement, and the induction of apoptosis.

Extrinsic apoptosis is initiated by several receptor-ligand complexes, and the pathway was first defined by studying the first apoptosis signal (FAS) receptor (CD95) and its ligand FASL. Other complexes include TNF-related apoptosis-inducing ligand (TRAIL)-TRAIL receptor (TRAILR), TNF-TNFR1 as well as LPS-TLR4 (176, 177). While disruption of both the late and early cell death checkpoint sensitizes the cells to TNF-induced cell death, the mode of cell death induced are different in the two scenarios (Figure 1.6). Extrinsic apoptosis through TNF-TNFR1 can be initiated when the induced expression of pro-survival molecules by NF-κB, the

late cell death checkpoint, is inhibited and RIPK1 subsequently dissociates from the membrane bound complex. RIPK1 is released into the cytosol in a deubiquitylated state, mediated by CYLD and A20 (Figure 1.7). Deubiquitylated RIPK1 subsequently interacts with TRADD, FAS-associated death domain protein (FADD) and pro-caspase 8, making up a cytosolic death complex (177). Complex formation is in this scenario independent of the kinase activity of RIPK1 and have also been termed complex IIa (177, 178). Importantly, RIPK1-dependent apoptosis can also be RIPK1-kinase dependent. This can occur when the early NF-κB independent cell death checkpoint is disrupted such as depletion of cIAP1/2, either by genetical deletion or chemical inhibition. Non-ubiquitylated RIPK1 forms a complex with FADD, RIPK3, and pro-caspase 8 which has been named complex IIb, and complex formation is here RIPK1-kinase dependent (161, 164, 179) (Figure 1.7).

Caspase 8 is the key enzyme controlling extrinsic apoptosis. Its catalytic activity is additionally critical for embryonic development in mice as both *CASP8* null and *CASP8* catalytically dead mutations are embryonically lethal (180-182). Caspase 8 interacts with FADD through its DED which prompts the recruitment of additional caspase 8 molecules resulting in filament formation (183). This caspase 8 filament enables the proteolytic domains of the pro-caspase 8 molecules to homodimerize (184). The homodimerization of pro-caspase 8 results in the autoproteolytic cleavage between the large and small catalytic subunit (p10), generating p10, p41 and p43 fragments (185). The p41/p43 fragments are subsequently cleaved leading to the release of the large catalytic p18 subunit. Catalytically active caspase 8 consists of two p18 and two p10 subunits. Active caspase 8 subsequently cleaves the executioner caspase 3 and -7, providing the link between complex formation and the initiation of apoptosis (185, 186). In addition to its major role in apoptosis, caspase 8 also functions as a molecular switch in necroptosis and pyroptosis. Although RIPK1 initiates the assembly of the apoptotic complex, it must be inactivated to prevent the induction of caspase-independent cell death. This is mediated by caspase 8 which cleaves and inactivates RIPK1 and RIPK3, thereby inhibiting necroptosis (100). The role of caspase 8 in pyroptosis will be described in chapter 1.4.4.

As previously mentioned, a key regulator of caspase 8 activity is cFLIP. cFLIP is encoded by the NF-κB regulated gene *CFLAR* which is alternatively spliced into several isoforms, including cFLIP long ($cFLIP_L$), cFLIP short ($cFLIP_S$), and cFLIP Raji ($cFLIP_R$) (187-189). The best described isoform is $cFLIP_L$, primarily known as an anti-apoptotic regulator. As for caspase 8, the cFLIP structure contains DEDs and this structural similarity makes it able to

inhibit apoptosis, either through competitive binding to FADD or by forming heterodimers with caspase 8 thereby mitigating enzymatic activity (190-192) (Figure 1.7). In addition to preventing apoptosis, $cFLIP_L$ is also a regulator of necroptosis. The caspase 8-$cFLIP_L$ heterodimers retain their enzymatic activity and are thus able to cleave RIPK1 and RIPK3 thereby blocking necroptosis (193, 194). In contrast, the caspase 8-$cFLIP_S$ heterodimers lack this enzymatic activity and increased expression of $cFLIP_S$ over $cFLIP_L$ promotes necroptosis as the kinase activity of RIPK1 and RIPK3 are preserved (193).

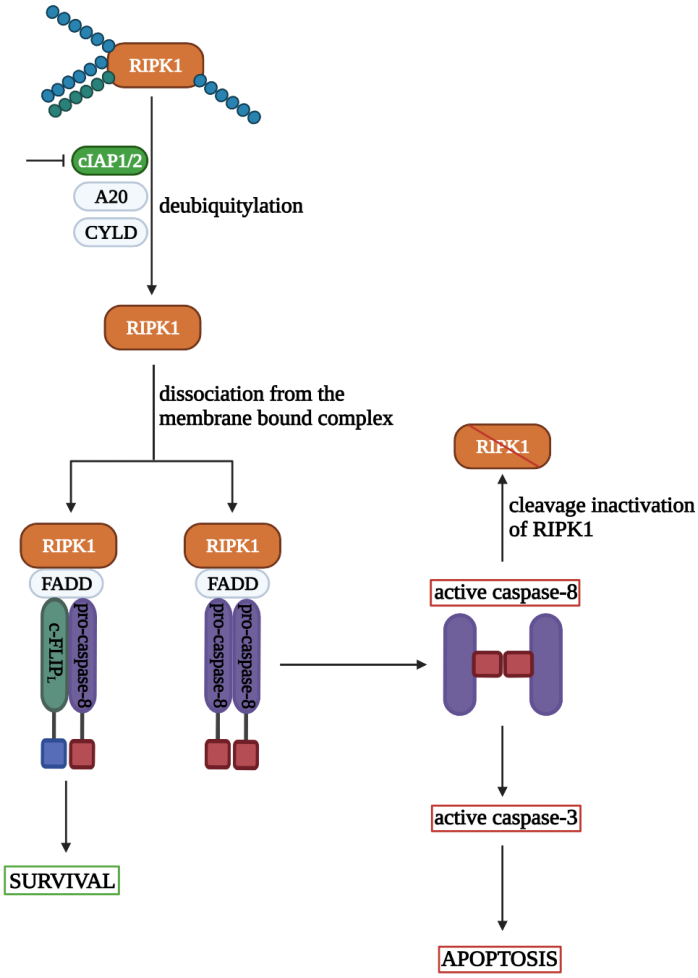

Figure 1.7 RIPK1-dependent apoptosis. Deubiquitylation of RIPK1 is mediated either by deubiquitylating enzymes like A20 or CYLD, or by inhibiting ubiquitin ligases like cIAP1/2 and TRAF2. This leads to the

dissociation of RIPK1 from the membrane bound receptor complex. In the cytosol, RIPK1 interacts with FADD and pro-caspase 8. Active caspase 8 is generated by the pro-caspase 8 homodimer. Pro-caspase 8 additionally forms heterodimers with $FLIP_L$ which promote cell survival by blocking caspase 8 activity. To prevent caspase-independent cell death, RIPK1 must be cleaved and thus inactivated either by fully activated caspase 8 or the pro-caspase 8 - $FLIP_L$ heterodimer. Modified from (100). The figure is created with biorender.com

1.4.3. RIPK1-dependent necroptosis

Necroptosis is a programmed form of necrotic cell death. In contrast to apoptosis, necroptosis is pro-inflammatory, lytic and independent of caspase activity (195, 196). It is characterized by swelling of cell organelles and loss of membrane integrity resulting in cell rupture (172). This causes spilling of cellular content like DAMPs such as ATP and high mobility group box 1 (HMGB1) and inflammatory cytokines into the extracellular space inducing inflammatory responses and cell death (171, 197, 198).

Necroptosis can be initiated through several receptors including CD95, TNFR1, TLR4 and Z-DNA binding protein 1 (ZBP1, also known as DAI) (89, 171, 199). TNF-TNFR1 signaling induces necroptosis in a context where RIPK1 is de- or non-ubiquitylated and caspase 8 is chemically or genetically inactivated (194, 196). Initiation of necroptosis relies on the kinase activities of RIPK1 and RIPK3 which is sustained as the caspase 8 mediated cleavage is inhibited (89, 200). RIPK3 is indispensable for necroptosis and RIPK1 recruits and activates numerous RIPK3 molecules through a mechanism involving interactions between their RHIM domains and the kinase activity of RIPK1(200-202). This is followed by a series of trans-phosphorylation or auto-phosphorylation events on serine residues on RIPK1 and RIPK3, resulting in the formation of an amyloid complex named the necrosome (Figure 1.7) (171, 200).

Assembly of the necrosome and phosphorylation of RIPK3 leads to the subsequent recruitment and phosphorylation of mixed lineage kinase domain like pseudokinase (MLKL) (Figure 1.8) (100, 203). MLKL is an indispensable substrate for RIPK3 for induction of necroptosis. Even though the pseudokinase domain of MLKL binds to ATP, it is catalytically inactive, and it is the RIPK3-mediated phosphorylation of MLKL that is essential for downstream signaling (204). Phosphorylated MLKL form oligomers that translocate to the plasma membrane through binding to membrane lipids (205-207). Oligomerized MLKL punctures the membrane by forming pores, leading to influx of ions and water resulting in permeabilization, release of DAMPs and inflammatory cytokines and necroptosis (Figure 1.8) (171).

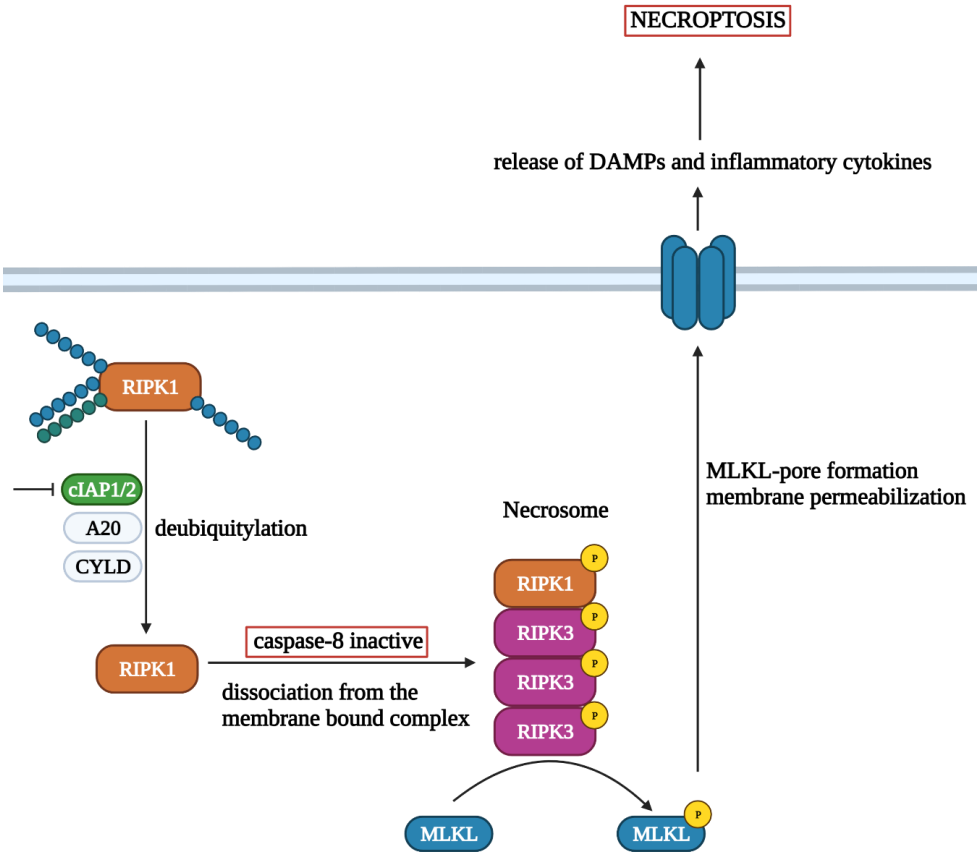

Figure 1.8 RIPK1-dependent necroptosis. The necrosome is formed upon the deubiquitylation and release of RIPK1 from the membrane bound complex when caspase 8 activity is reduced or blocked. RIPK1 recruit numerous RIPK3 where both is activated upon trans- and auto-phosphorylation. Subsequent activation of MLKL through phosphorylation induces pore formation, membrane permeabilization and necroptosis. Modified from (100). The figure is created by biorender.com.

1.4.4. The inflammasome and pyroptosis

Pyroptosis is a highly inflammatory mode of lytic cell death that is triggered upon microbial infections or stress. A pyroptotic cell is characterized by DNA fragmentation, swelling and leakage of cellular content (208). In contrast to necroptosis, pyroptosis is caspase-dependent and activated through the inflammasome. The inflammasome is a multimeric protein complex comprised of a sensor, adaptor, and effector protein. The sensor initiates the assembly of the inflammasome complex upon sensing of DAMPs or PAMPs and based on their structural

features are grouped into nucleotide-binding domain-line receptors (NLRs), absent in melanoma 2-like receptors (ALRs) and pyrins (209). Most inflammasomes require an adaptor known as apoptosis-associated speck-like protein containing CARD (ASC). As the name implies, the CARD domain of ASC recruits the effector, the inflammatory caspase-1,-11, -4 or -5 (210).

The best characterized NLR is NLR pyrin 3 (NLRP3) and inflammasome activation requires two steps, priming and activation (211). Priming is initiated when PAMPs or DAMPs activate PRRs such as LPS binding to TLR4, and result in transcriptional expression of pro-inflammatory mediators like pro-IL-1β and NLRP3. Necroptosis-induced membrane permeabilization can also function as an activation signal for the NLRP3 inflammasome (209, 212). Activation is the inflammasome-forming step initiated by DAMPs and PAMPS and result in the autoproteolytic cleavage and activation of caspase 1. Active caspase 1 then goes on to cleave pro-IL-1β into its mature form. Caspase 1 additionally cleaves gasdermin D (GSDMD) and the N-terminal p30 subunit of GSDMD translocate to the membrane and induce pore formation by binding to phospholipids. The GSDMD pore permeabilize the plasma membrane leading to release of IL-1β and efflux of ions, inducing pyroptosis (Figure 1.9) (213, 214).

Caspase 8 is primarily described as an apoptotic initiator caspase, but recent studies have demonstrated that it can also function as an inflammatory caspase in pyroptosis (Figure 1.9). Caspase 8 has been shown to trigger the NLRP3 inflammasome and might also function as an alternative mechanism when caspase 1 is inhibited (215-217). Activated caspase 8 have additionally been demonstrated to cleave pro-IL-1β and GSDMD which leads to the maturation of IL-1β and the induction of both pyroptosis and apoptosis (91, 218). Caspase 8 can additionally cleave and activate pro-caspase 1 and -3 (219, 220). Active caspase 3 is also able to cleave GSDMD, but to a p43 form that inhibits the N-terminal GSDMD thereby restraining pyroptosis (220).

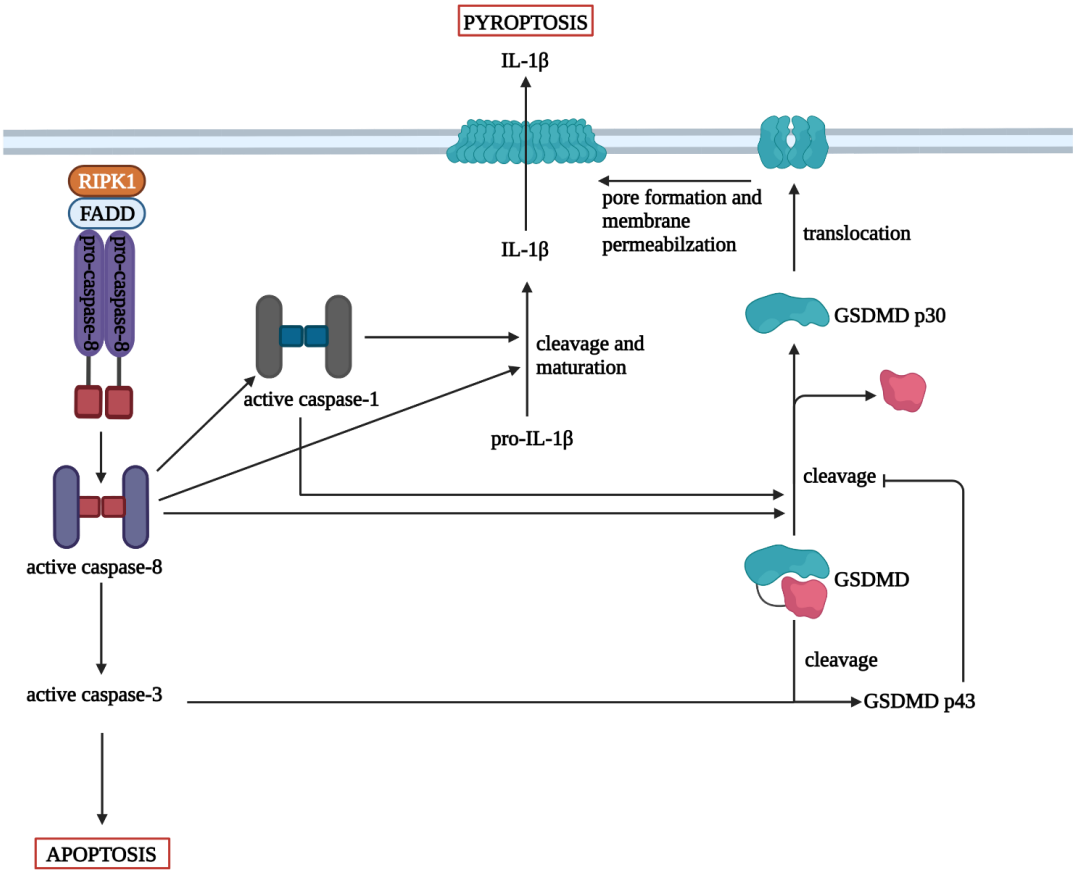

Figure 1.9 Caspase 8 mediated pyroptosis. Catalytically active caspase 8 cleaves and activates caspase 3 and in certain cases caspase 1. GSDMD and pro-IL-1β can be cleaved by caspase 8 either directly or indirectly via caspase 1. Cleavage of GSDMD results in the translocation of the p30 form to the plasma membrane and subsequent pore formation and permeabilization of the membrane. This induces pyroptosis and release of mature IL-1β through the GSDMD p30 pores. Active caspase 3 results in cleavage of GSDMD p43 and inhibits the cleavage to the p30 form thereby restraining pyroptosis. Modified from (208, 220). The figure is created with biorender.com.

1.5. Pharmaceutical targeting of the RIPK1 pathway

1.5.1. Inhibiting RIPK1-dependent cell death

As RIPK1 function as a switch between inflammation and cell death it has emerged as an attractive therapeutic target (221). Several RIPK1 kinase inhibitors have been developed and include the small molecule drug necrostatin-1s (Nec-1s) that has been extensively used to investigate the role of RIPK1 both in animal models for human diseases and mechanistic studies (89, 222, 223). RIPK1 inhibitors were primarily considered as an alternative to anti-TNF therapies in autoimmune diseases. However, they offer several advantages such as being safe in the nervous system and targeting a broader array of inflammatory activities since RIPK1 is not only restricted to TNF-signaling (223, 224). Other inhibitors targeting excessive RIPK1-dependent cell death have also been thoroughly studied and include drugs inhibiting MLKL and RIPK3 (195, 203, 225, 226). This includes necrosulfonamide (NSA) that blocks MLKL polymer formation and GSK872 that inhibits RIPK3 kinase activity (203, 227, 228). Pharmaceutical targeting of RIPK1, RIPK3 and MLKL and *in vivo* studies, such as knock-in mice that express catalytically inactive RIPK1, have established the importance of RIPK1-dependent cell death in a wide array of diseases. This includes as ischemia-reperfusion injury and several neurodegenerative, autoimmune and inflammatory pathologies (88, 89, 222, 223, 229-231).

1.5.2. Smac-mimetics

cIAPs regulate inflammation and cell death though their ubiquitin E3 ligase activity of RIPK1 (232). They are overexpressed in many cancers, suppress apoptosis and increase drug-resistance of tumor cells, and they are associated with poor prognosis (233-235). In addition, patients expressing high levels of Smac, the natural antagonist of cIAPs, has higher remission rates and longer overall survival (236) The development of IAP-inhibitors (also termed smac-mimetics, SM) have therefore gained attention as novel treatment strategies in cancer and chronic inflammatory diseases (100, 161, 237). Several SM are currently undergoing phase II clinical trials for solid and hematological cancers (235, 238). Smac binds the BIR domains of IAPs via its IBM motif (115). The IBM motif is formed by the four N-terminus amino acid residues known as the AVPI segment. As the name implies, SM mimic this AVPI segment of Smac, and are thus able to bind to the BIR domains of cIAP1/2 and XIAP (115). As previously described, loss of IAP activity induces cell death through a dual mechanism. SM-treatment

results in stabilization of NIK, NF-κB2 activation and production of TNF (232). Blocking of cIAP-activity by SM will additionally result in non-ubiquitinated RIPK1, thus turning off the early NF-κB independent cell death checkpoint. Autocrine TNF stimulation of the deubiquitylated RIPK1 complex ultimately results in the induction of programmed cell death (58, 100). However, SM-treatment have been demonstrated to induce cytokine release syndrome, a systemic inflammatory response caused by a rapid and vast release of inflammatory cytokines characterized by fever, headaches, and nausea (239).

1.5.3. TAK1-inhibitors

TAK1 is an important part of the pro-inflammatory node of the RIPK1-pathway through its activation of NF-κB and MAPKs (75). NF-κB and MAPK signaling are implicated in the pathogenesis of several inflammatory processes. By being a key mediator of these pathways, TAK1 has been proposed as a potential therapeutic target in treatment of inflammatory diseases like rheumatoid arthritis and inflammatory bowel disease (240-242). In addition, dysregulation NF- κB and MAPKs are implicated in several cancers. Due to this and its role in developing chemo resistance, TAK1-inhibitors are also a potential anti-tumor therapy (243). Treatment with TAK1-inhibitors shuts of the RIPK1-dependent pro-survival NF-κB and MAPK pathways and induce cell death in several types of cancer (244, 245). In some cases, TAK1-inhibitors must be simultaneously combined with other stimulants to induce tumor cell death. This includes combination with cytokines such as TNF and TGF-β or in the presence of chemotherapy which activates TAK1 due to genotoxic stress (246).

1.6. Multiple myeloma

Multiple myeloma (MM) is the second most common hematological malignancy worldwide. It is an incurable cancer characterized by malignant transformation of clonal plasma cells within the BM often accompanied by secretion of monoclonal immunoglobulins (247). Many myeloma patients suffer from hypercalcemia, renal failure, anemia and bone disease, commonly referred to as CRAB (247-249). There are about 500 (506 in 2019) new cases reported in Norway each year, with a higher prevalence in men (incidence rate 10.8 per 100 000 per year) than women (incidence rate 7.0) (250). Minimal residual disease (MRD) is an important reason as to why MM remain an incurable malignancy. MRD is a term used to describe the small number of tumor cells that remain in the BM after treatment and are the

major cause of relapse (251). MRD is caused by intrinsic cancer cell drug resistance, and microenvironmental factors such as nutrients from bone degradation, and an inflammatory environment. The degree of MRD varies with the amount of remaining cells and increasing cell numbers decrease time of progression-free survival. An intense treatment regime is used to minimize MRD in order to prolong time to relapse, but this put serious strain on patients, a problem that has increased as patients live longer with the disease (252).

In most cases, MM is preceded by a pre-malignant state of plasma cell proliferation (253). This pre-malignant state is characterized as either monoclonal gammopathy of undetermined significance (MGUS) or smoldering multiple myeloma (SMM) depending on the degree of plasma cell infiltration in the BM and concentration of tumor-secreted monoclonal immunoglobulins (254). In addition, changes in the BM microenvironment and genetic and epigenetic alterations of normal plasma cells are important factors in the development and progression of MM (255, 256). The criteria for diagnosis of MM revised by the International Myeloma Working Group are the presence of ≥ 10% of clonal plasma cell in the BM and the presence of minimum one myeloma defining event (257). A myeloma defining event is either meeting the CRAB criteria or one or more biomarkers of malignancy.

Many myeloma cells have constitutive activation of NF-κB and MAPK signaling pathways, and over 80% of MM patients have elevated NF-κB target gene expression (258). NF-κB and MAPK makes the tumor cells more tolerant to cytotoxic stress such as genomic instability, reactive oxygen species and accumulation of misfolded proteins such as immunoglobulins (259). They induce transcription of intracellular survival factors, and secreted inflammatory cytokines such as IL-6, and IL-8, that create a low-grade inflammation that further contributes to cell survival. In addition, constitutive activation of NF-κB promotes OC differentiation promoting the clinical manifestation of myeloma bone disease (MBD) (260, 261).

1.6.1. Myeloma bone disease

MBD is a severe complication of MM affecting about 80% of patients (47). MBD is defined as the major cause of pain, reducing the quality of life of patients due to bone fractures and hypercalcemia. In normal bone remodeling, there is a tightly regulated balance between OB deposition and OC resorption of the bone. OC and OB reciprocally regulate each other's differentiation, recruitment, and activity through cytokine-mediated signaling and cell-cell contact. In MBD however, there is a pathological increase in OC and reduction in OB activity

compromising bone homeostasis as osteolytic bone-destruction is not followed by reactive formation of new bone (47). The shift in OB-OC homeostasis makes MBD distinctively different than other cancers that metastasize to bone like breast and prostate cancer, were OC-mediated bone-destruction is followed by OB-mediated bone-formation (262).

There is a multitude of factors that promote osteoclastogenesis or suppress OB activity and formation. They are secreted by MM cells or other cells in the BM microenvironment (Figure 1.10). MM cells secrete OC activating factors (OAFs) like RANKL and TNF and induce stromal cells to secrete osteoclastogenic factors like CSF-1 and IL-6 (263). OC also reversely stimulate MM cells by secreting tumor-promoting factors (264). MM cells also influence OB and stromal cells to decrease the production of OC inhibitory factors like OPG (265). OB activation is reduced by MM cell-induced production of OB inhibitory factors (OBIFs) either directly or via other cells in the BM microenvironment. This complex interplay between MM cells and other cells in the BM creates a vicious cycle of uncontrolled bone-degradation resulting in the release of growth factors and nutrients promoting tumor growth, survival and drug resistance (266, 267).

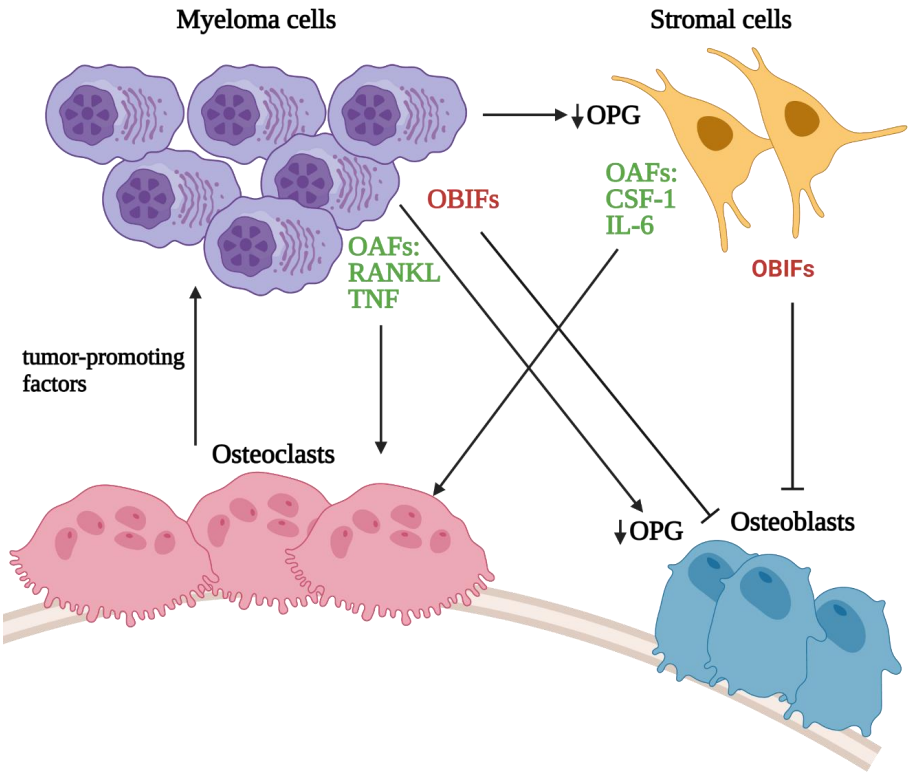

Figure 1.10 Mechanism of multiple myeloma induced bone lesions. MM cells induce a shift in bone homeostasis by the secretion OAFs and OBIFs either directly or via cells in the BM microenvironment like stromal cells. This results in increased osteoclastogenesis, reduced osteoblast activity and tumor-promotion. OAFs, OC activating factors; OBIFs, OB inhibiting factors. Modified from (263). The figure is created with biorender.com.

1.6.2. Current treatment strategies of MM

Although the overall survival has increased in the recent years, MM is still an incurable disease. The first line of therapy for patients are autologous stem cell transplantation (ASCT) (268). ASCT involves collecting the patient's own stem cells and reinserting them after high dose chemotherapy with or without radiation therapy with the goal to restore the body's own ability to produce normal blood cells. Patients are treated with combinations of different drugs like steroids, immunomodulatory agents, monoclonal antibodies, proteasome inhibitors and alkylators (248). In addition, bisphosphonates and the monoclonal antibody denosumab that mimics OPG are used in treatment for MBD (49, 269, 270). Of note, the previously described SM are currently undergoing clinical trials in treatment of MM (238).

Alkylators are DNA-damaging agents used in treatment of several cancers, including MM. They were the first effective group of drugs used in MM treatment, and therapy with the alkylator melphalan and the steroid prednisone was the standard for newly diagnosed patients for over 40 years (271, 272). Today, one of the options for first line of therapy in MM are high dose melphalan therapy in combination with ASCT (273, 274). Several other alkylators are also used in MM treatment including cyclophosphamide that have a similar mechanism of action as melphalan (274). Alkylators induce DNA damage by adding alkyl groups to DNA bases inducing mutagenic and cytotoxic lesions. Bifunctional alkylators like melphalan contain two reactive groups that bind different DNA bases forming interstrand crosslinks (275). Alkylator-induced DNA-damage activate several signaling pathways, including TAK1 as described previously.

2 Aims of study

The main aim of this thesis was to contribute to a better understanding of pharmaceutical induction of RIPK1-dependent cell death in human macrophage systems. Much of the mechanistic insights on regulated cell death originate from pathogen experiments on murine immune cells such as macrophages. As cell death is context dependent and differently regulated in humans and mice, more insight into how RIPK1-dependent cell death can be drug-induced in human macrophages are needed. To ensure efficacy and avoid detrimental side effects, knowledge on context-specific drug responses are necessary. Based on this, we chose to study a broad repertoire of human macrophage subtypes including osteoclasts and pro- and anti-inflammatory macrophages.

SM and TAK1-inhibitors are extensively studied inducers of RIPK1-dependent cell death, but studies on primary human osteoclasts and other macrophage subtypes have been limited. SM are currently in phase II clinical trials in MM, and as osteoclasts are a major contributor to the disease pathology we sought to investigate if SM holds therapeutic potential in reducing bone disease as well. Preliminary studies in our group found that TAK1-inhibitors were cytotoxic to osteoclasts and MM cells. As the literature states that TAK1 is necessary for osteoclastogenesis and can be a driver of MM, this focus was included in this thesis.

In order to contribute to a better insight on how pharmaceutically induced RIPK1-dependent is regulated in human macrophage systems, our specific aims were as follow:

1. Investigate the effect of SM-treatment on human osteoclasts and the possible beneficial role in multiple myeloma therapy. This was the topic of paper I.

2. Study the effect of pro- and anti-inflammatory pretreatment on SM-induced cell death in human macrophages. This was the focus of paper II.

3. Investigate the effect of TAK1-inhibitor treatment on MM cells both alone and in combination treatment with DNA-damaging agents, and the possible double beneficial role on human osteoclasts. This was the topic of paper III.

3 Summary of papers

Paper I: **Smac-mimetics reduce numbers and viability of human osteoclasts**

The bone is continuously degraded and rebuilt, and the process involves the activity of bone-degrading osteoclasts (OC) and bone-forming osteoblasts. A pathological increase in OC activity contributes to bone-resorption in diseases such as myeloma bone disease (MBD), a hallmark of multiple myeloma (MM). Several proinflammatory cytokines promote osteoclastogenesis, including TNF. Receptor-interacting protein kinase 1 (RIPK1) is a key regulator of inflammation and cell death and is recruited to the TNFR1-complex where it is ubiquitinated and activates NF-κB and MAPK signaling. RIPK1-dependent signaling can be targeted by treatment with Smac-mimetics (SM) that block ubiquitination of RIPK1 and shifts signaling towards cell death. SM has gained attention as novel treatment strategies for both cancer and chronic inflammatory pathologies, but limited information exists on the effect on human OC.

In this paper, our aim was to investigate the effect of SM-treatment on human OC and the possible beneficial role in MM therapy. As LCL-161 is in phase 2 clinical studies for MM, we proposed that SM might possess additional benefits in reducing bone degradation in myeloma patients. We found that the SM birinapant and LCL-161 reduced the number and viability of primary human OC and induced TNF-dependent cell death in osteoclast precursors. We demonstrated that birinapant was more cytotoxic than LCL-161 and induced apoptosis and necroptosis, the latter independent of blocking caspase activity. Both inhibitors blocked osteoclastogenesis induced by myeloma patient bone-marrow aspirates. Taken together, we here show that SM restrain human osteoclastogenesis, and that these compounds may represent promising drug candidates for reducing pathological bone degradation.

Paper II: **Pro- and anti-inflammatory treatment dictates Smac-mimetic cytotoxicity in human macrophages**

Macrophages are a heterogenous group of multifunctional immune cells of the monocytic lineage. They are key players in the innate immune response against pathogen infection as well as in tissue homeostasis, clearing of apoptotic cells and wound healing. The expression of anti-apoptotic proteins like cellular inhibitor of apoptosis proteins (cIAPs) maintain macrophage survival. IAPs are ubiquitin ligases and key regulators of receptor-interacting protein kinase 1 (RIPK1)-dependent signaling induced by TNFR1- and TLR4-signaling. Smac-mimetics (SM) are a group of drugs targeting cIAPs, shifting macrophages from inflammation to RIPK1-dependent apoptosis or necroptosis. SM are novel therapeutic options in both cancer like multiple myeloma and chronic diseases such as psoriasis and inflammatory bowel disease, but the effect on different human macrophage subtypes is limited.

Our aim in this paper was to study the effect of pro- and anti-inflammatory pretreatment on SM-induced cell death in human macrophage types. We found that pro- and anti-inflammatory pretreatment dictated the SM-induced death mechanism and sensitivity of human macrophages. Macrophages pretreated with LPS were more susceptible to cell death induced by the SM birinapant and LCL-161, compared to other tested macrophage types and monocytes. This was caused by a specific increase in apoptosis while the other tested macrophage types depended on the necroptotic machinery for full birinapant cytotoxicity. This was demonstrated to be a SM-specific effect as we did not observe an up-regulation of the apoptotic machinery in pro-inflammatory macrophages. Apoptosis induced by birinapant in LPS pretreated macrophages was followed by the secretion of IL-1β independent of caspase 1, whereas IL-1β release was not observed in the subtypes displaying necroptosis. Our findings suggest that treatment with SM is a therapeutic potential in disease settings where upregulation of pro-inflammatory macrophages is involved.

Paper III: **TAK1-inhibitors are cytotoxic for multiple myeloma cells alone and in combination with melphalan**

Multiple myeloma (MM) is the second most common hematological malignancy worldwide. It is an incurable cancer characterized by malignant transformation of clonal plasma cells within the bone marrow often accompanied by secretion of monoclonal immunoglobulins. TGF-β-activated kinase 1 (TAK1) is an important regulator of NF-κB and MAPK signaling. In MM, NF-κB and MAPK are often constitutively activated and control the expression of several genes vital for driving the drug resistance in MM. In cells where TAK1 is activated, it is an attractive drug target as inhibition switches pro-inflammatory signaling towards cell death.

In this paper, our aim was to investigate the effect of TAK1-inhibitor treatment on MM cells both alone and in combination treatment with DNA-damaging agents, and the possible double beneficial role on human osteoclasts. We found that patients with high *TAK1* expression displayed shorter overall and progression free survival. The TAK1-inhibitors NG25 and 5Z-7-oxozeaenol (5Z-7) were demonstrated to be cytotoxic to both MM cell lines and patient cells. NG25 reduced the expression of MYC and E2F controlled genes which are involved in tumor growth, cell cycle progression and drug resistance. Genotoxic stress is known to activate TAK1. We found that the alkylator melphalan, used in high-dose therapy in MM, activated TAK1 in MM cells. NG25 and 5Z-7 induced both synergistic and additive cytotoxicity in combination with melphalan.

Myeloma bone disease is a hallmark of MM and is connected to poor prognosis and pain in patients. NG25 and 5Z-7 reduced number and viability of human bone degrading osteoclasts independent on their antitumor effect. This suggests that TAK1-inhibition can have a double beneficial effect in treatment of MM. In sum, we here presented *in vitro* data showing that TAK1 is a promising drug target for MM treatment.

4 Discussion

The RIPK1-pathway is a key regulator of inflammation and cell death and a central player in the immune system (86, 222). Regulated cell death has been extensively studied in murine immune cells like macrophages. However, as cell death is context dependent and differently regulated in humans and mice, more insight on drug-induced cell death in human macrophage systems are needed. As macrophages adopt to a variety of environmental stimuli it is necessary to investigate context specific drug responses to understand how cell death is regulated and how these cells can be targeted in human pathologies. Consequently, our aim in this thesis was to contribute to a better understanding of pharmaceutical induction of RIPK1-dependent cell death in human macrophage systems.

SM and TAK1-inhibitors are well studied inducers of RIPK1-dependent cell, but studies featuring SM on primary human OC and other macrophage types have been warranted (100, 237). SM are being investigated as novel treatment options in MM and as OC are a driver of myeloma-induced bone disease, we proposed a potential therapeutic benefit. Preliminary studies in our group found that TAK1-inhibitors were cytotoxic to OC and MM cells and as literature states that TAK1 is necessary for osteoclastogenesis and can be a driver of MM, this focus was included.

In this thesis we had three specific aims, and the first objective in **paper I** was to investigate the effect of SM-treatment on human OC. Secondly, we wanted to study the effect of SM on pro- and anti-inflammatory pretreated human macrophages. This was the focus of **paper II**. Lastly in **paper III,** we sought to investigate the effect of TAK1-inhibitor treatment on MM cells both alone and in combination with DNA-damaging agents, and the possible double beneficial role on human osteoclasts.

4.1. Differential response to SM on macrophage subtypes and implications in inflammatory disease settings

SM are small molecule drugs targeting cIAPs. They are overexpressed in several tumors and are currently undergoing clinical trials in solid and hematological cancers (114, 235, 238). As the expression and abundance of cIAPs are also increased in several chronic inflammatory conditions like psoriasis and inflammatory bowel disease, SM might be a therapeutic option in such settings as well (276, 277). In this thesis, we exploited the effect of pharmaceutical targeting of cIAPs by SM in human OC (**paper I**) and pro- and anti-inflammatory macrophage (**paper II**) systems. Treatment with the SM birinapant and LCL-161 induced cell death across

all subtypes independent of additional cytokine stimuli. Birinapant was more potent than LCL-161, an effect that was conserved across all subtypes. This difference might be explained by the nature of mono- and bivalent SM. LCL-161 is a monovalent SM that contain one AVPI segment, while bivalent SM like birinapant has two such motifs. Bivalent SM thus have higher binding affinities to cIAPs and result in higher potency and possibly increased efficiency in preclinical models (235, 237). One must however consider that bivalent SM might cause on-target toxicities. On the other hand, birinapant has been well tolerated in phase I clinical studies (233). Previous studies have established that SM induce cell death through autocrine TNF-signaling (179, 278). Consistent with this, we demonstrated in **paper I** that inhibiting TNF blocked SM-induced cell death in human pre-OC. We did not observe induction of *TNF* transcription after SM-treatment but rather detected constitutive low levels of TNF in the medium. This indicates that SM exploits human OC own production of TNF to induce its pharmaceutical effect, and that low TNF-levels might be sufficient. This could be beneficial in TNF-driven hyperinflammatory disease settings like rheumatoid arthritis, where OC dysregulation is part of the pathogenesis (279). However, we found that TNF was only partly involved in SM-induced inhibition of osteoclastogenesis. This warrants caution in combining SM with TNF-blocking antibodies as a treatment strategy for inflammatory diseases.

Recruited pro-inflammatory macrophages are involved in several chronic autoimmune and inflammatory diseases such as rheumatoid arthritis and atherosclerosis (14, 280). In **paper II**, we identified that pro-inflammatory macrophages were considerably more susceptible to SM-induced cell death compared to the other tested macrophage types. SM might thus be a treatment rationale in disease settings with inflammatory upregulation of pro-inflammatory macrophages. One must however consider that downregulation of inflammation can cause severe side effects as susceptibility to infections as shown for anti-TNF therapy, as a “just right” inflammatory response is necessary for proper immune function (281). We additionally demonstrated in **paper II** that LPS pretreated macrophages (M(LPS)) were substantially more inclined to SM-induced cell death than those pretreated with TNF and blocking TNF did not restrain cell death in M(LPS). Thus, the rationale of targeting these cells in chronic inflammatory settings like rheumatoid arthritis could be limited. However, this might be more beneficial in pathogen-induced inflammatory sepsis and cytokine storm.

4.2. SM and TAK1-inhibitors reduce human OC activity

MBD is a severe complication of MM associated with poor prognosis and pain in patients (47). Bisphosphonates are an established treatment option in MBD but display side effects as severe

musculoskeletal pain and upper gastrointestinal symptoms (282). This underlines the need for safer and more effective therapies targeting OC activity in MBD-patients. LCL-161 is currently undergoing phase II clinical trials as treatment of MM (235, 238, 239). Our hypothesis in **paper I** was that SM might have a beneficial role in reducing pathological bone degradation in addition to its antitumorigenic property in MM. We found that SM restrained osteoclastogenesis and shifted human OC to cell death. In addition, SM efficiently blocked myeloma BM aspirate-driven osteoclastogenesis. Treatment with SM could therefore have a beneficial effect in MM by reducing MBD in patients. Studies done by Zhou *et al.* further underlines that the SM birinapant could be a potential MM drug (283). They found a synergistic effect of co-treatment of birinapant with the proteasome inhibitor bortezomib through inactivation of NF-κB signaling and induction of caspase 8-dependent apoptosis. As they demonstrate that caspase 8-dependent cell death can be triggered in MM this is also consistent with our findings in **paper III.**

In **paper III** we demonstrated that the TAK1-inhibitors NG25 and 5Z-7-oxozeaneol (5Z-7) blocked osteoclastogenesis, suggesting a beneficial treatment rationale in MM patients by potentially limiting MBD. By comparing the effect of SM (**paper I**) and TAK1-inhibitors (**paper III**) on pre-OC it is evident that targeting different components of the RIPK1-pathway might possess distinctive implications in MM-treatment. While SM did not affect MM cell viability, TAK1-inhibitors were cytotoxic to both myeloma cells and OC. Previous studies found that biallelic inactivation of cIAP1 and cIAP2 affects around 15% of MM patients included in the COMMpass data set (284). In contrast, Chesi *et al.* showed that LCL-161 induced anti-myeloma activity in relapsed refractory MM patients (238). Interestingly, the anti-myeloma effect was accomplished through an inflammatory type I IFN response activating macrophages and DCs to phagocytose tumor cells, and not a direct effect on the tumor cells. As we in **paper II** suggested that anti-inflammatory macrophages, such as TAMs, might be less sensitive to SM this could be another positive effect in treatment of MM. In sum, both SM and TAK1-inhibitors show promising results as agents blocking OC activity, underlining the importance of RIPK1-mediated pro-inflammatory signaling in OC survival and differentiation.

4.3. SM-treatment display RIPK1-dependent cell death plasticity

Previous studies have demonstrated that SM primarily sensitize cells to apoptosis and that necroptosis is only obtained upon caspase inhibition or depletion (233, 239, 285). In **paper I** we found that birinapant induced apoptosis in pre-OC but also necroptosis in some donors. We detected cleaved forms of caspase 8 and -3 as well as phosphorylated RIPK1 and RIPK3

suggesting that both the apoptotic and necroptotic machinery were functional, and that necroptosis could be activated without caspase 8 inhibition. In addition, pre-OC were only rescued from SM-induced cell death when subjected to both caspase and MLKL or RIPK1 kinase inhibition. This is an exciting finding as we here show that SM can induce necroptosis in a setting where apoptosis also can be activated. It is unclear how this happens mechanistically, but physiological examples of necroptosis exist in several contexts.

Necroptosis has been described as a back-up death mechanism when apoptosis is defective. It is an important anti-viral response in combatting the virus-mediated inhibition of apoptosis and promoting an innate immune response through the release of inflammatory mediators (202, 286-288). Knockout of *CASP3* and *CASP8* are respectively perinatal and embryonical lethal in mice (289). Interestingly, necroptosis-resistant mice carrying *RIPK1* kinase dead knock-in, or *RIPK3* or *MLKL* knockout mutations are viable and display no developmental defects (95, 290-293). In addition, necroptosis is identified as a contributor to pathology in several human diseases such as neurodegenerative disorders like multiple sclerosis and Alzheimer's disease, hyperinflammatory settings like sepsis, and ischemia-reperfusion injury (222, 294-296). In sum, the literature presents that necroptosis might be predominantly activated in pathological conditions, but our studies in **paper I** demonstrate that inhibitor-treatment is able to spontaneously activate necroptosis. This underlines its importance besides being an alternative cell death pathway upon apoptotic inhibition.

In **paper II** we showed that SM-induced sensitivity and death mechanism were dictated by pro- and anti-inflammatory pretreatment in human macrophages. M(LPS) were considerably more susceptible to SM-induced cell death compared to the other tested macrophage types and monocytes. This was caused by a potentiation of apoptosis in M(LPS). We detected cleaved caspase 8 and -3 while MLKL and RIPK1 kinase inhibition did not rescue birinapant-induced cell death. In contrast, the other tested macrophage types depended on the necroptotic machinery for full birinapant cytotoxicity as cell death was restrained when subjected to MLKL or RIPK1 kinase inhibition. Other studies have showed that anti-inflammatory macrophages are prone to necroptosis upon TAK1-inhibitor and SM treatment, but here following combination with the pan-caspase inhibitor zVAD (198, 297). Combination with zVAD did not affect birinapant cytotoxicity in M(LPS) but rather displayed an increase in phosphorylated RIPK1 as well as blocking caspase cleavage. This demonstrates that the necroptotic machinery is functional in M(LPS) and that they can be re-directed to necroptosis upon caspase inhibition.

Interestingly, a newly published paper by Huang *et al.* showed that caspase inhibition prolongs inflammation in response to LPS by promoting a signaling complex with RIPK1 where activated RIPK1 promotes its own scaffold function to regulate NF-κB-mediated proinflammatory signaling (298). SM-treated M(LPS) also induced IL-1β release but as this was found to be independent of caspase 1 and as the pore-forming GSDMD p30 form were not detected, this indicates no involvement of pyroptosis. Sagulenko *et al.* and Ørning *et al.* have demonstrated that caspase 8 is able to cleave IL-1β and this might be the case in our system as well (91, 218). We did however not determine if IL-1β existed in the pro- or cleaved form. LPS treatment of macrophages has been demonstrated to transcriptionally upregulate IL-1β production (299). One hypothesis could be that LPS-induced IL-1β is only released by membrane rupture mediated by secondary necrosis occurring after initial apoptosis (300, 301).

How macrophage subtypes are wired towards different cell death modes upon SM-treatment is an interesting further perspective. In the project related to **paper I** we performed a mass spectrometry study but no general re-wiring of the proteome regarding up-regulation of necroptotic factors in OC were found (data not shown). Other factors that could contribute to necroptosis in OC are increased levels of calcium and reactive oxygen species during osteoclastogenesis that has been found to trigger the phosphorylation of RIPK1 through the JNK pathway (302-304). In addition, recent studies by Yang *et al.* proposed that caspase 8 mediated blockade of necroptosis is eliminated *in vivo* by p90 ribosomal S6 kinase (RSK) which phosphorylates pro-caspase 8 thereby bypassing necroptotic inhibition (305). In **paper II**, our MS study did not reveal a general up- or down-regulation of apoptotic or necroptotic proteins between Mϕ and M(LPS+IFN-γ) that could explain the potentiation of apoptosis in pro-inflammatory macrophages. In addition, we showed that other cell death inducers did not yield the same cell death pattern, suggesting SM-specific effects rather than a general re-wiring of the cell death machinery. Lastly, the gain-of-apoptosis in M(LPS) was correlated with increased $cFLIP_L$ and $cFLIP_S$ protein levels, contrary to the literature that states that $cFLIP_L$-caspase 8 block apoptosis and $cFLIP_S$ promote necroptosis (100). Taken together our findings in **paper II** are surprising given a model where caspase 8 activity dictates cell death outcomes. This suggest that caspase 8 can be specifically restrained in human macrophages, and that proinflammatory stimuli in combination with SM releases caspase 8 activity, resulting in a more potent cell death response.

Importantly, our results demonstrating that treatment with SM induce cell death in human OC and macrophages are in line with existing literature describing that treatment with SM disrupt the early NF-κB independent cell death checkpoint in the TNFR1 signaling pathway (161, 179, 306). However, recent evidence demonstrates that the ubiquitylation of RIPK1 by cIAP1/2 only repress RIPK1 indirectly. The inhibition of RIPK1 kinase-dependent cell death requires a two-step mechanism where the ubiquitylation of RIPK1 is a prerequisite for the IKKα/β-mediated phosphorylation of RIPK1 (166). How this phosphorylation restricts cell death is unclear and theories include the prevention of RIPK1 to dissociate from the membrane bound complex, alteration of its enzymatic activity or influencing binding of RIPK1 to the cytosolic death inducing complexes (110). In the case of cIAP1/2 depletion, the NF-κB2 kinase NIK has been demonstrated to phosphorylate RIPK1 which in contrast to IKKα/β-mediated phosphorylation of RIPK1 mediates the assembly of complex IIb (307). In **paper I** and **paper II,** we observed apoptosis in the situation of SM-treatment this indicates induction of RIPK1-kinase dependent apoptosis (complex IIb). Of note, as cIAP1/2 is a NF-κB inducible pro-survival molecule cIAP1/2 depletion can result in RIPK1 kinase-independent apoptosis (complex IIa) as well. In sum, further investigation on the SM-induced modifications on RIPK1 are necessary to further understand how cell death is induced in this context in human OC and macrophages.

Our observation that SM can induce both apoptosis and necroptosis in human macrophage systems is an exciting finding as it demonstrates that these cells can shift between different cell death modes when required. This is consistent with a proposed concept of cell death plasticity by Malireddi *et al.* named PANoptosis (pyro-apo-necroptosis) (308, 309). They established that there is extensive crosstalk between the death pathways and proposed that a complex of apoptotic, necroptotic and pyroptotic components regulate cell death in a different manner than previously believed (310). In an autoinflammatory setting in mice it has been demonstrated that combined deletion of *RIPK3*, *CASP1* and *CASP8* rescued the mice from osteomyelitis while inhibition of a single cell death arm was not sufficient (311, 312). Interestingly, recent research has demonstrated that PANoptosis can be induced in SARS-CoV-2 infection upon inflammatory stimuli (313). As they found that PANoptosis mediated by inflammatory cytokines are a key driver of pathology, SM might not be a potential treatment option for COVID-19 patients. However, it might be more complicated as our MS data in **paper II** suggests that SM-treatment targets macrophages involved in COVID-19. Another paper by Malireddi *et al.* found that LPS priming of TAK1-deficient macrophages induced a RIPK1 kinase independent complex inducing caspase 8-dependent apoptosis and NRLP3-driven

pyroptosis (308). They additionally found fully functional RIPK1 kinase activity that induced necroptosis independent of this apoptotic-pyroptotic complex. This underlines the complexity that exists in our research interest of RIPK1-dependent cell death and a more comprehensive understanding of this regulation in our systems is a desired aim in further investigation.

4.4. Targeting the RIPK1-pathway in human versus mice systems

The consequence of treatment with SM on mice systems have been extensively studied, but the effect on human OC and other macrophage systems are less described. In **paper I** we found species-specific differences in the response to SM treatment in human and mouse OC. While SM efficiently reduced human OCt numbers and viability, low doses increased this in murine OC. In addition, a considerably higher SM-concentration was needed to restrain osteoclastogenesis murine OC compared to humans. The fact that SM are able to increase OC numbers have been confirmed by others, supporting our findings (314, 315).

For further studies it would be interesting to investigate if there are species-specific differences in response to SM treatment in other macrophage types as well. Recent studies by Ali *et al*. showed a similar effect between mice and human macrophages when treated with LCL-161. In contrast, Lawlor *et al*. demonstrated that birinapant treatment in LPS pretreated murine macrophages does not induce a high degree of cell death, no IL-1β production, and that a change in sensitivity is only obtained when knocking out *XIAP* (210, 316). Their experimental setup is comparable to ours in **paper II,** but as it contradicts our findings it might indicate that the SM-response is different in mouse and human macrophage systems.

Lamothe *et al.* have demonstrated that TAK1 is a key factor in regulating OC activity and osteoclastogenesis in mice (50, 83). Consistent with this, we demonstrated in **paper III** that the TAK1-inhibitors NG25 and 5Z-7 blocked osteoclastogenesis and were cytotoxic to human pre-OC at higher doses. Collectively, the results in this thesis demonstrate that there are species-specific differences in response to SM between mouse and human OC, but that the response to TAK1-inhibitors might be more comparable. In other words, targeting different components in the RIPK1-pathway might possess differences in how translational the effect is from mice to human systems. As our results is only from *in vitro* human OC systems, the response to SM in human *in vivo* systems might display significant differences. This warrants caution in future clinical trials of SM-based therapy with respect to effect on OC activity.

4.5. Pharmacological inhibitors versus genetic approach in inhibiting TAK1

In **paper III**, we used a pharmacological approach with the TAK1-inhibitors NG25 and 5Z-7. The use of inhibitors versus genetic approaches such as CRISPR-Cas9 and knockout mice is an interesting discussion where both approaches have their advantages and limitations. On one side, genetic approaches potentially remove all transcripts of the gene of interest giving a permanent and stable knockdown. Inhibitors on the other hand bind and inhibit the protein directly but the protein remains present. This can have important implications as the protein may lack certain activity but might still interact with some binding partners or assemble into macromolecular complexes.

An important factor when deciding between a genetic approach or pharmacological inhibition is the purpose of the research project in question. If the goal is to decipher the biological function of a gene such as *TAK1*, CRISPR-Cas9 or knockout models would be appropriate. In **paper III**, we wanted to study the effect of TAK1-inhibition on MM cells both alone and in combination with alkylating agents which are well-established myeloma drugs. As we here focused on the potential of TAK1-inhibitors for clinical use i.e. its drugability and thus the effect of the inhibitors rather than the effect of the enzyme, a pharmacological approach was chosen.

Well-known challenges with pharmacological inhibitors are the possibilities of off-targets effects, unspecific dose-effects, or resistance. 5Z-7 has been demonstrated to exhibit inhibitory activity against other kinases than TAK1 i.e. causing off-target effects, but importantly shows specific inhibition of the TAK1-pathway in hematological cancer cells (317). Of note, even though genetic approaches such as CRISPR-Cas9 have been proven to be much more specific and thus safer than inhibitors, off-target modifications can still be a possible challenge (318). However, it is very unlikely that different approaches for inhibiting the function of a protein exhibits similar off-target effects. Thus, the strongest argument for describing the cellular or physiological role of a protein such as TAK1 is to demonstrate similar effects across different approaches, such as pharmacological inhibition and genetic knockout.

4.6. TAK1-inhibitors and SM as possible treatment options in MM

NF-κB and MAPK signaling regulate immune- and oncological survival and induce the expression of genes involved in MRD and drug resistance in MM (319). TAK1 is a key activator of NF-κB and MAPK and our analysis of data from the MMRF CoMMpass study in

paper III revealed that MM patients with high expression of *TAK1* had decreased overall and progression free survival. Based on this, we hypothesized that targeting TAK1 could be a promising therapeutic option in MM. We found that the TAK1-inhibitors NG25 and 5Z-7 were cytotoxic to both myeloma cell lines and patient samples. We additionally demonstrated that TAK1-inhibitors had an additional antitumorigenic effect through blocking osteoclastogenesis and could thus limit MBD in patients. These findings are supported by previous work and has highlighted the novelty of TAK1-inhibitors as possible MM drugs as they could potentially be used in combination with existing treatment options and target the interaction between MM cells and the surrounding microenvironment (320, 321).

The inhibition of TAK1 has been demonstrated to shut off the early NF-κB independent cell death checkpoint and consequently induce RIPK1 kinase-dependent apoptosis without influencing the ubiquitylation of RIPK1 (164). This has been shown to be due to an IKKα/β-induced inhibiting phosphorylation of RIPK1 on serine 25 (166, 167). However, the role of TAK1 in repressing RIPK1 cytotoxicity has been proven to be even more complex. TAK1 are also involved in the activation of the p38 MAPK pathway and recent publications has demonstrated that the p38-substrate MK2 additionally phosphorylate RIPK1 to restrict cell death (322-324). In the case of TAK1-inhibition, further studies on the cytotoxicity on the myeloma cells and OC should be performed to provide a broader understanding of the mode of cell death induced including the NF-κB independent regulation of RIPK1 cytotoxicity by TAK1.

The alkylators melphalan and cyclophosphamide are used in high-dose therapy of MM patients, but are associated with side effects and development of drug resistance (325). As genotoxic stress induces TAK1-signaling we proposed that TAK1-inhibitors would render MM cells more sensitive to melphalan. In **paper III** we demonstrated that combination with TAK1-inhibitors decreased the IC50 of melphalan in MM cells. Thus, this combination might be a beneficial treatment option by lowering the doses of DNA-damaging drugs possibly reducing side effects, drug resistance and MRD. However, this assumes that TAK1-inhibitor treatment displays minimal side effects and needs further investigation. An interesting future objective of the use of alkylators in anti-cancer treatment was proposed by Sriram *et al*. which found that DNA-damaged tumor cells can work as an adjuvant in anti-tumor immunity as an alternative to immune checkpoint therapy (326). They showed that cells injured by DNA-damaging agents induced strong DC-dependent T-cell priming and expansion. In **paper III** we also demonstrated that TAK1-inhibition induced caspase-dependent apoptosis. Further

investigation on the involvement of other cell death pathways are however needed. A newly published paper by Han *et al*. showed that radiation therapy activates the inflammasome and that IL-1β production is necessary for the anti-tumor activity of immune cells (327). An interesting future aspect is thus if therapy-induced DNA-damage promote a similar beneficial inflammatory effect.

In sum, the studies in this thesis demonstrates that pharmaceutical targeting of the RIPK1-pathway by SM induce apoptosis and necroptosis in human macrophage subtypes. As SM and TAK1-inhibitors restrained osteoclastogenesis and shifted OC to cell death, treatment could potentially limit MBD in MM-patients. In **paper I** we showed that SM blocks osteoclastogenesis and induce TNF-dependent cytotoxicity through both apoptosis and necroptosis in human OC. SM-treatment additionally dampened MM-driven osteoclastogenesis, indicating a possible beneficial role in reducing MBD in patients. In, **paper II** we found that SM-treatment affect macrophages differently depending on pro- or anti-inflammatory pretreatment. Pro-inflammatory treatment potentiated SM-induced apoptosis in human macrophages which could be useful in pathologies where inflammatory over-activation of macrophages is a challenge. In **paper III** we demonstrated that TAK1-inhibitors induce cytotoxicity in MM cells and OC. TAK1-inhibitors also potentiated the cytotoxicity of the DNA-damaging drug melphalan, suggesting a beneficial combination in MM treatment. We additionally demonstrated that TAK1-inhibitors blocked osteoclastogenesis, and treatment could thus have a beneficial antitumorigenic effect by reducing MBD in MM patients.

5 Future perspectives

In the studies presented in this thesis we have focused on how pharmaceutical targeting of the RIPK1-pahthway induce cell death in human macrophage systems and a possible therapeutic option in MM. In **paper I** we found that treatment with SM blocked osteoclastogenesis and induced cytotoxicity in human OC and that treatment with SM might possess an additional benefit in MM by reducing bone degradation. **Paper II** focused on that pro- and anti-inflammatory pretreatment dictated SM-induced cell death in human macrophages. In **paper III** we demonstrated that TAK1-inhibitors were cytotoxic to MM and patient cells and reduced differentiation and viability of human OC.

The immediate perspectives in the continuation of these studies is understand how macrophage subtypes are wired towards different cell death modes upon SM-treatment. For future studies it could be interesting to perform RNA-seq and MS analysis to determine which inflammatory genes are expressed in the different subtypes and up-regulated during cell-death stimuli. Immunoprecipitation and confocal microscopy studies could be used to identify which components are involved in initiation and execution of cell death in the different subtypes. In addition, it would be interesting to determine the inflammatory profile of necroptosis upon SM-treatment by analyzing the secretome by MS for DAMPs, and multiplex analysis for inflammatory cytokines.

In this thesis we studied pharmaceutical targeting of IAPs through treatment with SM. For future studies it would be interesting to study other bivalent SM to deduce if the observed cell death potency is a birinapant- or bivalent SM-specific effect. Another future perspective would be to perform Crispr-Cas9 or siRNA studies of cIAP1 and cIAP2 in human primary macrophages to determine whether they have specific functions in determining cell death outcomes.

As we demonstrated that treatment with SM and TAK1-inhibitors blocked osteoclastogenesis and induced cytotoxicity in human OC, we proposed a possible beneficial role in treatment of MM. Further studies on the effect on bone resorption activity should be performed to conclude with this. It would also be interesting to co-culture MM cells and OC to get a better understanding of the interplay between these cells upon SM- and TAK1-inhibitor-treatment.

6 Conclusions

RIPK1-dependent cell death regulates inflammation and homeostasis in macrophage systems. Several drugs including Smac-mimetics and TAK1-inhibitors have been extensively studied in chronic diseases and cancers, but the effect on human primary OC and other macrophage subtypes have been limited. Further studies are necessary to investigate context-specific drug responses to ensure effectiveness and avoid adverse side effects.

The three studies presented in this thesis are focused on pharmaceutical targeting of RIPK1-signaling by SM and TAK1-inhibitors in human macrophage systems and their therapeutic potential in MM. In this thesis we demonstrated that treatment with SM and TAK1-inhibitors blocks osteoclastogenesis and induce cytotoxicity in human OC. SM-treatment induced both RIPK1 kinase dependent and caspase dependent cell death through necroptosis and apoptosis, consistent with the concept of cell death plasticity. SM-treatment also dampened MM-driven osteoclastogenesis which might possess an additional benefit by reducing MBD in patients. We also demonstrated that SM-treatment affects macrophages differently depending on pro- or anti-inflammatory pretreatment. Pro-inflammatory treatment potentiated SM-induced apoptosis in human macrophages accompanied by IL-1β release. Taken together, our findings suggest that SM holds therapeutic potential in disease setting were upregulation of pro-inflammatory macrophages is involved. Lastly, we demonstrated that TAK1-inhibitors induce cytotoxicity in MM cells and OC. TAK1-inhibitors also potentiated the cytotoxicity of the DNA-damaging drug melphalan, suggesting a beneficial combination in MM treatment. TAK1-inhibitors were also shown to block osteoclastogenesis, which could have a beneficial antitumorigenic effect by reducing bone disease in patients.

Altogether, this work contributes to the understanding of pharmaceutical targeting of RIPK1-signaling in human macrophage systems and as potential therapy candidates for treatment of inflammatory conditions and cancers such as multiple myeloma.

7 References

1. Italiani P, Boraschi D. From Monocytes to M1/M2 Macrophages: Phenotypical vs. Functional Differentiation. Frontiers in Immunology. 2014;5(514).
2. Sprangers S, de Vries TJ, Everts V. Monocyte Heterogeneity: Consequences for Monocyte-Derived Immune Cells. J Immunol Res. 2016;2016:1475435.
3. Hettinger J, Richards DM, Hansson J, Barra MM, Joschko AC, Krijgsveld J, et al. Origin of monocytes and macrophages in a committed progenitor. Nat Immunol. 2013;14(8):821-30.
4. Auffray C, Fogg DK, Narni-Mancinelli E, Senechal B, Trouillet C, Saederup N, et al. CX3CR1+ CD115+ CD135+ common macrophage/DC precursors and the role of CX3CR1 in their response to inflammation. J Exp Med. 2009;206(3):595-606.
5. Akashi K, Traver D, Miyamoto T, Weissman IL. A clonogenic common myeloid progenitor that gives rise to all myeloid lineages. Nature. 2000;404(6774):193-7.
6. Schütt C, Schumann R. [The endotoxin receptor CD14]. Immun Infekt. 1993;21(2):36-40.
7. Yeap WH, Wong KL, Shimasaki N, Teo ECY, Quek JKS, Yong HX, et al. CD16 is indispensable for antibody-dependent cellular cytotoxicity by human monocytes. Scientific Reports. 2016;6(1):34310.
8. Ginhoux F, Jung S. Monocytes and macrophages: developmental pathways and tissue homeostasis. Nature Reviews Immunology. 2014;14(6):392-404.
9. Shi C, Pamer EG. Monocyte recruitment during infection and inflammation. Nature Reviews Immunology. 2011;11(11):762-74.
10. Chistiakov DA, Myasoedova VA, Revin VV, Orekhov AN, Bobryshev YV. The impact of interferon-regulatory factors to macrophage differentiation and polarization into M1 and M2. Immunobiology. 2018;223(1):101-11.
11. Lin W, Xu D, Austin CD, Caplazi P, Senger K, Sun Y, et al. Function of CSF1 and IL34 in Macrophage Homeostasis, Inflammation, and Cancer. Frontiers in Immunology. 2019;10(2019).
12. Liu YC, Zou XB, Chai YF, Yao YM. Macrophage polarization in inflammatory diseases. Int J Biol Sci. 2014;10(5):520-9.
13. Cho KJ, Roche P. Regulation of MHC Class II-Peptide Complex Expression by Ubiquitination. Frontiers in Immunology. 2013;4(369).
14. Shapouri-Moghaddam A, Mohammadian S, Vazini H, Taghadosi M, Esmaeili SA, Mardani F, et al. Macrophage plasticity, polarization, and function in health and disease. J Cell Physiol. 2018;233(9):6425-40.
15. Amit I, Winter DR, Jung S. The role of the local environment and epigenetics in shaping macrophage identity and their effect on tissue homeostasis. Nat Immunol. 2016;17(1):18-25.
16. Jenkins SJ, Ruckerl D, Cook PC, Jones LH, Finkelman FD, van Rooijen N, et al. Local macrophage proliferation, rather than recruitment from the blood, is a signature of TH2 inflammation. Science. 2011;332(6035):1284-8.
17. Jones CV, Ricardo SD. Macrophages and CSF-1: implications for development and beyond. Organogenesis. 2013;9(4):249-60.
18. Dai XM, Ryan GR, Hapel AJ, Dominguez MG, Russell RG, Kapp S, et al. Targeted disruption of the mouse colony-stimulating factor 1 receptor gene results in osteopetrosis, mononuclear phagocyte deficiency, increased primitive progenitor cell frequencies, and reproductive defects. Blood. 2002;99(1):111-20.

19. Pollard JW, Stanley ER. Pleiotropic Roles for CSF-1 in Development Defined by the Mouse Mutation Osteopetrotic. In: Wassarman PM, editor. Advances in Developmental Biochemistry. 4: Academic Press; 1996. p. 153-93.
20. Isidro RA, Appleyard CB. Colonic macrophage polarization in homeostasis, inflammation, and cancer. Am J Physiol Gastrointest Liver Physiol. 2016;311(1):G59-73.
21. Murray PJ, Allen JE, Biswas SK, Fisher EA, Gilroy DW, Goerdt S, et al. Macrophage activation and polarization: nomenclature and experimental guidelines. Immunity. 2014;41(1):14-20.
22. Hume DA. The Many Alternative Faces of Macrophage Activation. Front Immunol. 2015;6:370.
23. Vidyarthi A, Khan N, Agnihotri T, Negi S, Das DK, Aqdas M, et al. TLR-3 Stimulation Skews M2 Macrophages to M1 Through IFN-αβ Signaling and Restricts Tumor Progression. Frontiers in Immunology. 2018;9(1650).
24. Wang N, Liang H, Zen K. Molecular Mechanisms That Influence the Macrophage M1–M2 Polarization Balance. Frontiers in Immunology. 2014;5(614).
25. Labonte AC, Tosello-Trampont AC, Hahn YS. The role of macrophage polarization in infectious and inflammatory diseases. Mol Cells. 2014;37(4):275-85.
26. Murray PJ, Wynn TA. Protective and pathogenic functions of macrophage subsets. Nat Rev Immunol. 2011;11(11):723-37.
27. Rosas M, Davies LC, Giles PJ, Liao CT, Kharfan B, Stone TC, et al. The transcription factor Gata6 links tissue macrophage phenotype and proliferative renewal. Science. 2014;344(6184):645-8.
28. Arpaia N, Green JA, Moltedo B, Arvey A, Hemmers S, Yuan S, et al. A Distinct Function of Regulatory T Cells in Tissue Protection. Cell. 2015;162(5):1078-89.
29. Kotwal GJ, Chien S. Macrophage Differentiation in Normal and Accelerated Wound Healing. Results Probl Cell Differ. 2017;62:353-64.
30. Edholm ES, Rhoo KH, Robert J. Evolutionary Aspects of Macrophages Polarization. Results Probl Cell Differ. 2017;62:3-22.
31. Rhee I. Diverse macrophages polarization in tumor microenvironment. Arch Pharm Res. 2016;39(11):1588-96.
32. Van Dyken SJ, Locksley RM. Interleukin-4- and interleukin-13-mediated alternatively activated macrophages: roles in homeostasis and disease. Annu Rev Immunol. 2013;31:317-43.
33. Pan XQ. The mechanism of the anticancer function of M1 macrophages and their use in the clinic. Chin J Cancer. 2012;31(12):557-63.
34. Lin Y, Xu J, Lan H. Tumor-associated macrophages in tumor metastasis: biological roles and clinical therapeutic applications. Journal of Hematology & Oncology. 2019;12(1):76.
35. Galdiero MR, Garlanda C, Jaillon S, Marone G, Mantovani A. Tumor associated macrophages and neutrophils in tumor progression. J Cell Physiol. 2013;228(7):1404-12.
36. Sica A, Larghi P, Mancino A, Rubino L, Porta C, Totaro MG, et al. Macrophage polarization in tumour progression. Semin Cancer Biol. 2008;18(5):349-55.
37. EC GOL. M2-like macrophages and tumor-associated macrophages: overlapping and distinguishing properties en route to a safe therapeutic potential. Integr Cancer Sci Therap. 2016;3.
38. Georgoudaki AM, Prokopec KE, Boura VF, Hellqvist E, Sohn S, Östling J, et al. Reprogramming Tumor-Associated Macrophages by Antibody Targeting Inhibits Cancer Progression and Metastasis. Cell Rep. 2016;15(9):2000-11.

39. Lee Y, Biswas SK. Rewiring macrophages for anti-tumour immunity. Nature Cell Biology. 2016;18(7):718-20.
40. Gutiérrez-González A, Martínez-Moreno M, Samaniego R, Arellano-Sánchez N, Salinas-Muñoz L, Relloso M, et al. Evaluation of the potential therapeutic benefits of macrophage reprogramming in multiple myeloma. Blood. 2016;128(18):2241-52.
41. Sommerfeldt DW, Rubin CT. Biology of bone and how it orchestrates the form and function of the skeleton. Eur Spine J. 2001;10 Suppl 2(Suppl 2):S86-95.
42. Florencio-Silva R, Sasso GR, Sasso-Cerri E, Simões MJ, Cerri PS. Biology of Bone Tissue: Structure, Function, and Factors That Influence Bone Cells. Biomed Res Int. 2015;2015:421746.
43. Touaitahuata H, Blangy A, Vives V. Modulation of osteoclast differentiation and bone resorption by Rho GTPases. Small GTPases. 2014;5:e28119.
44. Teitelbaum SL. Bone resorption by osteoclasts. Science. 2000;289(5484):1504-8.
45. Cappellen D, Luong-Nguyen NH, Bongiovanni S, Grenet O, Wanke C, Susa M. Transcriptional program of mouse osteoclast differentiation governed by the macrophage colony-stimulating factor and the ligand for the receptor activator of NFkappa B. J Biol Chem. 2002;277(24):21971-82.
46. Sugatani T, Vacher J, Hruska KA. A microRNA expression signature of osteoclastogenesis. Blood. 2011;117(13):3648-57.
47. Hameed A, Brady JJ, Dowling P, Clynes M, O'Gorman P. Bone disease in multiple myeloma: pathophysiology and management. Cancer Growth Metastasis. 2014;7:33-42.
48. Feng X. RANKing intracellular signaling in osteoclasts. IUBMB Life. 2005;57(6):389-95.
49. Lacey DL, Boyle WJ, Simonet WS, Kostenuik PJ, Dougall WC, Sullivan JK, et al. Bench to bedside: elucidation of the OPG-RANK-RANKL pathway and the development of denosumab. Nat Rev Drug Discov. 2012;11(5):401-19.
50. Lamothe B, Lai Y, Xie M, Schneider MD, Darnay BG. TAK1 is essential for osteoclast differentiation and is an important modulator of cell death by apoptosis and necroptosis. Mol Cell Biol. 2013;33(3):582-95.
51. Tanaka S, Nakamura K, Takahasi N, Suda T. Role of RANKL in physiological and pathological bone resorption and therapeutics targeting the RANKL-RANK signaling system. Immunol Rev. 2005;208:30-49.
52. Ginaldi L, De Martinis M. Osteoimmunology and Beyond. Curr Med Chem. 2016;23(33):3754-74.
53. Del Fattore A, Teti A, Rucci N. Osteoclast receptors and signaling. Arch Biochem Biophys. 2008;473(2):147-60.
54. Itonaga I, Sabokbar A, Sun SG, Kudo O, Danks L, Ferguson D, et al. Transforming growth factor-beta induces osteoclast formation in the absence of RANKL. Bone. 2004;34(1):57-64.
55. Abu-Amer Y. NF-κB signaling and bone resorption. Osteoporos Int. 2013;24(9):2377-86.
56. Kim JH, Kim N. Regulation of NFATc1 in Osteoclast Differentiation. J Bone Metab. 2014;21(4):233-41.
57. Baron R. Molecular mechanisms of bone resorption by the osteoclast. Anat Rec. 1989;224(2):317-24.
58. Boyce BF, Xiu Y, Li J, Xing L, Yao Z. NF-κB-Mediated Regulation of Osteoclastogenesis. Endocrinol Metab (Seoul). 2015;30(1):35-44.
59. Pahl HL. Activators and target genes of Rel/NF-κB transcription factors. Oncogene. 1999;18(49):6853-66.
60. Sun SC. Non-canonical NF-κB signaling pathway. Cell Res. 2011;21(1):71-85.

61. Liu T, Zhang L, Joo D, Sun SC. NF-κB signaling in inflammation. Signal Transduct Target Ther. 2017;2:17023-.
62. Hayden MS, Ghosh S. Shared principles in NF-kappaB signaling. Cell. 2008;132(3):344-62.
63. Vallabhapurapu S, Karin M. Regulation and function of NF-kappaB transcription factors in the immune system. Annu Rev Immunol. 2009;27:693-733.
64. Taniguchi K, Karin M. NF-κB, inflammation, immunity and cancer: coming of age. Nature Reviews Immunology. 2018;18(5):309-24.
65. Hoffmann A, Baltimore D. Circuitry of nuclear factor kappaB signaling. Immunol Rev. 2006;210:171-86.
66. Sun SC. The non-canonical NF-κB pathway in immunity and inflammation. Nat Rev Immunol. 2017;17(9):545-58.
67. Zarnegar BJ, Wang Y, Mahoney DJ, Dempsey PW, Cheung HH, He J, et al. Noncanonical NF-kappaB activation requires coordinated assembly of a regulatory complex of the adaptors cIAP1, cIAP2, TRAF2 and TRAF3 and the kinase NIK. Nat Immunol. 2008;9(12):1371-8.
68. Zhang W, Liu HT. MAPK signal pathways in the regulation of cell proliferation in mammalian cells. Cell Research. 2002;12(1):9-18.
69. Huangfu WC, Omori E, Akira S, Matsumoto K, Ninomiya-Tsuji J. Osmotic stress activates the TAK1-JNK pathway while blocking TAK1-mediated NF-kappaB activation: TAO2 regulates TAK1 pathways. J Biol Chem. 2006;281(39):28802-10.
70. Mihaly SR, Ninomiya-Tsuji J, Morioka S. TAK1 control of cell death. Cell Death Differ. 2014;21(11):1667-76.
71. Cargnello M, Roux PP. Activation and function of the MAPKs and their substrates, the MAPK-activated protein kinases. Microbiol Mol Biol Rev. 2011;75(1):50-83.
72. Shaulian E, Karin M. AP-1 in cell proliferation and survival. Oncogene. 2001;20(19):2390-400.
73. Bretones G, Delgado MD, León J. Myc and cell cycle control. Biochim Biophys Acta. 2015;1849(5):506-16.
74. Yamaguchi K, Shirakabe K, Shibuya H, Irie K, Oishi I, Ueno N, et al. Identification of a member of the MAPKKK family as a potential mediator of TGF-beta signal transduction. Science. 1995;270(5244):2008-11.
75. Dai L, Aye Thu C, Liu XY, Xi J, Cheung PC. TAK1, more than just innate immunity. IUBMB Life. 2012;64(10):825-34.
76. Criswell T, Leskov K, Miyamoto S, Luo G, Boothman DA. Transcription factors activated in mammalian cells after clinically relevant doses of ionizing radiation. Oncogene. 2003;22(37):5813-27.
77. Janssens S, Tschopp J. Signals from within: the DNA-damage-induced NF-kappaB response. Cell Death Differ. 2006;13(5):773-84.
78. Wu ZH, Miyamoto S. Many faces of NF-kappaB signaling induced by genotoxic stress. J Mol Med (Berl). 2007;85(11):1187-202.
79. Shiloh Y, Ziv Y. The ATM protein kinase: regulating the cellular response to genotoxic stress, and more. Nature Reviews Molecular Cell Biology. 2013;14(4):197-210.
80. Yang Y, Xia F, Hermance N, Mabb A, Simonson S, Morrissey S, et al. A cytosolic ATM/NEMO/RIP1 complex recruits TAK1 to mediate the NF-kappaB and p38 mitogen-activated protein kinase (MAPK)/MAPK-activated protein 2 responses to DNA damage. Mol Cell Biol. 2011;31(14):2774-86.
81. Wu Z-H, Wong ET, Shi Y, Niu J, Chen Z, Miyamoto S, et al. ATM- and NEMO-Dependent ELKS Ubiquitination Coordinates TAK1-Mediated IKK Activation in Response to Genotoxic Stress. Molecular Cell. 2010;40(1):75-86.

82. Cicenas J, Zalyte E, Rimkus A, Dapkus D, Noreika R, Urbonavicius S. JNK, p38, ERK, and SGK1 Inhibitors in Cancer. Cancers (Basel). 2017;10(1).
83. Qi B, Cong Q, Li P, Ma G, Guo X, Yeh J, et al. Ablation of Tak1 in osteoclast progenitor leads to defects in skeletal growth and bone remodeling in mice. Scientific Reports. 2014;4(1):7158.
84. Pasparakis M, Vandenabeele P. Necroptosis and its role in inflammation. Nature. 2015;517(7534):311-20.
85. Silke J, Rickard JA, Gerlic M. The diverse role of RIP kinases in necroptosis and inflammation. Nature Immunology. 2015;16(7):689-97.
86. Ofengeim D, Yuan J. Regulation of RIP1 kinase signalling at the crossroads of inflammation and cell death. Nat Rev Mol Cell Biol. 2013;14(11):727-36.
87. Tao P, Sun J, Wu Z, Wang S, Wang J, Li W, et al. A dominant autoinflammatory disease caused by non-cleavable variants of RIPK1. Nature. 2020;577(7788):109-14.
88. Cuchet-Lourenço D, Eletto D, Wu C, Plagnol V, Papapietro O, Curtis J, et al. Biallelic RIPK1 mutations in humans cause severe immunodeficiency, arthritis, and intestinal inflammation. Science. 2018;361(6404):810-3.
89. Degterev A, Huang Z, Boyce M, Li Y, Jagtap P, Mizushima N, et al. Chemical inhibitor of nonapoptotic cell death with therapeutic potential for ischemic brain injury. Nat Chem Biol. 2005;1(2):112-9.
90. Li Y, Führer M, Bahrami E, Socha P, Klaudel-Dreszler M, Bouzidi A, et al. Human RIPK1 deficiency causes combined immunodeficiency and inflammatory bowel diseases. Proc Natl Acad Sci U S A. 2019;116(3):970-5.
91. Orning P, Weng D, Starheim K, Ratner D, Best Z, Lee B, et al. Pathogen blockade of TAK1 triggers caspase-8-dependent cleavage of gasdermin D and cell death. Science. 2018;362(6418):1064-9.
92. Kelliher MA, Grimm S, Ishida Y, Kuo F, Stanger BZ, Leder P. The death domain kinase RIP mediates the TNF-induced NF-kappaB signal. Immunity. 1998;8(3):297-303.
93. Rickard JA, O'Donnell JA, Evans JM, Lalaoui N, Poh AR, Rogers T, et al. RIPK1 regulates RIPK3-MLKL-driven systemic inflammation and emergency hematopoiesis. Cell. 2014;157(5):1175-88.
94. Dannappel M, Vlantis K, Kumari S, Polykratis A, Kim C, Wachsmuth L, et al. RIPK1 maintains epithelial homeostasis by inhibiting apoptosis and necroptosis. Nature. 2014;513(7516):90-4.
95. Polykratis A, Hermance N, Zelic M, Roderick J, Kim C, Van TM, et al. Cutting edge: RIPK1 Kinase inactive mice are viable and protected from TNF-induced necroptosis in vivo. J Immunol. 2014;193(4):1539-43.
96. Newton K, Sun X, Dixit VM. Kinase RIP3 is dispensable for normal NF-kappa Bs, signaling by the B-cell and T-cell receptors, tumor necrosis factor receptor 1, and Toll-like receptors 2 and 4. Mol Cell Biol. 2004;24(4):1464-9.
97. Berger SB, Kasparcova V, Hoffman S, Swift B, Dare L, Schaeffer M, et al. Cutting Edge: RIP1 kinase activity is dispensable for normal development but is a key regulator of inflammation in SHARPIN-deficient mice. J Immunol. 2014;192(12):5476-80.
98. Faustman D, Davis M. TNF receptor 2 pathway: drug target for autoimmune diseases. Nat Rev Drug Discov. 2010;9(6):482-93.
99. Hsu H, Xiong J, Goeddel DV. The TNF receptor 1-associated protein TRADD signals cell death and NF-kappa B activation. Cell. 1995;81(4):495-504.
100. Brenner D, Blaser H, Mak TW. Regulation of tumour necrosis factor signalling: live or let die. Nat Rev Immunol. 2015;15(6):362-74.
101. Haglund K, Dikic I. Ubiquitylation and cell signaling. Embo j. 2005;24(19):3353-9.

102. Hershko A. Ubiquitin and the Biology of the Cell1998.
103. Chen ZJ, Sun LJ. Nonproteolytic functions of ubiquitin in cell signaling. Mol Cell. 2009;33(3):275-86.
104. Vince JE, Pantaki D, Feltham R, Mace PD, Cordier SM, Schmukle AC, et al. TRAF2 must bind to cellular inhibitors of apoptosis for tumor necrosis factor (tnf) to efficiently activate nf-{kappa}b and to prevent tnf-induced apoptosis. J Biol Chem. 2009;284(51):35906-15.
105. Kanayama A, Seth RB, Sun L, Ea CK, Hong M, Shaito A, et al. TAB2 and TAB3 activate the NF-kappaB pathway through binding to polyubiquitin chains. Mol Cell. 2004;15(4):535-48.
106. Ea CK, Deng L, Xia ZP, Pineda G, Chen ZJ. Activation of IKK by TNFalpha requires site-specific ubiquitination of RIP1 and polyubiquitin binding by NEMO. Mol Cell. 2006;22(2):245-57.
107. Wu CJ, Conze DB, Li T, Srinivasula SM, Ashwell JD. Sensing of Lys 63-linked polyubiquitination by NEMO is a key event in NF-kappaB activation [corrected]. Nat Cell Biol. 2006;8(4):398-406.
108. Komander D, Reyes-Turcu F, Licchesi JD, Odenwaelder P, Wilkinson KD, Barford D. Molecular discrimination of structurally equivalent Lys 63-linked and linear polyubiquitin chains. EMBO Rep. 2009;10(5):466-73.
109. Rahighi S, Ikeda F, Kawasaki M, Akutsu M, Suzuki N, Kato R, et al. Specific recognition of linear ubiquitin chains by NEMO is important for NF-kappaB activation. Cell. 2009;136(6):1098-109.
110. Ting AT, Bertrand MJM. More to Life than NF-κB in TNFR1 Signaling. Trends Immunol. 2016;37(8):535-45.
111. Graber TE, Holcik M. Distinct roles for the cellular inhibitors of apoptosis proteins 1 and 2. Cell Death & Disease. 2011;2(3):e135-e.
112. Salvesen GS, Duckett CS. IAP proteins: blocking the road to death's door. Nature Reviews Molecular Cell Biology. 2002;3(6):401-10.
113. Estornes Y, Bertrand MJ. IAPs, regulators of innate immunity and inflammation. Semin Cell Dev Biol. 2015;39:106-14.
114. Hunter AM, LaCasse EC, Korneluk RG. The inhibitors of apoptosis (IAPs) as cancer targets. Apoptosis. 2007;12(9):1543-68.
115. Morrish E, Brumatti G, Silke J. Future Therapeutic Directions for Smac-Mimetics. Cells. 2020;9(2).
116. Gyrd-Hansen M, Meier P. IAPs: from caspase inhibitors to modulators of NF-kappaB, inflammation and cancer. Nat Rev Cancer. 2010;10(8):561-74.
117. Hinds MG, Norton RS, Vaux DL, Day CL. Solution structure of a baculoviral inhibitor of apoptosis (IAP) repeat. Nat Struct Biol. 1999;6(7):648-51.
118. Gyrd-Hansen M, Darding M, Miasari M, Santoro MM, Zender L, Xue W, et al. IAPs contain an evolutionarily conserved ubiquitin-binding domain that regulates NF-kappaB as well as cell survival and oncogenesis. Nat Cell Biol. 2008;10(11):1309-17.
119. Darding M, Feltham R, Tenev T, Bianchi K, Benetatos C, Silke J, et al. Molecular determinants of Smac mimetic induced degradation of cIAP1 and cIAP2. Cell Death Differ. 2011;18(8):1376-86.
120. Dueber EC, Schoeffler AJ, Lingel A, Elliott JM, Fedorova AV, Giannetti AM, et al. Antagonists induce a conformational change in cIAP1 that promotes autoubiquitination. Science. 2011;334(6054):376-80.
121. Lopez J, John SW, Tenev T, Rautureau GJ, Hinds MG, Francalanci F, et al. CARD-mediated autoinhibition of cIAP1's E3 ligase activity suppresses cell proliferation and migration. Mol Cell. 2011;42(5):569-83.

122. Mahoney DJ, Cheung HH, Mrad RL, Plenchette S, Simard C, Enwere E, et al. Both cIAP1 and cIAP2 regulate TNFalpha-mediated NF-kappaB activation. Proc Natl Acad Sci U S A. 2008;105(33):11778-83.
123. Eckelman BP, Salvesen GS, Scott FL. Human inhibitor of apoptosis proteins: why XIAP is the black sheep of the family. EMBO Rep. 2006;7(10):988-94.
124. Eckelman BP, Salvesen GS. The Human Anti-apoptotic Proteins cIAP1 and cIAP2 Bind but Do Not Inhibit Caspases*. Journal of Biological Chemistry. 2006;281(6):3254-60.
125. Choi YE, Butterworth M, Malladi S, Duckett CS, Cohen GM, Bratton SB. The E3 ubiquitin ligase cIAP1 binds and ubiquitinates caspase-3 and -7 via unique mechanisms at distinct steps in their processing. J Biol Chem. 2009;284(19):12772-82.
126. Du C, Fang M, Li Y, Li L, Wang X. Smac, a mitochondrial protein that promotes cytochrome c-dependent caspase activation by eliminating IAP inhibition. Cell. 2000;102(1):33-42.
127. Huang Y, Rich RL, Myszka DG, Wu H. Requirement of both the second and third BIR domains for the relief of X-linked inhibitor of apoptosis protein (XIAP)-mediated caspase inhibition by Smac. J Biol Chem. 2003;278(49):49517-22.
128. Blankenship JW, Varfolomeev E, Goncharov T, Fedorova AV, Kirkpatrick DS, Izrael-Tomasevic A, et al. Ubiquitin binding modulates IAP antagonist-stimulated proteasomal degradation of c-IAP1 and c-IAP2(1). Biochem J. 2009;417(1):149-60.
129. Yang QH, Du C. Smac/DIABLO selectively reduces the levels of c-IAP1 and c-IAP2 but not that of XIAP and livin in HeLa cells. J Biol Chem. 2004;279(17):16963-70.
130. Ciesielska A, Matyjek M, Kwiatkowska K. TLR4 and CD14 trafficking and its influence on LPS-induced pro-inflammatory signaling. Cellular and Molecular Life Sciences. 2021;78(4):1233-61.
131. Mogensen TH. Pathogen recognition and inflammatory signaling in innate immune defenses. Clin Microbiol Rev. 2009;22(2):240-73, Table of Contents.
132. Yu B, Wright SD. Catalytic Properties of Lipopolysaccharide (LPS) Binding Protein: TRANSFER OF LPS TO SOLUBLE CD14 (∗). Journal of Biological Chemistry. 1996;271(8):4100-5.
133. Gioannini TL, Teghanemt A, Zhang D, Levis EN, Weiss JP. Monomeric endotoxin:protein complexes are essential for TLR4-dependent cell activation. J Endotoxin Res. 2005;11(2):117-23.
134. Fitzgerald KA, Palsson-McDermott EM, Bowie AG, Jefferies CA, Mansell AS, Brady G, et al. Mal (MyD88-adapter-like) is required for Toll-like receptor-4 signal transduction. Nature. 2001;413(6851):78-83.
135. Laird MH, Rhee SH, Perkins DJ, Medvedev AE, Piao W, Fenton MJ, et al. TLR4/MyD88/PI3K interactions regulate TLR4 signaling. J Leukoc Biol. 2009;85(6):966-77.
136. Liu S, Cai X, Wu J, Cong Q, Chen X, Li T, et al. Phosphorylation of innate immune adaptor proteins MAVS, STING, and TRIF induces IRF3 activation. Science. 2015;347(6227):aaa2630.
137. Liu L, Lalaoui N. 25 years of research put RIPK1 in the clinic. Seminars in Cell & Developmental Biology. 2021;109:86-95.
138. Into T, Inomata M, Takayama E, Takigawa T. Autophagy in regulation of Toll-like receptor signaling. Cellular Signalling. 2012;24(6):1150-62.
139. Annibaldi A, Meier P. Checkpoints in TNF-Induced Cell Death: Implications in Inflammation and Cancer. Trends Mol Med. 2018;24(1):49-65.
140. Beg AA, Baltimore D. An essential role for NF-kappaB in preventing TNF-alpha-induced cell death. Science. 1996;274(5288):782-4.

141. Van Antwerp DJ, Martin SJ, Kafri T, Green DR, Verma IM. Suppression of TNF-alpha-induced apoptosis by NF-kappaB. Science. 1996;274(5288):787-9.
142. Micheau O, Lens S, Gaide O, Alevizopoulos K, Tschopp J. NF-kappaB signals induce the expression of c-FLIP. Mol Cell Biol. 2001;21(16):5299-305.
143. Micheau O, Tschopp J. Induction of TNF receptor I-mediated apoptosis via two sequential signaling complexes. Cell. 2003;114(2):181-90.
144. Wang CY, Guttridge DC, Mayo MW, Baldwin AS, Jr. NF-kappaB induces expression of the Bcl-2 homologue A1/Bfl-1 to preferentially suppress chemotherapy-induced apoptosis. Mol Cell Biol. 1999;19(9):5923-9.
145. Wang CY, Mayo MW, Korneluk RG, Goeddel DV, Baldwin AS, Jr. NF-kappaB antiapoptosis: induction of TRAF1 and TRAF2 and c-IAP1 and c-IAP2 to suppress caspase-8 activation. Science. 1998;281(5383):1680-3.
146. Lee EG, Boone DL, Chai S, Libby SL, Chien M, Lodolce JP, et al. Failure to regulate TNF-induced NF-kappaB and cell death responses in A20-deficient mice. Science. 2000;289(5488):2350-4.
147. He KL, Ting AT. A20 inhibits tumor necrosis factor (TNF) alpha-induced apoptosis by disrupting recruitment of TRADD and RIP to the TNF receptor 1 complex in Jurkat T cells. Mol Cell Biol. 2002;22(17):6034-45.
148. Wertz IE, O'Rourke KM, Zhou H, Eby M, Aravind L, Seshagiri S, et al. De-ubiquitination and ubiquitin ligase domains of A20 downregulate NF-κB signalling. Nature. 2004;430(7000):694-9.
149. Draber P, Kupka S, Reichert M, Draberova H, Lafont E, de Miguel D, et al. LUBAC-Recruited CYLD and A20 Regulate Gene Activation and Cell Death by Exerting Opposing Effects on Linear Ubiquitin in Signaling Complexes. Cell Rep. 2015;13(10):2258-72.
150. Mevissen TE, Hospenthal MK, Geurink PP, Elliott PR, Akutsu M, Arnaudo N, et al. OTU deubiquitinases reveal mechanisms of linkage specificity and enable ubiquitin chain restriction analysis. Cell. 2013;154(1):169-84.
151. De A, Dainichi T, Rathinam CV, Ghosh S. The deubiquitinase activity of A20 is dispensable for NF-κB signaling. EMBO Rep. 2014;15(7):775-83.
152. Lu TT, Onizawa M, Hammer GE, Turer EE, Yin Q, Damko E, et al. Dimerization and ubiquitin mediated recruitment of A20, a complex deubiquitinating enzyme. Immunity. 2013;38(5):896-905.
153. Sun SC. CYLD: a tumor suppressor deubiquitinase regulating NF-kappaB activation and diverse biological processes. Cell Death Differ. 2010;17(1):25-34.
154. Wright A, Reiley WW, Chang M, Jin W, Lee AJ, Zhang M, et al. Regulation of early wave of germ cell apoptosis and spermatogenesis by deubiquitinating enzyme CYLD. Dev Cell. 2007;13(5):705-16.
155. Kovalenko A, Chable-Bessia C, Cantarella G, Israël A, Wallach D, Courtois G. The tumour suppressor CYLD negatively regulates NF-kappaB signalling by deubiquitination. Nature. 2003;424(6950):801-5.
156. Trompouki E, Hatzivassiliou E, Tsichritzis T, Farmer H, Ashworth A, Mosialos G. CYLD is a deubiquitinating enzyme that negatively regulates NF-kappaB activation by TNFR family members. Nature. 2003;424(6950):793-6.
157. Brummelkamp TR, Nijman SM, Dirac AM, Bernards R. Loss of the cylindromatosis tumour suppressor inhibits apoptosis by activating NF-kappaB. Nature. 2003;424(6950):797-801.
158. O'Donnell MA, Legarda-Addison D, Skountzos P, Yeh WC, Ting AT. Ubiquitination of RIP1 regulates an NF-kappaB-independent cell-death switch in TNF signaling. Curr Biol. 2007;17(5):418-24.

159. O'Donnell MA, Ting AT. Chronicles of a death foretold: dual sequential cell death checkpoints in TNF signaling. Cell Cycle. 2010;9(6):1065-71.
160. O'Donnell MA, Ting AT. RIP1 comes back to life as a cell death regulator in TNFR1 signaling. Febs j. 2011;278(6):877-87.
161. Bertrand MJ, Milutinovic S, Dickson KM, Ho WC, Boudreault A, Durkin J, et al. cIAP1 and cIAP2 facilitate cancer cell survival by functioning as E3 ligases that promote RIP1 ubiquitination. Mol Cell. 2008;30(6):689-700.
162. Legarda-Addison D, Hase H, O'Donnell MA, Ting AT. NEMO/IKKgamma regulates an early NF-kappaB-independent cell-death checkpoint during TNF signaling. Cell Death Differ. 2009;16(9):1279-88.
163. Delanghe T, Dondelinger Y, Bertrand MJM. RIPK1 Kinase-Dependent Death: A Symphony of Phosphorylation Events. Trends Cell Biol. 2020;30(3):189-200.
164. Dondelinger Y, Aguileta MA, Goossens V, Dubuisson C, Grootjans S, Dejardin E, et al. RIPK3 contributes to TNFR1-mediated RIPK1 kinase-dependent apoptosis in conditions of cIAP1/2 depletion or TAK1 kinase inhibition. Cell Death Differ. 2013;20(10):1381-92.
165. Annibaldi A, Wicky John S, Vanden Berghe T, Swatek KN, Ruan J, Liccardi G, et al. Ubiquitin-Mediated Regulation of RIPK1 Kinase Activity Independent of IKK and MK2. Mol Cell. 2018;69(4):566-80.e5.
166. Dondelinger Y, Jouan-Lanhouet S, Divert T, Theatre E, Bertin J, Gough PJ, et al. NF-κB-Independent Role of IKKα/IKKβ in Preventing RIPK1 Kinase-Dependent Apoptotic and Necroptotic Cell Death during TNF Signaling. Mol Cell. 2015;60(1):63-76.
167. Dondelinger Y, Delanghe T, Priem D, Wynosky-Dolfi MA, Sorobetea D, Rojas-Rivera D, et al. Serine 25 phosphorylation inhibits RIPK1 kinase-dependent cell death in models of infection and inflammation. Nature Communications. 2019;10(1):1729.
168. Ang RL, Chan M, Ting AT. Ripoptocide - A Spark for Inflammation. Front Cell Dev Biol. 2019;7:163.
169. Elmore S. Apoptosis: a review of programmed cell death. Toxicol Pathol. 2007;35(4):495-516.
170. Savill J. Apoptosis in resolution of inflammation. J Leukoc Biol. 1997;61(4):375-80.
171. Galluzzi L, Vitale I, Aaronson SA, Abrams JM, Adam D, Agostinis P, et al. Molecular mechanisms of cell death: recommendations of the Nomenclature Committee on Cell Death 2018. Cell Death & Differentiation. 2018;25(3):486-541.
172. Guo X, Yin H, Chen Y, Li L, Li J, Liu Q. TAK1 regulates caspase 8 activation and necroptotic signaling via multiple cell death checkpoints. Cell Death & Disease. 2016;7(9):e2381-e.
173. Shalini S, Dorstyn L, Dawar S, Kumar S. Old, new and emerging functions of caspases. Cell Death & Differentiation. 2015;22(4):526-39.
174. Eckhart L, Ballaun C, Hermann M, VandeBerg JL, Sipos W, Uthman A, et al. Identification of novel mammalian caspases reveals an important role of gene loss in shaping the human caspase repertoire. Mol Biol Evol. 2008;25(5):831-41.
175. McIlwain DR, Berger T, Mak TW. Caspase functions in cell death and disease. Cold Spring Harb Perspect Biol. 2013;5(4):a008656.
176. Lavrik I, Golks A, Krammer PH. Death receptor signaling. J Cell Sci. 2005;118(Pt 2):265-7.
177. Wilson NS, Dixit V, Ashkenazi A. Death receptor signal transducers: nodes of coordination in immune signaling networks. Nat Immunol. 2009;10(4):348-55.
178. Wang L, Du F, Wang X. TNF-α Induces Two Distinct Caspase-8 Activation Pathways. Cell. 2008;133(4):693-703.

179. Petersen SL, Wang L, Yalcin-Chin A, Li L, Peyton M, Minna J, et al. Autocrine TNFalpha signaling renders human cancer cells susceptible to Smac-mimetic-induced apoptosis. Cancer Cell. 2007;12(5):445-56.
180. Alvarez-Diaz S, Dillon CP, Lalaoui N, Tanzer MC, Rodriguez DA, Lin A, et al. The Pseudokinase MLKL and the Kinase RIPK3 Have Distinct Roles in Autoimmune Disease Caused by Loss of Death-Receptor-Induced Apoptosis. Immunity. 2016;45(3):513-26.
181. Newton K, Wickliffe KE, Maltzman A, Dugger DL, Reja R, Zhang Y, et al. Activity of caspase-8 determines plasticity between cell death pathways. Nature. 2019;575(7784):679-82.
182. Fritsch M, Günther SD, Schwarzer R, Albert MC, Schorn F, Werthenbach JP, et al. Caspase-8 is the molecular switch for apoptosis, necroptosis and pyroptosis. Nature. 2019;575(7784):683-7.
183. Fu TM, Li Y, Lu A, Li Z, Vajjhala PR, Cruz AC, et al. Cryo-EM Structure of Caspase-8 Tandem DED Filament Reveals Assembly and Regulation Mechanisms of the Death-Inducing Signaling Complex. Mol Cell. 2016;64(2):236-50.
184. Tummers B, Green DR. Caspase-8: regulating life and death. Immunol Rev. 2017;277(1):76-89.
185. Orning P, Lien E. Multiple roles of caspase-8 in cell death, inflammation, and innate immunity. Journal of Leukocyte Biology. 2021;109(1):121-41.
186. Algate K, Haynes DR, Bartold PM, Crotti TN, Cantley MD. The effects of tumour necrosis factor-α on bone cells involved in periodontal alveolar bone loss; osteoclasts, osteoblasts and osteocytes. J Periodontal Res. 2016;51(5):549-66.
187. Safa AR, Day TW, Wu CH. Cellular FLICE-like inhibitory protein (C-FLIP): a novel target for cancer therapy. Curr Cancer Drug Targets. 2008;8(1):37-46.
188. Telieps T, Ewald F, Gereke M, Annemann M, Rauter Y, Schuster M, et al. Cellular-FLIP, Raji isoform (c-FLIP R) modulates cell death induction upon T-cell activation and infection. Eur J Immunol. 2013;43(6):1499-510.
189. Busca A, Saxena M, Kryworuchko M, Kumar A. Anti-apoptotic genes in the survival of monocytic cells during infection. Curr Genomics. 2009;10(5):306-17.
190. Scaffidi C, Schmitz I, Krammer PH, Peter ME. The role of c-FLIP in modulation of CD95-induced apoptosis. J Biol Chem. 1999;274(3):1541-8.
191. Hillert LK, Ivanisenko NV, Busse D, Espe J, König C, Peltek SE, et al. Dissecting DISC regulation via pharmacological targeting of caspase-8/c-FLIP(L) heterodimer. Cell Death Differ. 2020;27(7):2117-30.
192. Kavuri SM, Geserick P, Berg D, Dimitrova DP, Feoktistova M, Siegmund D, et al. Cellular FLICE-inhibitory protein (cFLIP) isoforms block CD95- and TRAIL death receptor-induced gene induction irrespective of processing of caspase-8 or cFLIP in the death-inducing signaling complex. J Biol Chem. 2011;286(19):16631-46.
193. Feoktistova M, Geserick P, Kellert B, Dimitrova DP, Langlais C, Hupe M, et al. cIAPs block Ripoptosome formation, a RIP1/caspase-8 containing intracellular cell death complex differentially regulated by cFLIP isoforms. Mol Cell. 2011;43(3):449-63.
194. Oberst A, Dillon CP, Weinlich R, McCormick LL, Fitzgerald P, Pop C, et al. Catalytic activity of the caspase-8-FLIP(L) complex inhibits RIPK3-dependent necrosis. Nature. 2011;471(7338):363-7.
195. He S, Wang L, Miao L, Wang T, Du F, Zhao L, et al. Receptor interacting protein kinase-3 determines cellular necrotic response to TNF-alpha. Cell. 2009;137(6):1100-11.

196. Kaiser WJ, Upton JW, Long AB, Livingston-Rosanoff D, Daley-Bauer LP, Hakem R, et al. RIP3 mediates the embryonic lethality of caspase-8-deficient mice. Nature. 2011;471(7338):368-72.
197. Weir A, Hughes S, Rashidi M, Hildebrand JM, Vince JE. Necroptotic movers and shakers: cell types, inflammatory drivers and diseases. Curr Opin Immunol. 2021;68:83-97.
198. Varga Z, Molnár T, Mázló A, Kovács R, Jenei V, Kerekes K, et al. Differences in the sensitivity of classically and alternatively activated macrophages to TAK1 inhibitor-induced necroptosis. Cancer Immunology, Immunotherapy. 2020;69(11):2193-207.
199. Upton JW, Kaiser WJ, Mocarski ES. DAI/ZBP1/DLM-1 complexes with RIP3 to mediate virus-induced programmed necrosis that is targeted by murine cytomegalovirus vIRA. Cell Host Microbe. 2012;11(3):290-7.
200. Li J, McQuade T, Siemer AB, Napetschnig J, Moriwaki K, Hsiao YS, et al. The RIP1/RIP3 necrosome forms a functional amyloid signaling complex required for programmed necrosis. Cell. 2012;150(2):339-50.
201. Vandenabeele P, Declercq W, Van Herreweghe F, Vanden Berghe T. The role of the kinases RIP1 and RIP3 in TNF-induced necrosis. Sci Signal. 2010;3(115):re4.
202. Cho YS, Challa S, Moquin D, Genga R, Ray TD, Guildford M, et al. Phosphorylation-driven assembly of the RIP1-RIP3 complex regulates programmed necrosis and virus-induced inflammation. Cell. 2009;137(6):1112-23.
203. Sun L, Wang H, Wang Z, He S, Chen S, Liao D, et al. Mixed lineage kinase domain-like protein mediates necrosis signaling downstream of RIP3 kinase. Cell. 2012;148(1-2):213-27.
204. Murphy JM, Czabotar PE, Hildebrand JM, Lucet IS, Zhang JG, Alvarez-Diaz S, et al. The pseudokinase MLKL mediates necroptosis via a molecular switch mechanism. Immunity. 2013;39(3):443-53.
205. Cai Z, Jitkaew S, Zhao J, Chiang HC, Choksi S, Liu J, et al. Plasma membrane translocation of trimerized MLKL protein is required for TNF-induced necroptosis. Nat Cell Biol. 2014;16(1):55-65.
206. Chen X, Li W, Ren J, Huang D, He WT, Song Y, et al. Translocation of mixed lineage kinase domain-like protein to plasma membrane leads to necrotic cell death. Cell Res. 2014;24(1):105-21.
207. Wang H, Sun L, Su L, Rizo J, Liu L, Wang LF, et al. Mixed lineage kinase domain-like protein MLKL causes necrotic membrane disruption upon phosphorylation by RIP3. Mol Cell. 2014;54(1):133-46.
208. Shi J, Gao W, Shao F. Pyroptosis: Gasdermin-Mediated Programmed Necrotic Cell Death. Trends Biochem Sci. 2017;42(4):245-54.
209. Sharma D, Kanneganti TD. The cell biology of inflammasomes: Mechanisms of inflammasome activation and regulation. J Cell Biol. 2016;213(6):617-29.
210. Lawlor KE, Khan N, Mildenhall A, Gerlic M, Croker BA, D'Cruz AA, et al. RIPK3 promotes cell death and NLRP3 inflammasome activation in the absence of MLKL. Nature Communications. 2015;6(1):6282.
211. Man SM, Kanneganti TD. Regulation of inflammasome activation. Immunol Rev. 2015;265(1):6-21.
212. Yang Y, Wang H, Kouadir M, Song H, Shi F. Recent advances in the mechanisms of NLRP3 inflammasome activation and its inhibitors. Cell Death Dis. 2019;10(2):128.
213. Kovacs SB, Miao EA. Gasdermins: Effectors of Pyroptosis. Trends Cell Biol. 2017;27(9):673-84.

214. Liu X, Zhang Z, Ruan J, Pan Y, Magupalli VG, Wu H, et al. Inflammasome-activated gasdermin D causes pyroptosis by forming membrane pores. Nature. 2016;535(7610):153-8.
215. Vince JE, Silke J. The intersection of cell death and inflammasome activation. Cell Mol Life Sci. 2016;73(11-12):2349-67.
216. Rauch I, Deets KA, Ji DX, von Moltke J, Tenthorey JL, Lee AY, et al. NAIP-NLRC4 Inflammasomes Coordinate Intestinal Epithelial Cell Expulsion with Eicosanoid and IL-18 Release via Activation of Caspase-1 and -8. Immunity. 2017;46(4):649-59.
217. Mascarenhas DPA, Cerqueira DM, Pereira MSF, Castanheira FVS, Fernandes TD, Manin GZ, et al. Inhibition of caspase-1 or gasdermin-D enable caspase-8 activation in the Naip5/NLRC4/ASC inflammasome. PLoS Pathog. 2017;13(8):e1006502.
218. Sagulenko V, Thygesen SJ, Sester DP, Idris A, Cridland JA, Vajjhala PR, et al. AIM2 and NLRP3 inflammasomes activate both apoptotic and pyroptotic death pathways via ASC. Cell Death & Differentiation. 2013;20(9):1149-60.
219. Gurung P, Anand PK, Malireddi RK, Vande Walle L, Van Opdenbosch N, Dillon CP, et al. FADD and caspase-8 mediate priming and activation of the canonical and noncanonical Nlrp3 inflammasomes. J Immunol. 2014;192(4):1835-46.
220. Taabazuing CY, Okondo MC, Bachovchin DA. Pyroptosis and Apoptosis Pathways Engage in Bidirectional Crosstalk in Monocytes and Macrophages. Cell Chem Biol. 2017;24(4):507-14.e4.
221. Mifflin L, Ofengeim D, Yuan J. Receptor-interacting protein kinase 1 (RIPK1) as a therapeutic target. Nature Reviews Drug Discovery. 2020;19(8):553-71.
222. Yuan J, Amin P, Ofengeim D. Necroptosis and RIPK1-mediated neuroinflammation in CNS diseases. Nat Rev Neurosci. 2019;20(1):19-33.
223. Degterev A, Ofengeim D, Yuan J. Targeting RIPK1 for the treatment of human diseases. Proc Natl Acad Sci U S A. 2019;116(20):9714-22.
224. Dong Y, Fischer R, Naudé PJ, Maier O, Nyakas C, Duffey M, et al. Essential protective role of tumor necrosis factor receptor 2 in neurodegeneration. Proc Natl Acad Sci U S A. 2016;113(43):12304-9.
225. Zhao J, Jitkaew S, Cai Z, Choksi S, Li Q, Luo J, et al. Mixed lineage kinase domain-like is a key receptor interacting protein 3 downstream component of TNF-induced necrosis. Proc Natl Acad Sci U S A. 2012;109(14):5322-7.
226. Zhang DW, Shao J, Lin J, Zhang N, Lu BJ, Lin SC, et al. RIP3, an energy metabolism regulator that switches TNF-induced cell death from apoptosis to necrosis. Science. 2009;325(5938):332-6.
227. Mandal P, Berger SB, Pillay S, Moriwaki K, Huang C, Guo H, et al. RIP3 induces apoptosis independent of pronecrotic kinase activity. Mol Cell. 2014;56(4):481-95.
228. Kaiser WJ, Sridharan H, Huang C, Mandal P, Upton JW, Gough PJ, et al. Toll-like receptor 3-mediated necrosis via TRIF, RIP3, and MLKL. J Biol Chem. 2013;288(43):31268-79.
229. Zhou W, Yuan J. Necroptosis in health and diseases. Semin Cell Dev Biol. 2014;35:14-23.
230. Patel S, Webster JD, Varfolomeev E, Kwon YC, Cheng JH, Zhang J, et al. RIP1 inhibition blocks inflammatory diseases but not tumor growth or metastases. Cell Death & Differentiation. 2020;27(1):161-75.
231. Rosenbaum DM, Degterev A, David J, Rosenbaum PS, Roth S, Grotta JC, et al. Necroptosis, a novel form of caspase-independent cell death, contributes to neuronal damage in a retinal ischemia-reperfusion injury model. J Neurosci Res. 2010;88(7):1569-76.

232. Varfolomeev E, Goncharov T, Fedorova AV, Dynek JN, Zobel K, Deshayes K, et al. c-IAP1 and c-IAP2 are critical mediators of tumor necrosis factor alpha (TNFalpha)-induced NF-kappaB activation. J Biol Chem. 2008;283(36):24295-9.
233. Amaravadi RK, Schilder RJ, Martin LP, Levin M, Graham MA, Weng DE, et al. A Phase I Study of the SMAC-Mimetic Birinapant in Adults with Refractory Solid Tumors or Lymphoma. Mol Cancer Ther. 2015;14(11):2569-75.
234. Derakhshan A, Chen Z, Van Waes C. Therapeutic Small Molecules Target Inhibitor of Apoptosis Proteins in Cancers with Deregulation of Extrinsic and Intrinsic Cell Death Pathways. Clin Cancer Res. 2017;23(6):1379-87.
235. Noonan AM, Bunch KP, Chen JQ, Herrmann MA, Lee JM, Kohn EC, et al. Pharmacodynamic markers and clinical results from the phase 2 study of the SMAC mimetic birinapant in women with relapsed platinum-resistant or -refractory epithelial ovarian cancer. Cancer. 2016;122(4):588-97.
236. Fulda S, Vucic D. Targeting IAP proteins for therapeutic intervention in cancer. Nat Rev Drug Discov. 2012;11(2):109-24.
237. Jensen S, Seidelin JB, LaCasse EC, Nielsen OH. SMAC mimetics and RIPK inhibitors as therapeutics for chronic inflammatory diseases. Sci Signal. 2020;13(619).
238. Chesi M, Mirza NN, Garbitt VM, Sharik ME, Dueck AC, Asmann YW, et al. IAP antagonists induce anti-tumor immunity in multiple myeloma. Nat Med. 2016;22(12):1411-20.
239. Infante JR, Dees EC, Olszanski AJ, Dhuria SV, Sen S, Cameron S, et al. Phase I dose-escalation study of LCL161, an oral inhibitor of apoptosis proteins inhibitor, in patients with advanced solid tumors. J Clin Oncol. 2014;32(28):3103-10.
240. Niederberger E, Geisslinger G. The IKK-NF-κB pathway: a source for novel molecular drug targets in pain therapy? The FASEB Journal. 2008;22(10):3432-42.
241. Ji RR, Gereau RWt, Malcangio M, Strichartz GR. MAP kinase and pain. Brain Res Rev. 2009;60(1):135-48.
242. Kalliolias GD, Ivashkiv LB. TNF biology, pathogenic mechanisms and emerging therapeutic strategies. Nat Rev Rheumatol. 2016;12(1):49-62.
243. Hammaker D, Firestein GS. "Go upstream, young man": lessons learned from the p38 saga. Ann Rheum Dis. 2010;69 Suppl 1(Suppl 1):i77-82.
244. Buglio D, Palakurthi S, Byth K, Vega F, Toader D, Saeh J, et al. Essential role of TAK1 in regulating mantle cell lymphoma survival. Blood. 2012;120(2):347-55.
245. Singh A, Sweeney MF, Yu M, Burger A, Greninger P, Benes C, et al. TAK1 inhibition promotes apoptosis in KRAS-dependent colon cancers. Cell. 2012;148(4):639-50.
246. Melisi D, Xia Q, Paradiso G, Ling J, Moccia T, Carbone C, et al. Modulation of pancreatic cancer chemoresistance by inhibition of TAK1. J Natl Cancer Inst. 2011;103(15):1190-204.
247. Kumar SK, Rajkumar V, Kyle RA, van Duin M, Sonneveld P, Mateos MV, et al. Multiple myeloma. Nat Rev Dis Primers. 2017;3:17046.
248. Rajkumar SV. Multiple myeloma: 2018 update on diagnosis, risk-stratification, and management. Am J Hematol. 2018;93(8):981-1114.
249. Mikhael JR, Dingli D, Roy V, Reeder CB, Buadi FK, Hayman SR, et al. Management of newly diagnosed symptomatic multiple myeloma: updated Mayo Stratification of Myeloma and Risk-Adapted Therapy (mSMART) consensus guidelines 2013. Mayo Clin Proc. 2013;88(4):360-76.
250. Norway CRo. Cancer in Norway 2019 - Cancer incidence, mortality, survival and prevalence in Norway. Oslo: Cancer Registry of Norway, 2020; 2020.

251. Kostopoulos IV, Ntanasis-Stathopoulos I, Gavriatopoulou M, Tsitsilonis OE, Terpos E. Minimal Residual Disease in Multiple Myeloma: Current Landscape and Future Applications With Immunotherapeutic Approaches. Front Oncol. 2020;10:860.
252. Kumar SK, Rajkumar SV. The current status of minimal residual disease assessment in myeloma. Leukemia. 2014;28(2):239-40.
253. Landgren O. Monoclonal gammopathy of undetermined significance and smoldering multiple myeloma: biological insights and early treatment strategies. Hematology Am Soc Hematol Educ Program. 2013;2013:478-87.
254. Criteria for the classification of monoclonal gammopathies, multiple myeloma and related disorders: a report of the International Myeloma Working Group. Br J Haematol. 2003;121(5):749-57.
255. Bianchi G, Munshi NC. Pathogenesis beyond the cancer clone(s) in multiple myeloma. Blood. 2015;125(20):3049-58.
256. Prideaux SM, Conway O'Brien E, Chevassut TJ. The genetic architecture of multiple myeloma. Adv Hematol. 2014;2014:864058.
257. Rajkumar SV, Dimopoulos MA, Palumbo A, Blade J, Merlini G, Mateos MV, et al. International Myeloma Working Group updated criteria for the diagnosis of multiple myeloma. Lancet Oncol. 2014;15(12):e538-48.
258. Annunziata CM, Davis RE, Demchenko Y, Bellamy W, Gabrea A, Zhan F, et al. Frequent engagement of the classical and alternative NF-kappaB pathways by diverse genetic abnormalities in multiple myeloma. Cancer Cell. 2007;12(2):115-30.
259. Hu J, Hu WX. Targeting signaling pathways in multiple myeloma: Pathogenesis and implication for treatments. Cancer Lett. 2018;414:214-21.
260. Ang E, Pavlos NJ, Rea SL, Qi M, Chai T, Walsh JP, et al. Proteasome inhibitors impair RANKL-induced NF-kappaB activity in osteoclast-like cells via disruption of p62, TRAF6, CYLD, and IkappaBalpha signaling cascades. J Cell Physiol. 2009;220(2):450-9.
261. Hongming H, Jian H. Bortezomib inhibits maturation and function of osteoclasts from PBMCs of patients with multiple myeloma by downregulating TRAF6. Leuk Res. 2009;33(1):115-22.
262. Roodman GD. Pathogenesis of myeloma bone disease. Leukemia. 2009;23(3):435-41.
263. Silbermann R, Roodman GD. Myeloma bone disease: Pathophysiology and management. J Bone Oncol. 2013;2(2):59-69.
264. Mitsiades CS, McMillin DW, Klippel S, Hideshima T, Chauhan D, Richardson PG, et al. The role of the bone marrow microenvironment in the pathophysiology of myeloma and its significance in the development of more effective therapies. Hematol Oncol Clin North Am. 2007;21(6):1007-34, vii-viii.
265. Pearse RN, Sordillo EM, Yaccoby S, Wong BR, Liau DF, Colman N, et al. Multiple myeloma disrupts the TRANCE/ osteoprotegerin cytokine axis to trigger bone destruction and promote tumor progression. Proc Natl Acad Sci U S A. 2001;98(20):11581-6.
266. Terpos E, Ntanasis-Stathopoulos I, Gavriatopoulou M, Dimopoulos MA. Pathogenesis of bone disease in multiple myeloma: from bench to bedside. Blood Cancer J. 2018;8(1):7.
267. David Roodman G, Silbermann R. Mechanisms of osteolytic and osteoblastic skeletal lesions. Bonekey Rep. 2015;4:753.
268. Al Hamed R, Bazarbachi AH, Malard F, Harousseau JL, Mohty M. Current status of autologous stem cell transplantation for multiple myeloma. Blood Cancer J. 2019;9(4):44.

269. Berenson JR, Lichtenstein A, Porter L, Dimopoulos MA, Bordoni R, George S, et al. Long-term pamidronate treatment of advanced multiple myeloma patients reduces skeletal events. Myeloma Aredia Study Group. J Clin Oncol. 1998;16(2):593-602.
270. Henry DH, Costa L, Goldwasser F, Hirsh V, Hungria V, Prausova J, et al. Randomized, double-blind study of denosumab versus zoledronic acid in the treatment of bone metastases in patients with advanced cancer (excluding breast and prostate cancer) or multiple myeloma. J Clin Oncol. 2011;29(9):1125-32.
271. Alexanian R, Haut A, Khan AU, Lane M, McKelvey EM, Migliore PJ, et al. Treatment for multiple myeloma. Combination chemotherapy with different melphalan dose regimens. Jama. 1969;208(9):1680-5.
272. Kyle RA, Rajkumar SV. Multiple myeloma. N Engl J Med. 2004;351(18):1860-73.
273. Schesvold FO, A. . Current and Novel Alkylators in Multiple Myeloma. Preprints. 2021.
274. Röllig C, Knop S, Bornhäuser M. Multiple myeloma. Lancet. 2015;385(9983):2197-208.
275. Fu D, Calvo JA, Samson LD. Balancing repair and tolerance of DNA damage caused by alkylating agents. Nat Rev Cancer. 2012;12(2):104-20.
276. Wang H, Ran L, Hui K, Pei X, Wang X, Zheng Y. The inhibitor of apoptosis protein livin is upregulated in psoriasis vulgaris. J Eur Acad Dermatol Venereol. 2018;32(6):e245-e7.
277. Watanabe T, Minaga K, Kamata K, Sakurai T, Komeda Y, Nagai T, et al. RICK/RIP2 is a NOD2-independent nodal point of gut inflammation. Int Immunol. 2019;31(10):669-83.
278. Abhari BA, Cristofanon S, Kappler R, von Schweinitz D, Humphreys R, Fulda S. RIP1 is required for IAP inhibitor-mediated sensitization for TRAIL-induced apoptosis via a RIP1/FADD/caspase-8 cell death complex. Oncogene. 2013;32(27):3263-73.
279. Kahlenberg JM, Fox DA. Advances in the medical treatment of rheumatoid arthritis. Hand Clin. 2011;27(1):11-20.
280. Parisi L, Gini E, Baci D, Tremolati M, Fanuli M, Bassani B, et al. Macrophage Polarization in Chronic Inflammatory Diseases: Killers or Builders? J Immunol Res. 2018;2018:8917804.
281. Scott DL, Kingsley GH. Tumor necrosis factor inhibitors for rheumatoid arthritis. N Engl J Med. 2006;355(7):704-12.
282. Kennel KA, Drake MT. Adverse effects of bisphosphonates: implications for osteoporosis management. Mayo Clin Proc. 2009;84(7):632-7; quiz 8.
283. Zhou L, Zhang Y, Leng Y, Dai Y, Kmieciak M, Kramer L, et al. The IAP antagonist birinapant potentiates bortezomib anti-myeloma activity in vitro and in vivo. J Hematol Oncol. 2019;12(1):25.
284. Keats JJ, Fonseca R, Chesi M, Schop R, Baker A, Chng WJ, et al. Promiscuous mutations activate the noncanonical NF-kappaB pathway in multiple myeloma. Cancer Cell. 2007;12(2):131-44.
285. Brumatti G, Ma C, Lalaoui N, Nguyen NY, Navarro M, Tanzer MC, et al. The caspase-8 inhibitor emricasan combines with the SMAC mimetic birinapant to induce necroptosis and treat acute myeloid leukemia. Sci Transl Med. 2016;8(339):339ra69.
286. Benedict CA, Norris PS, Prigozy TI, Bodmer JL, Mahr JA, Garnett CT, et al. Three adenovirus E3 proteins cooperate to evade apoptosis by tumor necrosis factor-related apoptosis-inducing ligand receptor-1 and -2. J Biol Chem. 2001;276(5):3270-8.
287. Nichols DB, De Martini W, Cottrell J. Poxviruses Utilize Multiple Strategies to Inhibit Apoptosis. Viruses. 2017;9(8).

288. Jerome KR, Fox R, Chen Z, Sears AE, Lee H, Corey L. Herpes simplex virus inhibits apoptosis through the action of two genes, Us5 and Us3. J Virol. 1999;73(11):8950-7.
289. Zheng TS, Flavell RA. Divinations and surprises: genetic analysis of caspase function in mice. Exp Cell Res. 2000;256(1):67-73.
290. Shutinoski B, Alturki NA, Rijal D, Bertin J, Gough PJ, Schlossmacher MG, et al. K45A mutation of RIPK1 results in poor necroptosis and cytokine signaling in macrophages, which impacts inflammatory responses in vivo. Cell Death Differ. 2016;23(10):1628-37.
291. Duprez L, Takahashi N, Van Hauwermeiren F, Vandendriessche B, Goossens V, Vanden Berghe T, et al. RIP kinase-dependent necrosis drives lethal systemic inflammatory response syndrome. Immunity. 2011;35(6):908-18.
292. Liu Y, Fan C, Zhang Y, Yu X, Wu X, Zhang X, et al. RIP1 kinase activity-dependent roles in embryonic development of Fadd-deficient mice. Cell Death Differ. 2017;24(8):1459-69.
293. Meng H, Liu Z, Li X, Wang H, Jin T, Wu G, et al. Death-domain dimerization-mediated activation of RIPK1 controls necroptosis and RIPK1-dependent apoptosis. Proc Natl Acad Sci U S A. 2018;115(9):E2001-e9.
294. Cho YS. The role of necroptosis in the treatment of diseases. BMB Rep. 2018;51(5):219-24.
295. Bolognese AC, Yang WL, Hansen LW, Denning NL, Nicastro JM, Coppa GF, et al. Inhibition of necroptosis attenuates lung injury and improves survival in neonatal sepsis. Surgery. 2018.
296. Yoo H, Lee JY, Park J, Yang JH, Suh GY, Jeon K. Association of Plasma Level of TNF-Related Apoptosis-Inducing Ligand with Severity and Outcome of Sepsis. J Clin Med. 2020;9(6).
297. Ali H, Caballero R, Dong SXM, Gajnayaka N, Vranjkovic A, Ahmed D, et al. Selective killing of human M1 macrophages by Smac mimetics alone and M2 macrophages by Smac mimetics and caspase inhibition. J Leukoc Biol. 2021.
298. Huang X, Tan S, Li Y, Cao S, Li X, Pan H, et al. Caspase inhibition prolongs inflammation by promoting a signaling complex with activated RIPK1. J Cell Biol. 2021;220(6).
299. Madej MP, Töpfer E, Boraschi D, Italiani P. Different Regulation of Interleukin-1 Production and Activity in Monocytes and Macrophages: Innate Memory as an Endogenous Mechanism of IL-1 Inhibition. Front Pharmacol. 2017;8:335.
300. Silva MT. Secondary necrosis: the natural outcome of the complete apoptotic program. FEBS Lett. 2010;584(22):4491-9.
301. Sachet M, Liang YY, Oehler R. The immune response to secondary necrotic cells. Apoptosis. 2017;22(10):1189-204.
302. Dhanasekaran DN, Reddy EP. JNK-signaling: A multiplexing hub in programmed cell death. Genes Cancer. 2017;8(9-10):682-94.
303. Sun W, Wu X, Gao H, Yu J, Zhao W, Lu JJ, et al. Cytosolic calcium mediates RIP1/RIP3 complex-dependent necroptosis through JNK activation and mitochondrial ROS production in human colon cancer cells. Free Radic Biol Med. 2017;108:433-44.
304. Kim YS, Morgan MJ, Choksi S, Liu ZG. TNF-induced activation of the Nox1 NADPH oxidase and its role in the induction of necrotic cell death. Mol Cell. 2007;26(5):675-87.
305. Yang ZH, Wu XN, He P, Wang X, Wu J, Ai T, et al. A Non-canonical PDK1-RSK Signal Diminishes Pro-caspase-8-Mediated Necroptosis Blockade. Mol Cell. 2020;80(2):296-310.e6.

306. Moulin M, Anderton H, Voss AK, Thomas T, Wong WW, Bankovacki A, et al. IAPs limit activation of RIP kinases by TNF receptor 1 during development. Embo j. 2012;31(7):1679-91.
307. Boutaffala L, Bertrand MJ, Remouchamps C, Seleznik G, Reisinger F, Janas M, et al. NIK promotes tissue destruction independently of the alternative NF-κB pathway through TNFR1/RIP1-induced apoptosis. Cell Death Differ. 2015;22(12):2020-33.
308. Malireddi RKS, Gurung P, Kesavardhana S, Samir P, Burton A, Mummareddy H, et al. Innate immune priming in the absence of TAK1 drives RIPK1 kinase activity-independent pyroptosis, apoptosis, necroptosis, and inflammatory disease. J Exp Med. 2020;217(3).
309. Malireddi RKS, Kesavardhana S, Kanneganti T-D. ZBP1 and TAK1: Master Regulators of NLRP3 Inflammasome/Pyroptosis, Apoptosis, and Necroptosis (PAN-optosis). Frontiers in Cellular and Infection Microbiology. 2019;9(406).
310. Samir P, Malireddi RKS, Kanneganti TD. The PANoptosome: A Deadly Protein Complex Driving Pyroptosis, Apoptosis, and Necroptosis (PANoptosis). Front Cell Infect Microbiol. 2020;10:238.
311. Lukens JR, Gurung P, Vogel P, Johnson GR, Carter RA, McGoldrick DJ, et al. Dietary modulation of the microbiome affects autoinflammatory disease. Nature. 2014;516(7530):246-9.
312. Gurung P, Burton A, Kanneganti TD. NLRP3 inflammasome plays a redundant role with caspase 8 to promote IL-1β-mediated osteomyelitis. Proc Natl Acad Sci U S A. 2016;113(16):4452-7.
313. Karki R, Sharma BR, Tuladhar S, Williams EP, Zalduondo L, Samir P, et al. Synergism of TNF-α and IFN-γ Triggers Inflammatory Cell Death, Tissue Damage, and Mortality in SARS-CoV-2 Infection and Cytokine Shock Syndromes. Cell. 2021;184(1):149-68.e17.
314. Casimiro S, Alho I, Bettencourt M, Pires R, Lipton A, Costa L. RANKL enhances the effect of an antagonist of inhibitor of apoptosis proteins (cIAPs) in RANK-positive breast cancer cells. J Bone Oncol. 2013;2(3):116-22.
315. Yang C, Davis JL, Zeng R, Vora P, Su X, Collins LI, et al. Antagonism of inhibitor of apoptosis proteins increases bone metastasis via unexpected osteoclast activation. Cancer Discov. 2013;3(2):212-23.
316. Lawlor KE, Feltham R, Yabal M, Conos SA, Chen KW, Ziehe S, et al. XIAP Loss Triggers RIPK3- and Caspase-8-Driven IL-1β Activation and Cell Death as a Consequence of TLR-MyD88-Induced cIAP1-TRAF2 Degradation. Cell Reports. 2017;20(3):668-82.
317. Wu J, Powell F, Larsen NA, Lai Z, Byth KF, Read J, et al. Mechanism and in vitro pharmacology of TAK1 inhibition by (5Z)-7-Oxozeaenol. ACS Chem Biol. 2013;8(3):643-50.
318. Cho SW, Kim S, Kim Y, Kweon J, Kim HS, Bae S, et al. Analysis of off-target effects of CRISPR/Cas-derived RNA-guided endonucleases and nickases. Genome Res. 2014;24(1):132-41.
319. Demchenko YN, Kuehl WM. A critical role for the NFkB pathway in multiple myeloma. Oncotarget. 2010;1(1):59-68.
320. Teramachi J, Tenshin H, Hiasa M, Oda A, Bat-Erdene A, Harada T, et al. TAK1 is a pivotal therapeutic target for tumor progression and bone destruction in myeloma. Haematologica. 2021;106(5):1401-13.
321. Tenshin H, Teramachi J, Oda A, Amachi R, Hiasa M, Bat-Erdene A, et al. TAK1 inhibition subverts the osteoclastogenic action of TRAIL while potentiating its antimyeloma effects. Blood Adv. 2017;1(24):2124-37.

322. Dondelinger Y, Delanghe T, Rojas-Rivera D, Priem D, Delvaeye T, Bruggeman I, et al. MK2 phosphorylation of RIPK1 regulates TNF-mediated cell death. Nat Cell Biol. 2017;19(10):1237-47.
323. Jaco I, Annibaldi A, Lalaoui N, Wilson R, Tenev T, Laurien L, et al. MK2 Phosphorylates RIPK1 to Prevent TNF-Induced Cell Death. Mol Cell. 2017;66(5):698-710.e5.
324. Menon MB, Gropengießer J, Fischer J, Novikova L, Deuretzbacher A, Lafera J, et al. p38(MAPK)/MK2-dependent phosphorylation controls cytotoxic RIPK1 signalling in inflammation and infection. Nat Cell Biol. 2017;19(10):1248-59.
325. Chabner BA, Roberts TG, Jr. Timeline: Chemotherapy and the war on cancer. Nat Rev Cancer. 2005;5(1):65-72.
326. Sriram G, Milling L, Chen J-K, Abraham W, Handly ED, Irvine DJ, et al. The Injury Response to DNA Damage Promotes Anti-Tumor Immunity. bioRxiv. 2020:2020.04.26.062216.
327. Han C, Godfrey V, Liu Z, Han Y, Liu L, Peng H, et al. The AIM2 and NLRP3 inflammasomes trigger IL-1-mediated antitumor effects during radiation. Sci Immunol. 2021;6(59).

Paper I

Moen et al. *Cell Death Discovery* (2021)7:36
https://doi.org/10.1038/s41420-021-00415-1

Cell Death Discovery

ARTICLE Open Access

Smac-mimetics reduce numbers and viability of human osteoclasts

Ingrid Nyhus Moen[1,2], Marita Westhrin[1], Erling Håland[1], Markus Haug[1], Unni Nonstad[1], Merisa Klaharn[1], Therese Standal[1] and Kristian K. Starheim[1,2]

Abstract

Elevated activity of bone-degrading osteoclasts (OC) contributes to pathological bone degradation in diseases such as multiple myeloma. Several proinflammatory cytokines, including TNF, contribute to osteoclastogenesis. The receptor-interacting protein kinase 1 (RIPK1) regulates inflammation and cell death. It is recruited to the TNF-receptor complex, where it is ubiquitinated, and activates transcription factor NF-κB and mitogen-activated protein kinases (MAPK). Smac-mimetics (SM) is a group of drugs that block RIPK1 ubiquitination and shifts RIPK1 to activation of apoptosis or necroptosis. In this manuscript, we show that the two SM birinapant and LCL-161 reduced the number and viability of primary human OC, and induced TNF-dependent cell death in OC precursors (pre-OC). Birinapant was more cytotoxic than LCL-161 and induced predominantly apoptosis and to some degree necroptosis. Both inhibitors restrained osteoclastogenesis induced by myeloma patient bone-marrow aspirates. SM has gained attention as novel treatment strategies both for cancer and chronic inflammatory pathologies, but limited information has been available on interactions with primary human immune cells. As LCL-161 is in phase 2 clinical studies for multiple myeloma, we propose that SM might possess additional benefits in reducing bone degradation in myeloma patients. Taken together, we show that SM reduces human osteoclastogenesis, and that these compounds may represent promising drug candidates for pathological bone degradation.

Introduction

Bone is a dynamic tissue that is constantly degraded and re-built. Excessive bone loss is caused by estrogen depletion, genetic susceptibility factors, drug treatments, and chronic inflammation. It is the cause of osteoporosis, and a contributing factor in the pathology of inflammatory diseases such as osteoarthritis and rheumatoid arthritis. In addition, several cancers, such as multiple myeloma, induce bone degradation to increase nutrient availability or carve out metastatic niches, resulting in poorer prognosis and painful complications for the patient[1,2].

Bone homeostasis is a tightly regulated balance between bone-degrading osteoclasts (OC) and bone-forming osteoblasts (OB). Excessive bone degradation results when this balance is compromised, for example by an increase in cytokines necessary for osteoclastogenesis. The OC are multinucleated cells that are specialized to degrade mineralized bone matrix through secretion of lysosomal enzymes in bone-degrading pits between the OC and the bone. OC are of monocytic origin and can be considered a specialized macrophage subtype. In normal bone homeostasis, OB and OC reciprocally regulate each other through cytokine-mediated signaling and cell-cell contact. The most prominent osteoclastogenic factor, receptor activator of nuclear factor κB ligand (RANKL), is expressed on the surface of OB[3]. Additionally, OB and stromal cells secrete cytokines such as colony-stimulating factor 1 (CSF-1), as well as transforming growth factor beta (TGF-β), tumor necrosis factor (TNF), and interleukins 6 and 1β (IL-6, IL-1β) to stimulate osteoclastogenesis[3,4]. In addition, TGF-β promotes osteoclastogenesis in multiple myeloma bone disease[5]. TNF, IL-6, and IL-1β does not induce osteoclastogenesis alone but synergize with RANKL to

Correspondence: Kristian K. Starheim (kristian.starheim@ntnu.no)
[1]CEMIR Centre of Molecular Inflammation Research, IKOM, NTNU, Trondheim, Norway
[2]Department of Hematology, St. Olavs University Hospital, Trondheim, Norway
Edited by I. Lavrik

SPRINGER NATURE CDDpress

induce osteoclastogenesis even at very low RANKL-levels[4,6]. The result is increased production and activity, and decreased turnover of OC[1,6]. Antibodies blocking TNF and IL-6 have proven highly efficient in a subset of rheumatoid arthritis patients, but they are costly and have adverse side effects[7]. Also, responses vary between patients, with 30-40 % having no or insufficient responses[8].

The baculoviral IAP repeat-containing protein 2 and 3 (BIRC2/3, also named cellular inhibitor of apoptosis 1 and 2, cIAP1/2), and x-linked inhibitor of apoptosis (XIAP) proteins are ubiquitin ligases that restrict several forms of regulated cell death, such as apoptosis and necroptosis[9]. cIAP1/2 are partly redundant and regulate inflammation through binding and ubiquitination of the receptor-interacting protein kinase 1 (RIPK1). RIPK1 and IAP signaling are central in the regulation of the hematopoietic compartment and macrophage differentiation[10,11]. RIPK1 is recruited to the cytoplasmic domain of several ligand-bound cytokine- and pattern-recognition receptors, including tumor necrosis factor receptor 1 (TNFR1). Upon receptor binding, RIPK1 is ubiquitinated by the ubiquitin ligases TNF-receptor associated factors 2, 5, and 6 (TRAF2, 5, 6), cIAP1/2, and others. Ubiquitinated RIPK1 recruits the kinases inhibitor of nuclear factor κ-B kinase α/β (IKKα/β) and TGF-β activated kinase 1 (TAK1), that further activates proinflammatory signaling, cytokine production, and differentiation through nuclear factor (NF)-κB and mitogen-activated protein kinases (MAPK)[12]. TAK1 can also be activated by RANK, and is necessary for osteoclastogenesis in mice[13]. Prolonged NF-κB activation or blockade of NF-κB activation leads to de-ubiquitination of RIPK1. The non-ubiquitinated RIPK1 binds to caspase 8 and RIPK3 to activate two forms of regulated cell death: apoptosis and lytic necroptosis, and under some circumstances pyroptosis[12,14]. Necroptosis is dependent on RIPK1 kinase activity, while apoptosis can be both dependent and independent on RIPK1 kinase activity[12]. Whereas cIAP1/2 restrain cell death by acting on the RIPK1-receptor complex, XIAP inhibits apoptotic executioner caspases 3 and 7, and can also block necroptosis[15–17].

IAP-inhibitors (also named Smac-mimetics, SM) have gained attention as novel treatment strategies both for cancer and chronic inflammatory diseases, but studies on primary human immune cells have been warranted[12,18]. Loss of IAP-activity triggers cell death through a dual mechanism. IAP-inhibitors lead to stabilization of the kinase mitogen-activated protein kinase kinase kinase 14 (Map3K14/NIK), with subsequent cleavage and activation of the transcription factor RelB and TNF-production[19]. SM will in parallel keep RIPK1 in an un-ubiquitinated form. Autocrine TNF stimulation of the deubiquitinated RIPK1 complex will then lead to cell death[12,20].

We hypothesized that SM could shift osteoclasts to cell death. The SM birinapant and LCL-161 are under phase 2 clinical trials for several cancer forms, including multiple myeloma (LCL-161). We found that they reduced osteoclastogenesis and induced cell death in primary human OC. On the basis of this, we propose that IAP-inhibitors can specifically act to reduce osteoclast number and excessive bone degradation.

Results

LCL-161 and birinapant reduce numbers and viability of differentiating osteoclasts

To test whether SM affected OC differentiation and viability, human $CD14^+$ monocytes were grown in OC differentiation medium supplemented with the SM birinapant and LCL-161 throughout differentiation. Birinapant has undergone phase 2 clinical trials for solid tumors (clinical trials ID NCT01188499[21]). LCL-161 is under phase 2 clinical trials for multiple myeloma (clinical Trials ID NCT01955434[22]).

LCL-161 and birinapant reduced the amount of mature OC compared to controls (Fig. 1A–D, total OC numbers are given in Supplementary Fig. S1C, E). This was accompanied by reduced viability, but reduced viability could not completely account for the reduction in OC numbers (Fig. 1E, Supplementary Fig. S1C, E). Birinapant potently blocked OC formation at the tested doses. SM cytotoxicity is described to be TNF-dependent[23]. A biosimilar of the TNF-blocking antibody infliximab reduced the number of OC and the combination of LCL-161 and infliximab further lowered the number of osteoclasts, but in an additive manner (Fig. 1B)[24]. Infliximab increased the viability of birinapant-treated cells (Fig. 1E).

To investigate whether differentiating OCs were especially sensitive to SM as compared to macrophages, we did a side-by-side comparison with differentiating macrophages (Mϕ). SM was cytotoxic both to differentiating OC and Mϕ, but differentiating OC displayed higher sensitivity than differentiating Mϕ (Fig. 1F, G). This was visible already at day 3 of differentiation (Supplementary Fig. S1F, G). RANKL and TGF-β both contributed to this increased sensitivity, but the contribution of each varied between donors (Supplementary Fig. S1H, I).

Birinapant and LCL-161 induce TNF-dependent cell death in pre-OC

To determine the mechanism of SM-induced cytotoxicity we established a standardized setup for SM-treatment of primary human pre-OC. $CD14^+$ monocytes were differentiated for 7 days in the OC differentiation medium. This time point was chosen as binuclear cells would appear after about one week, although with some donor variations. Pre-OC were treated with SM for the indicated time points. Birinapant and LCL-161 induced degradation of cIAP1, but not XIAP (Fig. 2A). The effect on cIAP2 levels varied between donors (data not shown).

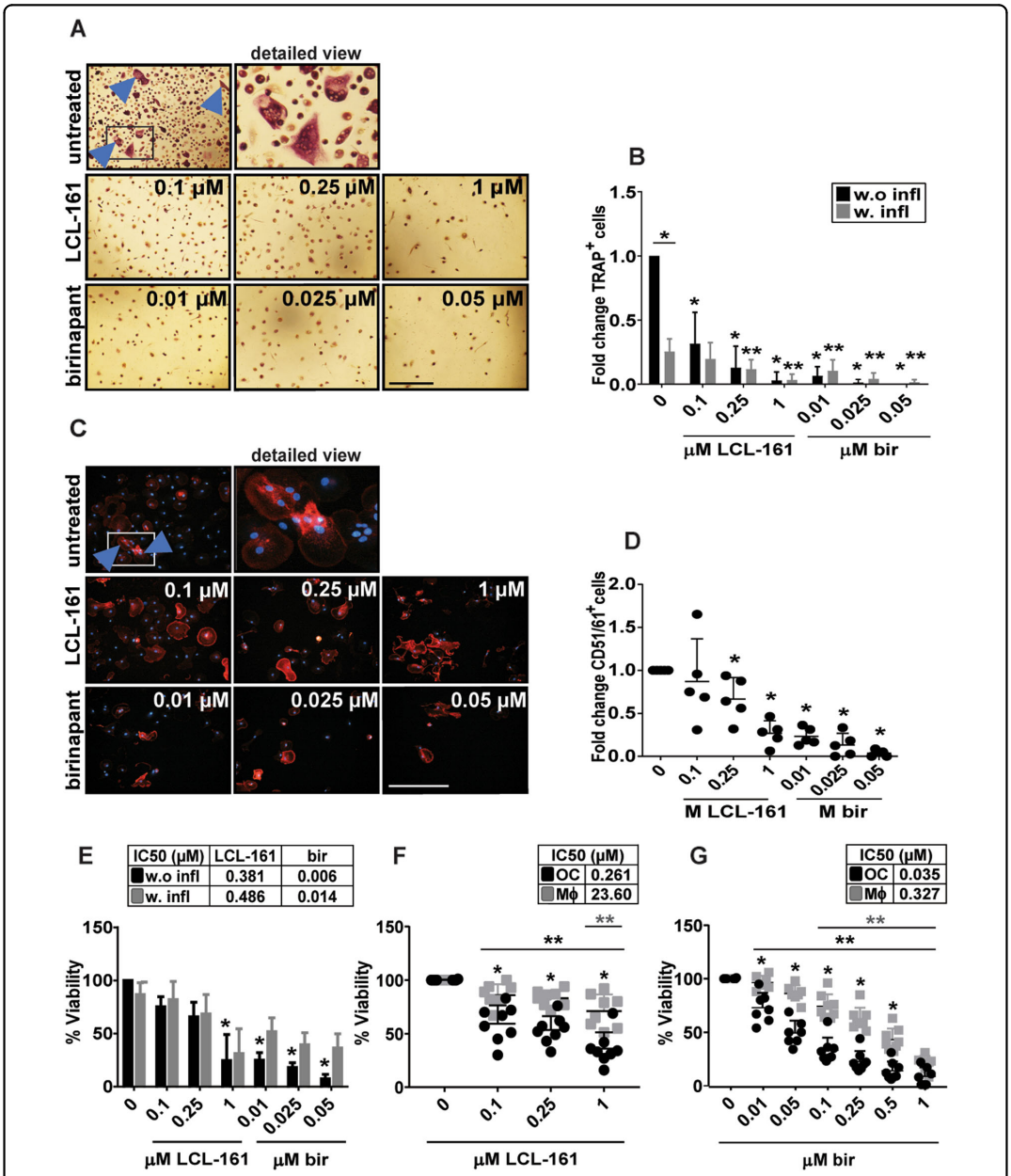

Fig. 1 (See legend on next page.)

Both inhibitors induced cell death, and birinapant was more potent than LCL-161. Co-treatment with TNF and SM gave a slight increase in cell death in some donors, but this was not consistent (Fig. 2B, C, Supplementary Fig. S2A, B). However, the TNF-binding antibody infliximab blocked SM-induced cell death (Fig. 2D, E). The same

(see figure on previous page)

Fig. 1 LCL-161 and birinapant reduce viability and number of differentiating OC. Human $CD14^+$-monocytes were treated with LCL-161 or birinapant at indicated concentrations throughout OC differentiation, typically 10-15 days (**A**–**E**). Representative phase-contrast images of $TRAP^+$-stained human OC, with arrowheads indicating multinuclear $TRAP^+$ cells. Frame in first column indicates cutout for detailed view. Bar is 150 μM (**A**). Fold change of $TRAP^+$ multinuclear cells after birinapant and LCL-161 treatment with or without infliximab (0.1 μg/ml) (**B**). Mean and standard deviations (SD) from 5 donors are shown. Single asterisk denotes statistical significance as compared to the untreated control or between indicated groups, double asterisk denotes statistical significance as compared to control treated with infliximab ($p < 0.05$, One-way ANOVA). Representative fluorescent microscope images of CD51/61-stained human OC, with arrowheads indicating multinuclear $CD51/61^+$ cells (**C**). Frame in first column indicates cutout for detailed view. Bar is 150 μM. Fold change of multinuclear $CD51/61^+$ cells after birinapant and LCL-161 treatment (**D**). 5 donors, mean and SD is shown. Asterisk denotes statistical significance as compared to the untreated control ($p < 0.05$, One-way ANOVA). Viability at the time of $TRAP^+$ quantification (**E**) shown as average and SD of 5 donors. Asterisk denotes statistical significance as compared to the untreated control ($p < 0.05$, One-way ANOVA). The viability of OC and Mϕ on day 10 of differentiation (F, G) measured with the Cell Titer Proliferation assay. 8 donors, mean, and SD are shown. Asterisk denotes statistical significance between groups, double asterisk denotes statistical significance between indicated controls (**F**, **G**) ($p < 0.05$, One-way ANOVA).

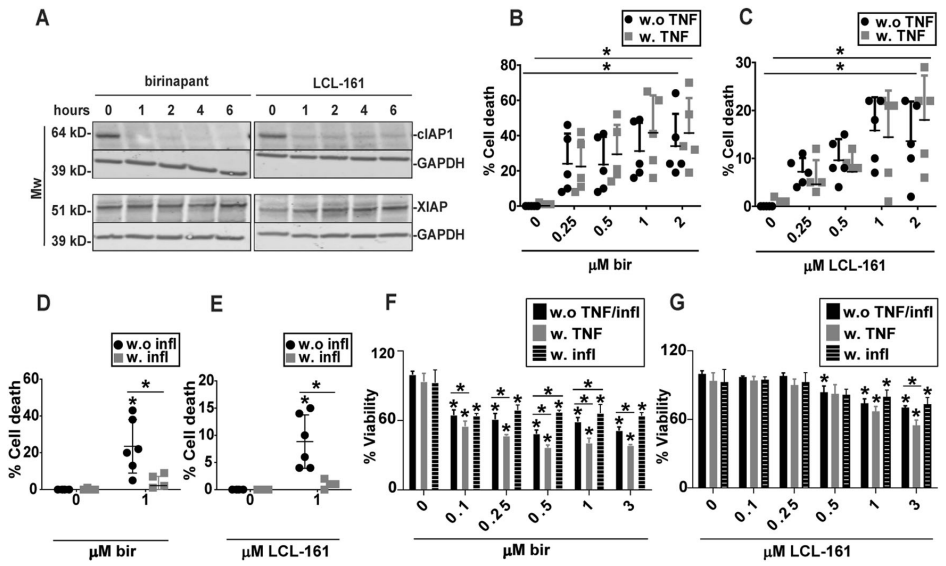

Fig. 2 Birinapant and LCL-161 trigger TNF-dependent cell death in pre-OC. Pre-OC were treated with 1 μM birinapant or LCL-161 at the indicated time points, and cell lysates were analyzed for cIAP1 and XIAP protein levels by immunoblotting. GAPDH is loading control, shown for corresponding membranes. One representative of three donors is shown (**A**). Pre-OC were treated with birinapant (**B**) or LCL-161 (**C**) alone or in combination with 25 ng/ml TNF for 18 h and analyzed for cell death. 5 donors, mean, and SD are shown. Pre-OCs were treated with 1 μM of birinapant (**D**) or LCL-161 (**E**) in combination with the TNF-blocking antibody infliximab (0.1 μg/ml) and analyzed for cell death. Cell death was measured by LDH-release (**B**–**E**), 6 donors, mean and are shown (**D**–**E**). Viability of hOCP after treatment with indicated concentrations of LCL-161 (**F**) and birinapant (**G**) alone or in combination with 25 ng/ml TNF for 18 h. Results are technical triplicates from one experiment. Cell viability was measured with the Cell Titer Glo assay. Asterisks indicate groups significantly different from control (**B**, **C**, **F**, **G**) or between indicated groups (**D**, **E**, **F**, **G**) ($p < 0.05$, One-way ANOVA).

effect was observed after treatment with the TNF-binding antibody 6H11 (Supplementary fig. S2C, D)[25].

We further wanted to investigate whether birinapant or LCL-161 induced TNF-production. We did not see SM-induced increase in the expression of *TNF*. Neither did we see changes in expression of the NF-κB controlled genes *IL6* or *CXCL8* by qPCR (Supplementary Fig. S2H, I, J). We did however detect TNF in the medium by ELISA (Supplementary Fig. S2F, G). This was in the picomolar range and did not change after SM treatment. This suggests that SM does not induce TNF-production in pre-OC, but rather that there is a low level of TNF in the culture that is sufficient to trigger cell death in concert with SM. The addition of RANKL, TGF-β or combination of the two did not affect SM sensitivity of pre-OC (Supplementary Fig. S2K, L).

As osteoclast cultures differentiated from primary monocytes contain cells of various differentiation status, we tested the effect of SM on purified human osteoclast

precursor cells (hOPC, Lonza). SM treatment of hOPC for 18 h gave a reduction in viability with birinapant being more potent than LCL-161. The addition of TNF weakly potentiated this effect (Fig. 2F, G). This was consistent with the effect observed in primary pre-OC. Co-treatment with infliximab reduced the loss of viability, demonstrating that at least part of the TNF is produced by the pre-OC themselves.

Birinapant induce apoptosis and necroptosis in pre-OC

TNF-driven SM cytotoxicity is mediated through RIPK1-dependent apoptosis or necroptosis. While apoptosis can be both dependent and independent of the RIPK1 kinase activity, necroptosis is RIPK1 kinase dependent[12]. To decipher the mode of cell death induced by SM we investigated whether the apoptotic and necroptotic inhibitors zVAD, necrosulfonamide (NSA) or necrostatin-1s (Nec-1s) were able to rescue pre-OC from SM-induced cell death. zVAD is a pan-caspase inhibitor that blocks apoptotic caspases, NSA inhibits the necroptotic effector MLKL while Nec-1s blocks RIPK1 kinase activity.

Nec-1s did not block birinapant cytotoxicity. Co-treatment with birinapant and zVAD potentiated birinapant. This can be explained by the function of caspase 8 in balancing cell death induction: inhibition can lead to excessive necroptosis[26]. The combination of zVAD and Nec-1s to a large extent neutralized birinapant + zVAD cytotoxicity (Fig. 3A). NSA alone did not significantly reduce birinapant-induced cytotoxicity, but it almost completely reversed birinapant + zVAD cytotoxicity (Fig. 3A).

LCL-161 treatment-induced low levels of cell death, and this was potentiated by zVAD. Combining LCL-161 + zVAD with Nec-1s or NSA blocked this cytotoxicity (Fig. 3B).

The RIPK3 inhibitor GSK872 did not affect birinapant-induced cell death (Supplementary Fig. S3A). However, the role of RIPK3 enzymatic activity in necroptosis is enigmatic, and it seems that RIPK3 kinase activity has several other roles besides phosphorylating and activating MLKL[27].

Birinapant-induced cleavage and activation of the apoptotic caspases 8 and 3, but kinetics differed between donors (Fig. 3C, Supplementary Fig. S7)[28]. RIPK1 and RIPK3 phosphorylation at serine 166 and 227, respectively was observed in a subset of donors, indicative of activation of the necroptotic kinase-cascade[29]. This supports a model where cell death can be mediated through both RIPK1 kinase dependent and independent death, necroptosis, and apoptosis, but with caspase 8/3 mediated apoptosis as the main pathway.

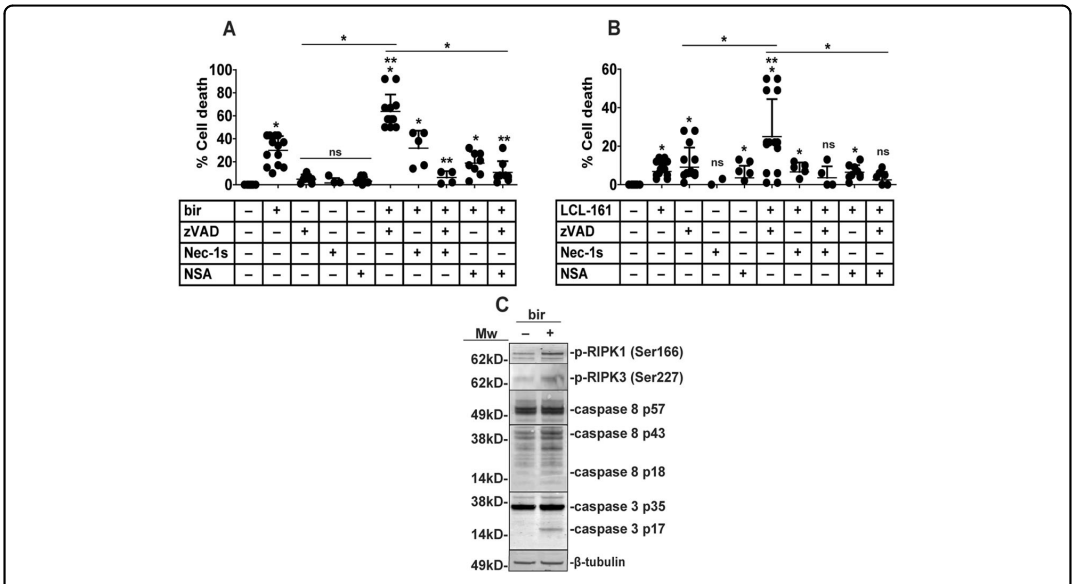

Fig. 3 Birinapant induces necroptosis and apoptosis in human pre-osteoclasts. Pre-OC were treated with birinapant (**A**) or LCL-161 (**B**) in combination with 20 μM zVAD, 1 μM NSA or 10 μM Nec-1s for 18 h before measuring the cytotoxicity by LDH-release, shown for 13 (A) and 15 (B) donors. Single asterisk denotes statistical significance as compared to the untreated control or between indicated groups, double asterisk denotes statistical significance as compared to SM treatment alone ($p < 0.05$, One-way ANOVA). Individual donors, average, and SD are shown. Pre-OC were treated with 1 μM birinapant for 4 h and cell lysates analyzed for caspase 8 cleavage, caspase 3 cleavage, RIPK1 serine 166 phosphorylation and RIPK3 serine 227 phosphorylation by immunoblotting (**C**). β-Tubulin is loading control. One representative of 7 donors is shown.

RIPK1-dependent apoptosis and necroptosis can trigger inflammasome activation and IL-1β release through caspase 8, RIPK3 as well as MLKL-induced membrane permeabilization[14,30,31]. We found no increased IL-1β levels in the medium of pre-OC IAP-treatment (Supplementary Fig. S3B, C).

Mouse osteoclasts display different dose-responses to SM than human OC

Loss of IAP-activity can increase osteoclastogenesis and bone degradation in mice[32,33]. This contrasts with our observed effects of SM on human OC. To test whether our findings were due to species differences or inhibitor-specific effects, we isolated monocytes from the bone marrow of C57BL/6 mice, differentiated them to OC and co-treated them with LCL-161 or birinapant throughout differentiation. Low doses of birinapant and LCL-161 and birinapant increased viability of differentiating OC, whereas higher doses recapitulated the effect observed in human differentiating OC (Fig. 4A–E, Supplementary Fig. S4A, B). Birinapant only reduced the number of $TRAP^+$ mouse OC numbers at 100-fold higher concentrations than what was observed for human OC (Fig. 4A, C, Supplementary Fig. S4B).

Both SM gave a dose-dependent reduction in viability in mouse pre-OCs (Supplementary Fig. S4C, D). Low doses of TNF were sufficient to potentiate SM cytotoxicity.

In sum, low doses of SM during differentiation increase the viability of mouse OCs while higher concentrations block osteoclastogenesis and reduce viability, with LCL-161 being more potent than birinapant.

LCL-161 and birinapant counter osteoclastogenesis driven by myeloma patient bone-marrow aspirate

To test whether LCL-161 and birinapant also had an effect on pathologically elevated osteoclastogenesis, we took advantage of our access to biobanked bone-marrow aspirate from multiple myeloma patients. Bone-marrow aspirate from myeloma patients is known to induce osteoclastogenesis and increase bone resorption. We differentiated osteoclasts in the presence of bone-marrow aspirate from myeloma patients or healthy controls. The effect of aspirate on SM sensitivity was calculated as fold change of $TRAP^+$ cells as compared to no aspirate. Buffy coat donors added some variation in absolute OC numbers (Supplementary Fig. S5A). 5% myeloma patient bone-marrow aspirate in OC differentiation medium was sufficient to increase osteoclastogenesis, while bone-marrow aspirate from healthy donors did not (Fig. 5A).

SM reduced OC numbers both for healthy controls and myeloma patients (Fig. 5A, Supplementary Fig. S5A). Thus, SM was efficient in blocking osteoclast formation also when osteoclastogenesis was pathologically elevated. Birinapant-induced cytotoxicity on the differentiating OC in the presence of bone-marrow aspirate, but this could not account for the full reduction in OC numbers (Fig. 5B). Neither LCL-161 nor birinapant reduced viability of human myeloma cell lines (Supplementary Fig. S5B–G), as has also been shown in other studies[22].

Discussion

In this work, we showed that the SM birinapant and LCL-161 reduced osteoclastogenesis and induced cell death in human differentiating OC and pre-OCs. They were also cytotoxic for differentiating human Mϕ, but with lower sensitivity. Birinapant was most potent, which is in accordance with earlier observations that bivalent SM is more potent than monovalent SM[18]. SM also dampened myeloma bone-marrow aspirate-driven osteoclastogenesis, giving a proof-of-concept that SM can neutralize pathologically induced osteoclastogenesis.

SM cytotoxicity in pre-OC was blocked by a biosimilar of the clinically approved TNF-blocking antibody infliximab. This is consistent with other studies showing that SM triggers cell death through an autocrine TNF-loop[34,35]. The observation that infliximab partly inhibit osteoclastogenesis, but reduce SM-induced death, warrant caution in combining SM with TNF-blocking antibodies as a treatment strategy for inflammatory diseases, and show that SM reduces viability of osteoclasts both in a TNF-dependent and independent manner: whereas low concentrations during differentiation reduced viability of OC independent of TNF, higher concentrations induced TNF-dependent cell death.

We did not observe an induction of *TNF* transcription after SM treatment. Rather, we observed a constitutive low level of TNF in the medium. This demonstrates that low levels of TNF might be sufficient to induce SM toxicity in pre-OCs.

Birinapant and LCL-161 cell death could go through both RIPK1 kinase dependent and caspase dependent. Birinapant-induced apoptosis in pre-OC, and also necroptosis in some donors. When caspases were inhibited by zVAD, this potentiated cell death through RIPK1 kinase and MLKL. On the other hand, necroptotic inhibitors did not affect cytotoxicity, and we speculate that cells then shift to apoptosis. These observations are consistent with a recently proposed concept of cell death plasticity, where cells can shift between different cell death mechanisms when required[36].

Both apoptosis and necroptosis can give inflammasome activation and IL-1β release, that is also involved in cytokine release syndrome[15,22]. Cytokine release syndrome is a dose limiting toxicity of SM[37,38]. Here, SM did not induce additional *TNF, IL6* or *CXCL8* expression, TNF, or IL-1β production, suggesting that SM trigger cell death without activating additional and possibly detrimental inflammation.

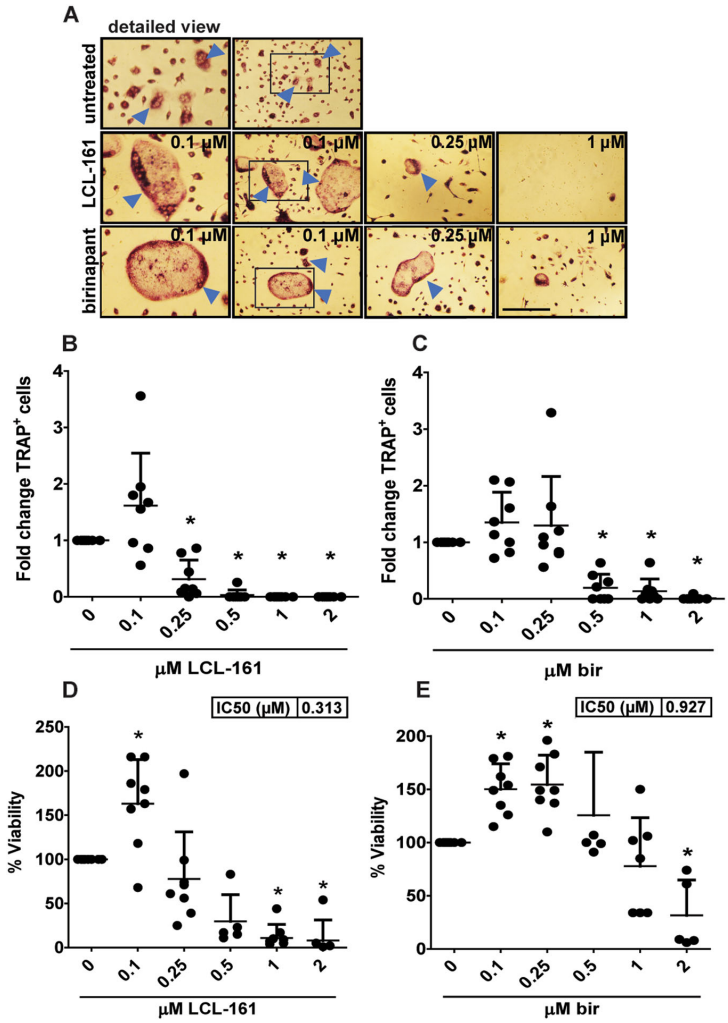

Fig. 4 SM induces dose-dependent effects on mouse osteoclasts. C57BL/6 mouse BMDMs were differentiated to OC and treated with LCL-161 and birinapant at indicated concentrations throughout OC differentiation (**A**–**E**). Representative phase-contrast images of TRAP-stained mouse OCs, with arrowheads indicating multinuclear TRAP$^+$ cells counted as OC. Frame in second column indicates cutout for detailed view. Bar is 150 µM (A). Fold change of TRAP$^+$ OCs after birinapant and LCL-161 treatment (**B**, **C**), shown for 8 donors. The viability of OC after differentiation SM was measured by the Cell Titer Proliferation Assay (**D**, **E**). Individual mice, mean, and SD are shown. Asterisk denotes statistical significance as compared to the untreated control ($p < 0.05$, One-way ANOVA).

Studies in mice have shown that SM can increase osteoclast numbers[32,33]. Consistent with this, we found that lower concentrations of SM increased viability and osteoclastogenesis in murine OCs, but that higher concentrations of SM reduced viability and numbers of mouse OC. We speculate that the increased osteoclast numbers in mice can be due to low concentrations of SM in the bone microenvironment. Birinapant reduced OC numbers at 100-fold higher concentrations than in human OC and was remarkably less cytotoxic, although showing similar effects in pre-OC. This confirms that there are species-specific differences in SM-response between mouse and humans, and warrants caution in extrapolating results from mouse models to humans. SM has been most

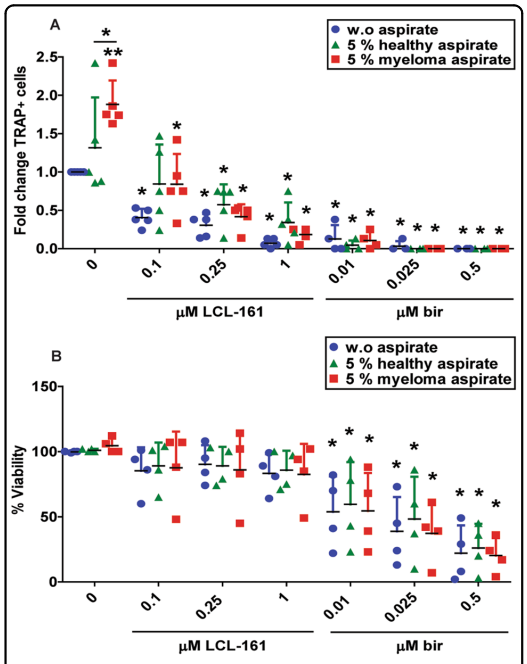

Fig. 5 SM blocks myeloma bone-marrow aspirate-driven osteoclastogenesis. Human CD14$^+$ monocytes were differentiated in OC differentiation medium supplemented with 5% bone-marrow aspirate from myeloma patients or healthy controls and treated with LCL-161 or birinapant at indicated concentrations throughout OC differentiation. TRAP$^+$ cells with 3 or more nuclei were counted as OC and represented as fold change of TRAP$^+$ cells as compared to no aspirate (w.o. aspirate) (**A**). Results are from 5 donors, mean and SD are indicated. Cell viability was measured by the Cell Titer Proliferation Assay (**B**). Results are from 4 donors, mean and SD is indicated. Single asterisk denotes statistical significance as compared to the untreated control within each group or between indicated groups. Double asterisk denotes statistical significance as compared to untreated control w.o aspirate ($p < 0.05$, One-way ANOVA).

extensively tested in neoplastic cell systems and mouse inflammatory models of cancer and inflammation, while studies in non-neoplastic human primary cells have been warranted[18].

In conclusion, we here present data in primary human osteoclasts that birinapant and LCL-161 blocks osteoclastogenesis and induce cytotoxicity in human OC. Both LCL-161 and birinapant are under clinical trials as cancer agents; LCL-161 is in phase 2 for multiple myeloma, and LCL-161 might therefore give an additional beneficial effect on reducing bone degradation in multiple myeloma patients. Based on our findings, birinapant and LCL-161 can also be relevant for treating pathological bone degradation, including those with chronic TNF-driven inflammation and osteoclastogenesis.

Materials and methods

Cell culture

To generate primary human osteoclasts and macrophages, peripheral blood mononuclear cells were isolated from healthy donors by density centrifugation. Buffy coats were provided by the Blood Bank (St. Olavs Hospital, Trondheim) with approval by the Regional Committee for Medical and Health Research Ethics (REC Central, Norway, No. 2009/2245). Subsequently, monocytes were isolated using CD14$^+$ magnetic bead separation according to the manufacturer's instructions (Miltenyi Biotec, Bergisch Gladbach, Germany, 130-050-201). The purity of isolated monocytes was assessed by flow cytometry. On average, 96% of the isolated monocytes expressed CD14 and frequencies of contaminating DC-, B-, T-, and NK-cell populations were below 0.5% (Supplementary fig. S1A, B). For human osteoclast differentiation, CD14$^+$ monocytes were plated in α minimum essential medium (αMEM, Thermo Fisher Scientific, Waltham, MA, USA, 41061-029) supplemented with 10% heat-inactivated human serum according to blood type, 30 ng/ml CSF-1 (216-MC), 10 ng/ml RANKL (390-TN-010), and 1 ng/ml TGF-β (240-B-002) (R&D systems, Minneapolis, MN, USA)[39,40]. In average, 2% of cells were scored as mature OC (Supplementary Fig. S1D). This is comparable to previous observations on primary human OC cultures[41]. Where indicated, bone-marrow aspirate from myeloma patients and healthy donors was added to the medium throughout differentiation to a final fraction of 5% (Fig. 5). Bone-marrow aspirate was provided by Biobank1 (St. Olavs Hospital, Trondheim) with approval by the Regional Committee for Medical and Health Research Ethics (REC Central, Norway, No. 2011/2029). Informed consent was obtained from all subjects, and samples were randomized for disease status. The cells were differentiated for 6-7 days to obtain osteoclast precursors (pre-OC), and until visible multinuclear cells for osteoclasts, typically 10-15 days. Macrophages were differentiated from CD14$^+$ monocytes cultured in αMEM supplemented with 10% heat-inactivated human serum according to blood type, and 100 ng/ml CSF-1.

For assessment of the effect of SM in a purified osteoclast system, human osteoclast precursor cells (hOCPs) were used (Lonza, Walkersville, MD, USA). The hOCPs were thawed, plated according to the manufacturer's instructions, and maintained in OCP medium (Lonza, PT-8201) in the presence of 33 ng/ml CSF-1 and 66 ng/ml RANKL. Cells were allowed to recover for 3 days before SM-treatment. To evaluate the purity of the hOCP, cells were differentiated for 5 days to obtain mature osteoclasts, and then TRAP-stained. We observed 67% multinuclear TRAP$^+$ cells after hOCP differentiation (Supplementary Fig. S2E).

The multiple myeloma cell line INA-6 (a kind gift from Dr. Martin Gramatzki, Erlangen, Germany[42]) was grown

in 10% heat-inactivated fetal calf serum (FCS) in RPMI-1640 medium (Sigma-Aldrich, St. Louis, MO, USA, R8758) supplemented with 1 ng/ml recombinant human IL-6 (Gibco, Thermo Fisher Scientific, PHC0061). JJN3 cells (a kind gift from Dr. Jennifer Ball, Department of Immunology, University of Birmingham, UK) were maintained in 10% heat-inactivated FCS in RPMI-1640 medium. RPMI-8226 cells (obtained from ATCC, Rockville, MD, USA) were grown in 20% heat-inactivated FCS in RPMI-1640 medium. All cell lines were routinely checked for mycoplasma contamination and the authenticity was confirmed using DNA-fingerprinting[43].

For the generation of mouse osteoclasts, bone marrow was isolated from mouse femurs of female and male C57BL/6 mice (between 2 and 10 months of age, FOTS ID 16832), red blood cells were removed by red blood cell lysis buffer (Thermo Fischer Scientific, 00-4333), and remaining cells were seeded out in 10 or 15 cm dishes in αMEM (Thermo Fisher Scientific) supplemented with 10% FCS and 100 ng/ml recombinant mouse CSF-1 (R&D Systems, 416-ML). Adherent bone-marrow-derived mononuclear cells (BMDM) were washed in sterile PBS and detached using Trypsin/EDTA and cell scraping. The cells were then spun down and resuspended in αMEM with 10% FCS, 30 ng/ml recombinant mouse CSF-1, 10 ng/ml recombinant mouse RANKL (R&D Systems, 462-TEC) and differentiated for 4–5 more days to obtain osteoclasts[13].

The following compounds were used in cell culture: 6H11 (TNF-binding antibody[25]), birinapant (Selleckchem, Munich, Germany, S7015), carbobenzoxy-valyl-alanyl-aspartyl-[O-methyl]-fluoromethylketone (zVAD, R&D Systems, FMK001), GSK872 (Selleckchem, S8465), infliximab biosimilar (Absolute Antibody, Redcar, UK, Ab00146-10.3), LCL-161 (Selleckchem, S7009), necrostatin-1s (Nec-1s, BioVision, Mountain View, CA, USA, 2263-1), necrosulfamide (NSA, BioVision, 9635-10), recombinant human and mouse TNF (PeproTech Nordic, Stockholm, Sweden, 300-01 A and R&D Systems, 410-MT-025).

Flow cytometry

After $CD14^+$ magnetic bead separation, purity of monocytes for osteoclast and macrophage differentiation was assessed by flow cytometry. A fraction of cells was stained with Fixable Viability Dye eFluor 780 (eBioscience, San Diego, CA, USA, 650865-14). Subsequently, Fc-receptors were blocked (Human SeroBlock, BioRad, BUF070B) and cells stained with fluorescent antibodies. Cells were stained for CD14 (PerCP/Cyanine 5.5, BD Biosciences, San Jose, CA, USA, 562692, or FITC, eBioscience, 11-0149-42), CD11b (PE, BD Biosciences, 333142) and CD45 (Alexa Fluor 700, eBioscience, 56-9459-42). Contaminating cell populations were identified by staining for CD3 (FITC, BioLegend, San Diego, CA, USA, 317306), CD19 (eFluor450, eBioscience, 48-0199-42), CD56 (APC, eBioscience, 17-0567-42), CD11c (PE/Cyanine, BioLegend, 331516), and CD303 (PerCP/Cyanine5.5, BioLegend, 354210). Staining with fluorescence-matched isotype control antibodies and staining for total peripheral blood mononuclear cells was performed as controls. Cells were analyzed on a BD LSRII flow cytometer and data were analyzed by FlowJo_V10 software (FlowJo, LLC, Ashland, OR, USA). Frequencies of $CD14^+$ monocytes and contaminating cells were identified from the viable cell population and quantified using GraphPad Prism6 (La Jolla, CA, USA) software (Supplementary fig. S1A, B).

Assessment of osteoclast differentiation

The number of mature osteoclasts was assessed by scoring the number of multinucleated cells (≥3 nuclei) that were positive for tartrate resistant acid phosphatase (TRAP) or integrin alpha V/ beta 3 (CD51/61)[41]. The cells were fixed and stained for TRAP using the Leukocyte Acid Phosphatase Kit (Sigma-Aldrich, 387A-1KT) according to the manufacturer's instructions. For CD51/61 scoring, cells were fixated by paraformaldehyde and stained for CD51/61 (BioLegend, 304416) and Hoechst 33342 as nuclear stain (Thermo Fisher Scientific, H3570). Cells were imaged using EVOS FL Auto 2 Cell Imaging System (Thermo Fisher Scientific, Norway).

Cytotoxicity and viability assays

For cell death assessment of pre-OC, cells were stimulated in Opti-MEM serum-free medium (Thermo Fisher Scientific, 11058-021), and cell death was calculated by measuring lactate dehydrogenase-release (LDH) in medium using a colorimetric assay according to the manufacturer's instructions (TaKaRa Bio, Saint-Germain-en-Laye, France, MK401). Cell viability was measured using the colorimetric Cell titer 96® AQueous One Solution Cell Proliferation Assay (Promega, Madison, WI, USA, G358C) or the luminescent CellTiter-Glo® 2.0 Cell Viability Assay (Promega, G9242).

ELISA

The levels of TNF and IL-1β in the medium were quantified by enzyme-linked immunosorbent assay (ELISA, R&D Systems, DY210, and DY201) according to the manufacturer's instructions. The absorption at 450 nm was immediately detected using a 96-well plate reader (Bio-Rad, Hercules, CA, USA, 16692) and the Microplate Manager Software (Bio-Rad).

RNA extraction and qPCR

Total RNA was extracted from SM treated pre-OC using RNeasy Mini kits including DNAse digestion with Qiacube (QIAGEN, Hilden, Germany, 74104). Synthesis of cDNA was carried out with the High-Capacity RNA-to-cDNA kit according to the manufacturer's instructions (Applied Biosystems, Thermo Fisher Scientific, 4387406). Relative gene expression of *TNF*, *IL6*, and *CXCL8* were quantified by

Real-Time Quantitative PCR and TaqMan Gene Expression Reagents (Applied Biosystems, 4364340) according to the manufacturer's instructions. *ACTB* was used as endogenous control. Samples were run in duplicates on StepOnePlus Real-Time PCR System (Applied Biosystems) and analyzed by the Applied Step One software 2.3 (Applied Biosystems). The following probes were used: *TNF* (Hs01113624_g1), *IL6* (Hs00985639_m1), *CXCL8* (Hs00174103_m1), and *ACTB* (Hs03023943_g1). Genes with a Ct value above 35 were considered as not detected.

Cell lysis and immunoblotting

Cells were washed with ice-cold phosphate-buffered saline (PBS) and lysed for 15 min on ice (50 mM tris-HCl, 1% TritonX-100, 150 mM NaCl, 5 mM EDTA, protease inhibitor cocktail (Roche, Basel, Switzerland, 1187358001), 1 mM Na_3VO_4 and 50 mM NaF). The samples were separated on NuPAGE Bis-Tris gels with MOPS or MES running buffer (Invitrogen, Thermo Fisher Scientific). Proteins were transferred from the gel onto a 0.2 µm nitrocellulose membrane using the iBlot gel transfer system (Life Technologies, Thermo Fisher Scientific). The membrane was blocked with 5% BSA in tris-buffered saline with 0.01% Tween 20 (TBS-T) and incubated with primary antibodies. Blots were washed with TBS-T before incubation with horse-radish peroxidase- or fluorophore-conjugated secondary antibodies (Dako, Agilent, Santa Clara, CA, USA and LiCor Biosciences, Lincoln, NE, USA). Membranes were analyzed on a LiCor Fc or xCT (LiCor Biosciences). For luminescence, a SuperSignal West Femto luminescence substrate was used (Thermo Fisher Scientific, 34096).

The following antigens were analyzed (antibodies in parenthesis): BIRC2/cIAP1 (Enzo, New York, NY, USA, ALX-803-335-C100), β-tubulin (Abcam, Cambridge, UK, Ab6046), β-actin (Cell Signaling Technologies (CST), Danvers, MA, USA, 4970), caspase 3 (CST, 9662), caspase 8 (Enzo, ALX-804-242-C100), GAPDH (CST, 2118), RIPK1 phospho-Ser166 (CST, 44590), RIPK3 phospho-Ser227 (CST, 93654), XIAP (CST, 20425).

Statistical analysis

Experiments were performed on individual donors. For cell death, viability, TRAP, and ELISA experiments, individual donors are displayed with average and standard deviation of donors indicated on the plot. Statistical analyses were performed using GraphPad Prism6 (La Jolla, CA, USA). A sample size of 5 or more donors was used for most primary cell experiments. For experiments performed on fewer than 5, no statistical tests were performed. Exceptions are Fig. 2F–G, Supplementary Fig. S2C-D, Supplementary Fig. S4C, D and Fig. 5B. This was due to limited availability of hOCP donors (Lonza), the TNF-blocking antibody 6H11, mice and bone-marrow aspirate from myeloma patients, respectively. The statistical tests used were one sample Student's *t* test for pair-wise comparison, and one-way ANOVA with Bonferroni correction for comparison of multiple groups. Statistical significance is marked with asterisk in the figures.

Acknowledgements

This work was supported by grants from The Norwegian Cancer Society (project ID 6799133), The Liaison Committee for education, research and innovation in Central Norway, the Joint Research Committee between St. Olavs Hospital and Faculty of Medicine and Health Science, NTNU, and the Research Council of Norway through its Center of Excellence funding scheme (project number 2223255/F50). Mice were provided by the Comparative medicine Core Facility (CoMed), NTNU. CoMed is funded by the Faculty of Medicine at NTNU and Central Norway Regional Health Authority. Imaging using the EVOS FL Auto 2 Cell Imaging System was performed at the Cellular and Molecular Imaging Core Facility (CMIC), NTNU. CMIC is funded by the Faculty of Medicine at NTNU and Central Norway Regional Health Authority. We thank Professor Terje Espevik (NTNU) for the 6H11 antibody, Marie Holter-Sørensen for technical assistance, Lill-Anny Grønseth (Biobank1) for assistance with patient samples, and professors Geir Bjørkøy and Egil Lien for input on the manuscript. We would also thank our user panel of myeloma patients for inspiring discussions.

Conflict of interest

The authors declare no competing interests.

Supplementary information The online version contains supplementary material available at https://doi.org/10.1038/s41420-021-00415-1.

Received: 10 December 2020 Accepted: 9 January 2021
Published online: 19 February 2021

References

1. Michalski, M. N. & McCauley, L. K. Macrophages and skeletal health. *Pharmacol. Ther.* **174**, 43–54 (2017).
2. Palumbo, A. & Anderson, K. Multiple myeloma. *N. Engl. J. Med.* **364**, 1046–1060 (2011).
3. Teitelbaum, S. L. Bone resorption by osteoclasts. *Science* **289**, 1504–1508 (2000).
4. Del Fattore, A., Teti, A. & Rucci, N. Osteoclast receptors and signaling. *Arch. Biochem. Biophys.* **473**, 147–160 (2008).
5. Itonaga, I. et al. Transforming growth factor-β induces osteoclast formation in the absence of RANKL. *Bone* **34**, 57–64 (2004).
6. Ginaldi, L. & De Martinis, M. Osteoimmunology and beyond. *Curr. Med. Chem.* **23**, 3754–3774 (2016).
7. Lenert, A. & Lenert, P. Tapering biologics in rheumatoid arthritis: a pragmatic approach for clinical practice. *Clin. Rheumatol.* **36**, 1–8 (2016).
8. Bek, S. et al. Systematic review and meta-analysis: pharmacogenetics of anti-TNF treatment response in rheumatoid arthritis. *Pharmacogenomics J.* **17**, 403–411 (2017).
9. Silke, J. & Vaux, D. L. IAP gene deletion and conditional knockout models. *Semin. Cell Dev. Biol.* **39**, 97–105 (2015).
10. Roderick, J. E. et al. Hematopoietic RIPK1 deficiency results in bone marrow failure caused by apoptosis and RIPK3-mediated necroptosis. *Proc. Natl Acad. Sci.* **111**, 14436–14441 (2014).
11. Wong, W. W. L. et al. cIAPs and XIAP regulate myelopoiesis through cytokine production in an RIPK1- And RIPK3-dependent manner. *Blood* **123**, 2562–2572 (2014).
12. Brenner, D., Blaser, H. & Mak, T. W. Regulation of tumour necrosis factor signalling: live or let die. *Nat. Rev. Immunol.* **15**, 362–374 (2015).
13. Lamothe, B., Lai, Y., Xie, M., Schneider, M. D. & Darnay, B. G. TAK1 is essential for osteoclast differentiation and is an important modulator of cell death by apoptosis and necroptosis. *Mol. Cell. Biol.* **33**, 582–595 (2013).

14. Orning, P. et al. Pathogen blockade of TAK1 triggers caspase-8–dependent cleavage of gasdermin D and cell death. *Science* **1069**, eaau2818 (2018).
15. Fulda, S. Molecular pathways: targeting death receptors and smac mimetics. *Clin. Cancer Res.* 20, 3915–3920 (2014).
16. Wicki, S. et al. Loss of XIAP facilitates switch to TNFα-induced necroptosis in mouse neutrophils. *Cell Death Dis.* **7**, e2422 (2016).
17. Lawlor, K. E. et al. XIAP loss triggers RIPK3- and Caspase-8-Driven IL-1β activation and cell death as a consequence of TLR-MyD88-induced cIAP1-TRAF2 degradation. *Cell Rep.* **20**, 668–682 (2017).
18. Jensen, S., Seidelin, J. B., LaCasse, E. C. & Nielsen, O. H. SMAC mimetics and RIPK inhibitors as therapeutics for chronic inflammatory diseases. *Sci. Signal.* **13**, eaax8295 (2020).
19. Varfolomeev, E. et al. c-IAP1 and c-IAP2 are critical mediators of tumor necrosis factor alpha (TNFalpha)-induced NF-kappaB activation. *J. Biol. Chem.* **283**, 24295–24299 (2008).
20. Boyce, B. F., Xiu, Y., Li, J., Xing, L. & Yao, Z. NF-κB-mediated regulation of osteoclastogenesis. *Endocrinol. Metab.* **30**, 35 (2015).
21. Noonan, A. M. et al. Pharmacodynamic markers and clinical results from the phase 2 study of the SMAC mimetic birinapant in women with relapsed platinum-resistant or -refractory epithelial ovarian cancer. *Cancer* **122**, 588–597 (2016).
22. Chesi, M. et al. IAP antagonists induce anti-tumor immunity in multiple myeloma. *Nat. Med.* **22**, 1411–1420 (2016).
23. Fulda, S. Targeting inhibitor of apoptosis proteins for cancer therapy: a double-edge sword? *J. Clin. Oncol.* **32**, 3190–3191 (2014).
24. Azuma, Y., Kaji, K., Katogi, R., Takeshita, S. & Kudo, A. Tumor necrosis factor-alpha induces differentiation of and bone resorption by osteoclasts. *J. Biol. Chem.* **275**, 4858–4864 (2000).
25. Liabakk, N. B., Nustad, K. & Espevik, T. A rapid and sensitive immunoassay for tumor necrosis factor using magnetic monodisperse polymer particles. *J. Immunol. Methods* **134**, 253–259 (1990).
26. Schworer, S. A. et al. Toll-like receptor-mediated downregulation of the deubiquitinase CYLD protects macrophages from necroptosis in wild-derived mice. *J. Biol. Chem.* **289**, 14422–14433 (2014).
27. Lawlor, K. E. et al. RIPK3 promotes cell death and NLRP3 inflammasome activation in the absence of MLKL. *Nat. Commun.* **6**, 6282 (2015).
28. Algate, K., Haynes, D. R., Bartold, P. M., Crotti, T. N. & Cantley, M. D. The effects of tumour necrosis factor-α on bone cells involved in periodontal alveolar bone loss; osteoclasts, osteoblasts and osteocytes. *J. Periodontal Res.* **51**, 549–566 (2016).
29. Galluzzi, L. et al. Molecular mechanisms of cell death: recommendations of the Nomenclature Committee on Cell Death 2018. *Cell Death Differ.* **25**, 486–541 (2018).
30. Vince, J. E. et al. Inhibitor of apoptosis proteins limit RIP3 kinase-dependent interleukin-1 activation. *Immunity* **36**, 215–227 (2012).
31. Gutierrez, K. D. et al. MLKL activation triggers NLRP3-mediated processing and release of IL-1β independently of gasdermin-D. *J. Immunol.* 198, 2156–2164 (2017).
32. Yang, C. et al. Antagonism of inhibitor of apoptosis proteins increases bone metastasis via unexpected osteoclast activation. *Cancer Discov.* **3**, 212–223 (2013).
33. Casimiro, S. et al. RANKL enhances the effect of an antagonist of inhibitor of apoptosis proteins (cIAPs) in RANK-positive breast cancer cells. *J. Bone Oncol.* **2**, 116–122 (2013).
34. Abhari, B. A. et al. RIP1 is required for IAP inhibitor-mediated sensitization for TRAIL-induced apoptosis via a RIP1/FADD/caspase-8 cell death complex. *Oncogene* **32**, 3263–3273 (2013).
35. Petersen, S. L. et al. Autocrine TNFalpha signaling renders human cancer cells susceptible to Smac-mimetic-induced apoptosis. *Cancer Cell.* **12**, 445–456 (2007).
36. Samir, P., Malireddi, R. K. S. & Kanneganti, T.-D. The PANoptosome: a deadly protein complex driving pyroptosis, apoptosis, and necroptosis (PANoptosis). *Front. Cell. Infect. Microbiol.* **10**, 238 (2020).
37. West, A. C. et al. The SMAC mimetic, LCL-161, reduces survival in aggressive MYC-driven lymphoma while promoting susceptibility to endotoxic shock. *Oncogenesis* **5**, e216–e216 (2016).
38. Infante, J. R. et al. Phase I dose-escalation study of LCL161, an oral inhibitor of apoptosis proteins inhibitor, in patients with advanced solid tumors. *J. Clin. Oncol.* **32**, 3103–3110 (2014).
39. Harre, U. et al. Glycosylation of immunoglobulin G determines osteoclast differentiation and bone loss. *Nat. Commun.* **6**, 6651 (2015).
40. Westhrin, M. et al. Monoclonal immunoglobulins promote bone loss in multiple myeloma. *Blood* **136**, 2656–2666 (2020).
41. Madel, M.-B., Ibáñez, L., Rouleau, M., Wakkach, A. & Blin-Wakkach, C. A novel reliable and efficient procedure for purification of mature osteoclasts allowing functional assays in mouse cells. *Front. Immunol.* **9**, 1–12 (2018).
42. Burger, R. et al. Gp130 and ras mediated signaling in human plasma cell line INA-6: a cytokine-regulated tumor model for plasmacytoma. *Hematol. J.* **2**, 42–53 (2001).
43. Keats, J. J., Chesi, M., Kuehl, W. M. & Bergsagel, P. L. A simple and reliable method to verify the authenticity and purity of human myeloma cell lines. *Blood* **110**, 2485–2485 (2007).

Supplementary material for

SMAC-MIMETICS REDUCE NUMBERS AND VIABILITY OF HUMAN OSTEOCLASTS

Ingrid Nyhus Moen (1, 2), Marita Westhrin (1), Erling Håland (1), Markus Haug (1), Unni Nonstad (1), Merisa Klaharn (1), Therese Standal (1), Kristian K. Starheim (1,2).

1) CEMIR Centre for Molecular Inflammation Research, IKOM, NTNU, Trondheim. Norway.

2) Department of Hematology, St. Olavs University Hospital, Trondheim, Norway.

Correspondence: Kristian K. Starheim, Faculty of Medicine and Health Sciences, Department for Clinical and Molecular Medicine (IKOM), Norwegian University of Technology and Natural Sciences (NTNU), Pb. 8905, N-7491 Trondheim, NORWAY. E-mail: Kristian.starheim@ntnu.no, tel. +4790178148.

Running title: Smac-mimetics reduce osteoclast numbers.

Conflict of interest: The authors declare no conflict of interest.

Disclosure: The authors have no disclosures.

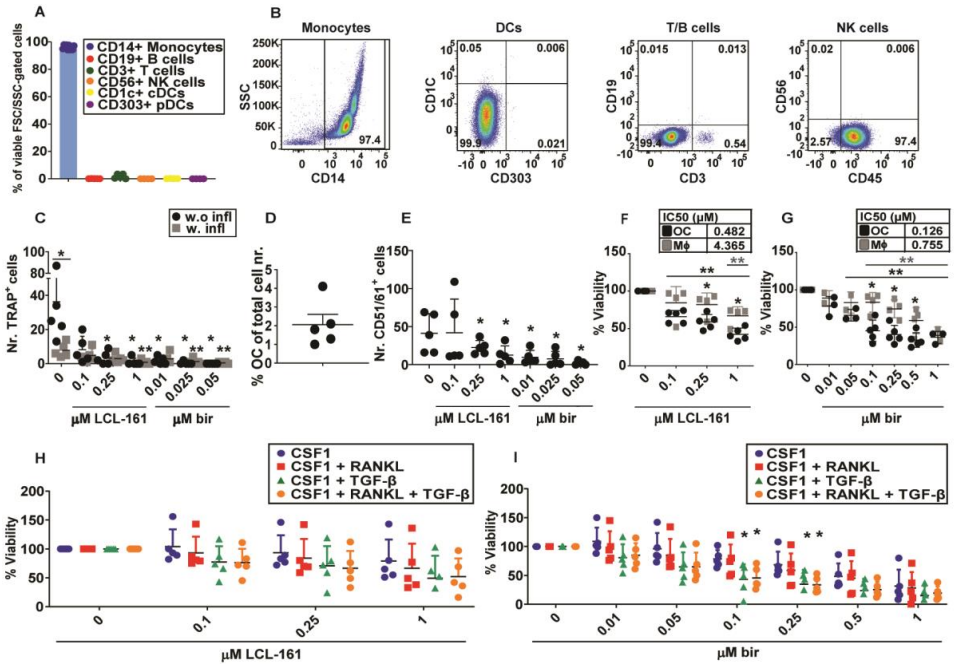

Supplementary Figure S1. Purity analysis of CD14-isolated monocytes, and sensitivity of OC and Mϕ to SM. Purity analysis of $CD14^+$ monocytes isolated from peripheral mononuclear blood cells and content of contaminating DC, T-, B- and NK-cells by flow cytometry (A, B). 10 ($CD14^+$), 5 ($CD19/CD3^+$) and 4 ($CD45/CD56^+$, $CD1C/CD303^+$) donors were quantified in (A), representative plots from one donor are shown in (B). Human $CD14^+$ monocytes were differentated to OC and treated with indicated concentrations of LCL-161 and birinapant with or without infliximab (0.1 µg) throughout differentation. $TRAP^+$ cells with 3 or more nuclei were counted as OC (C). Results are from 5 donors. Individual donors, average and SD are shown. Single asterisk denotes statistical significance as compared to untreated control or between indicated groups. Double asterisk denotes statistical significance as compared to control treated with infliximab ($p<0.05$, One-way ANOVA). % OC of total cell number (D) and number of OC (E) of $CD51/61^+$ cells with 3 or more nuclei counted as OC . Results are from 5 donors. Individual donors, average and SD are shown. Asterisk denotes statistical significance as compared to untreated control ($p<0.05$, Student's T-Test). Human $CD14^+$-monocytes were differentiated in OC differentiating medium or CSF-1 and treated with the indicated doses of SM for three days before viability was measured (F, G). Results are from 5 donors. Individual donors, average and SD are shown. Asterisk denotes statistical significance compared between groups. Double asterisk denotes statistical significance as compared to individual controls ($p<0.05$, One-way ANOVA). Viability of CSF-1, CSF-1 + RANKL, CSF-1 + TGF-β and CSF-1 + RANKL + TGF-β differentiated cells after LCL-161 (H) and birinapant (I) treatment measured by the Cell Titer Proliferation assay on day 10 of differentiation, shown for 5 donors. Individual donors, average and SD are shown. Asterisk denotes statistical significance as compared to cells cultured in CSF-1 ($p<0.05$, One-way ANOVA).

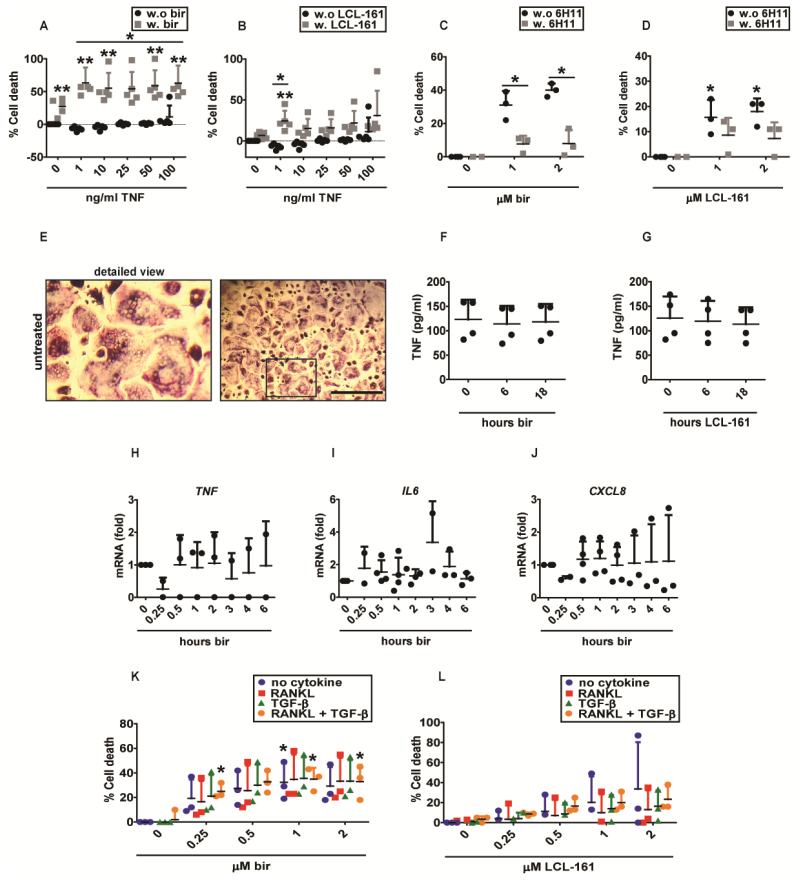

Supplementary Figure S2: LCL-161 and birianapant induce cell death in human pre-OCs dependent on TNF. Pre-OC were treated with 1 µM birinapant (A) or LCL-161 (B) in combination with indicated concentrations of TNF for 18 h, before cell ceath was measured by the LDH cytotoxcicity assay. Results are from 5 donors. Individual donors, average and SD are shown. Single asterisk denotes statistical significance as compared to untreated control. Double asterisk denotes statistical significance between groups ($p<0.05$, One-way ANOVA). Pre-OC were treated with 1 µM of birinapant (A) or LCL-161 (B) in combination with the TNF-binding antibody 6H11 for 18 h, before cell death was measured by the LDH cytotoxicity assay. Results are from 3 donors. Individual donors, average and SD are shown. Asterisk denotes statistical significance as compared to the untreated control or between indicated groups ($p<0.05$, One-way ANOVA). Representative phase-contrast image of TRAP-stained hOCP. Frame in second column indicate cutout for detailed view. Bar is 150 µM (E). Pre-OC were treated with 1 µM birinapant (F) or LCL-161 (G) for the indicated time points, and the concentration of TNF in medium was measured by ELISA, shown for 4 donors. Pre-OC were treated with 1 µM of birinapant for the indicated time points, RNA was isolated and analyzed for levels of *TNF*, *IL6* and *CXCL8* by qPCR (H-J), shown for 4 donors. Pre-OC were co-treated with the indicated doses of birinapant (K) or or LCL-161 (L) in combination with the indicated cytokines for 18 h before cell death was measured by the LDH cytotoxicity assay, shown for 3 donors. Individual donors, average and standard deviations are shown. Asterisk denotes statistical significance as compared to individual controls ($p<0.05$, One-way ANOVA).

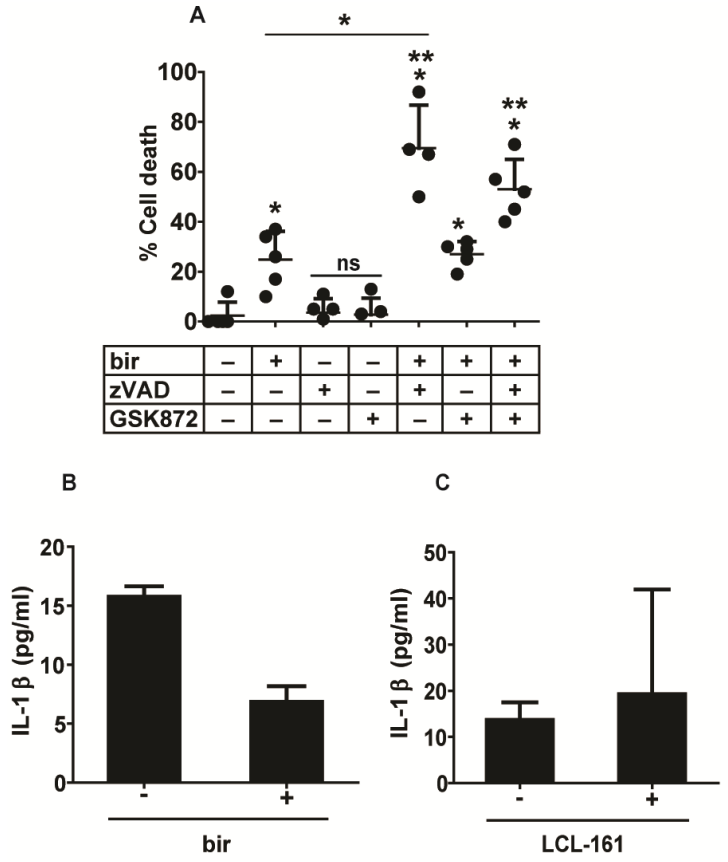

Supplementary Figure S3. **SM effects on RIPK3 inhibition and IL-1β production**. Pre-OC were treated with 1 µM birinapant in combination with 20 µM zVAD and/or 1 µM RIPK3 inhibitor GSK872 for 18 hours before measuring the cytotoxicity by LDH-release (A). Five donors, average and standard deviations are shown. Single asterisk denotes statistical significance as compared to the untreated control or between indicated groups, double asterisk indicates statistical significant difference from birinapant alone ($p<0.05$, One-way ANOVA). Pre-OC were treated with 1 µM birinapant (B) or LCL-161 (C) for 18 h, medium was collected, and the contentration of IL-1β was measured by ELISA. Average and SD for 3 individual donors is shown.

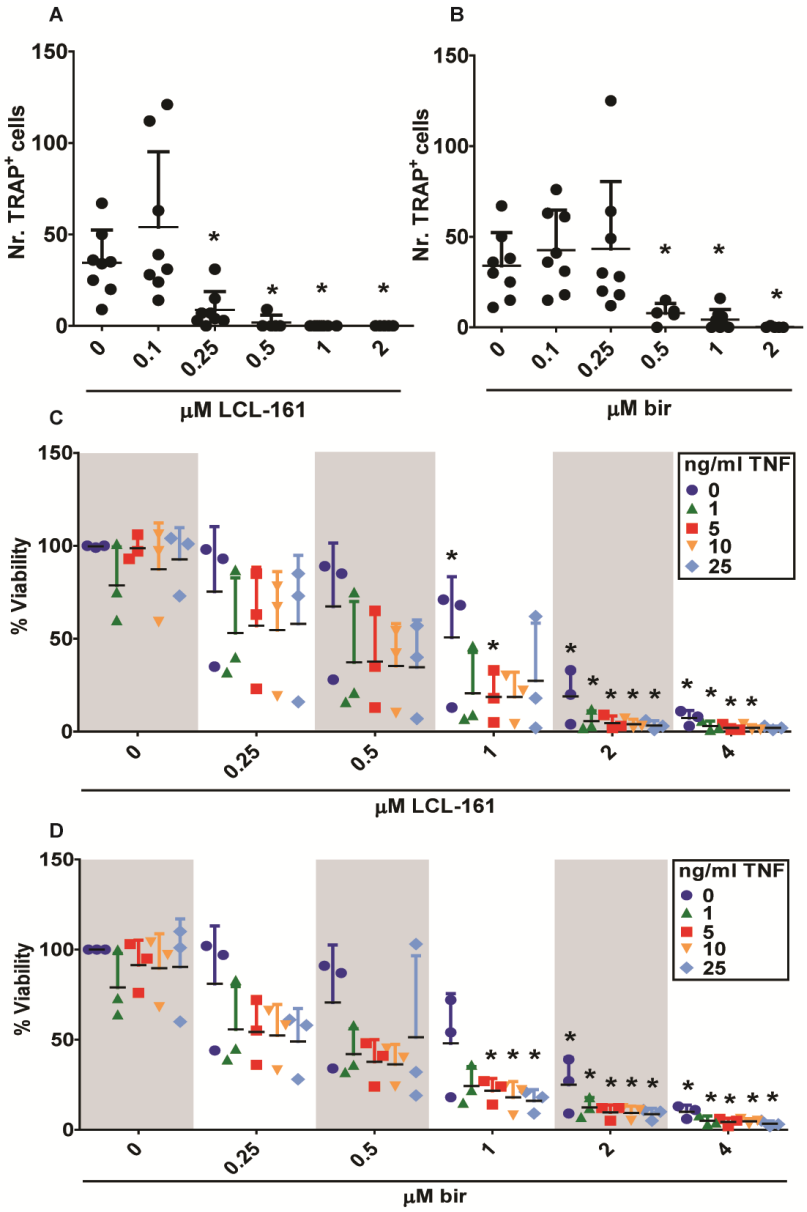

Supplementary Figure S4. Effect of SM on mouse OC. C57BL/6 mouse BDMDs were differentated to OC and treated with indicated concentrations of LCL-161 (A) and birinapant (B) throughout differentation. TRAP$^+$ cells with 3 or more nuclei were counted as OC (A, B), shown for 8 donors. Individual donors, mean and SD are shown. Asterisk denotes statistical significance as compared to the untreated control ($p<0.05$, One-way ANOVA). Viability of mouse pre-OC after treatment with indicated concentrations of LCL-161 (C) or birinapant (D) in combination with indicated concentrations of TNF for 18 h, shown for 3 donors. Viability was measured by the Cell Titer Glo assay. Individual donors, average and standard deviations are shown. Asterisk denotes statistical significance as compared to untreated controls ($p<0.05$, One-way ANOVA).

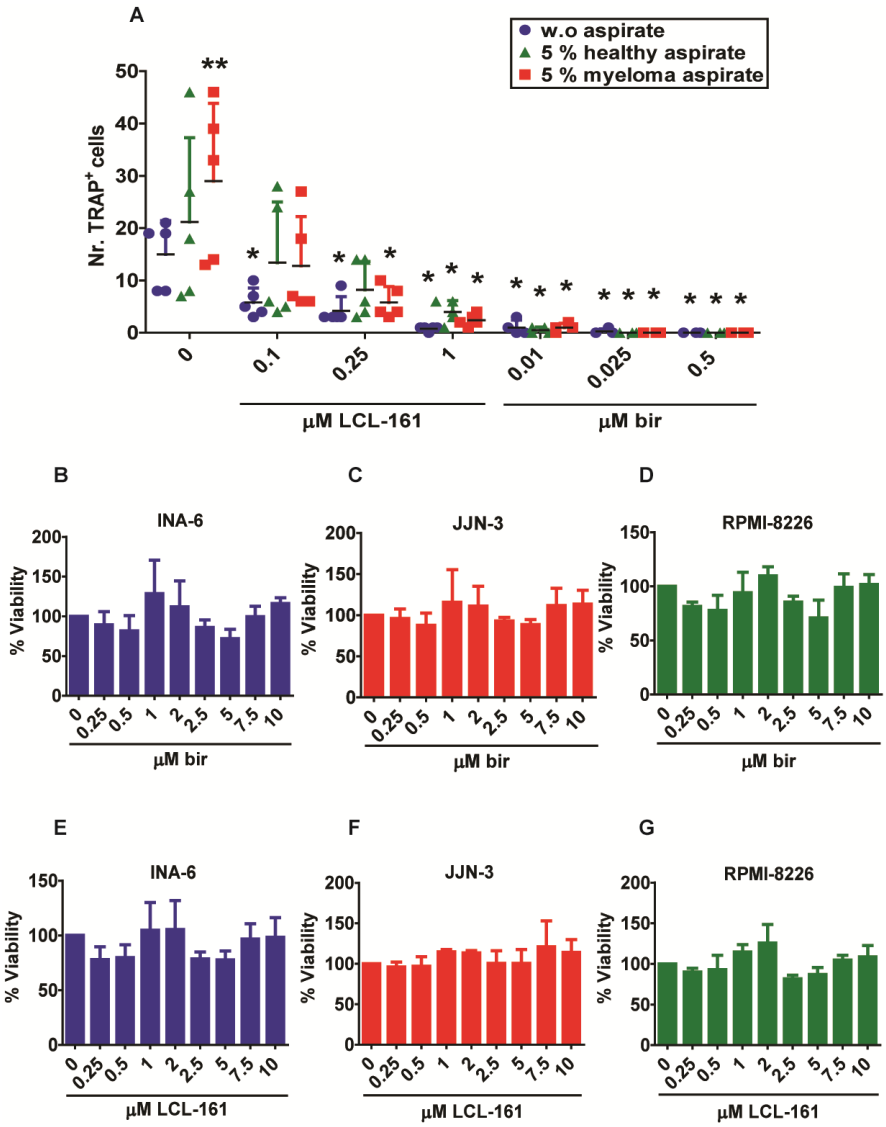

Supplementary S5. **Birinapant or LCL-161 effect on multiple myeloma driven osteoclastogenesis and multiple myeloma cell lines**. CD14^{+}-monocytes were differentiated in OC differentiation medium supplemented with 5% bone marrow aspirate from myeloma patients or healthy controls and treated with LCL-161 or birinapant at indicated concentrations throughout OC differentiation. TRAP^{+} cells with 3 or more nuclei were counted as OC (A), shown for 5 donors. Individual donors, average and SD are shown. Single asterisk denotes statistical significance compared to individual controls. Double asterisk denotes statistical significance as compared to no aspirate (w.o. aspirate) ($p<0.05$, One-way ANOVA). The multiple myeloma cell lines INA-6, JJN-3 and RPMI-8226 were treated with the indicated doses of birinapant (B-D) or LCL-161 (E-G) for 18 hours before cell viability was measured by Cell Titer Proliferation Assay. Average and SD from 3 independent experiments are shown, and we observed no significant differences ($p<0.05$, Student's T-Test).

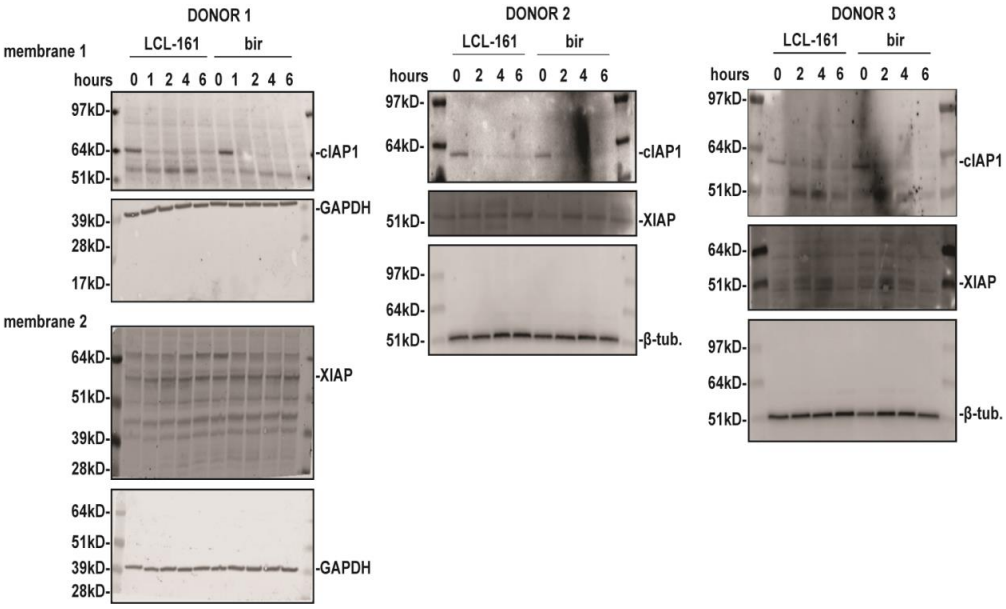

Supplementary Figure S6. **Donors and full immunoblots for SM effect on cIAP1 and XIAP protein levels**. Pre-OCs were treated with 1 µM birinapant or LCL-161 at indicated time points, and cell lysates were analyzed for cIAP1 and XIAP protein levels by immunoblotting. GAPDH as loading control for donor1, β-tubulin as loading control for donor 2 and 3. Donor 1 is same as in Figure 2A.

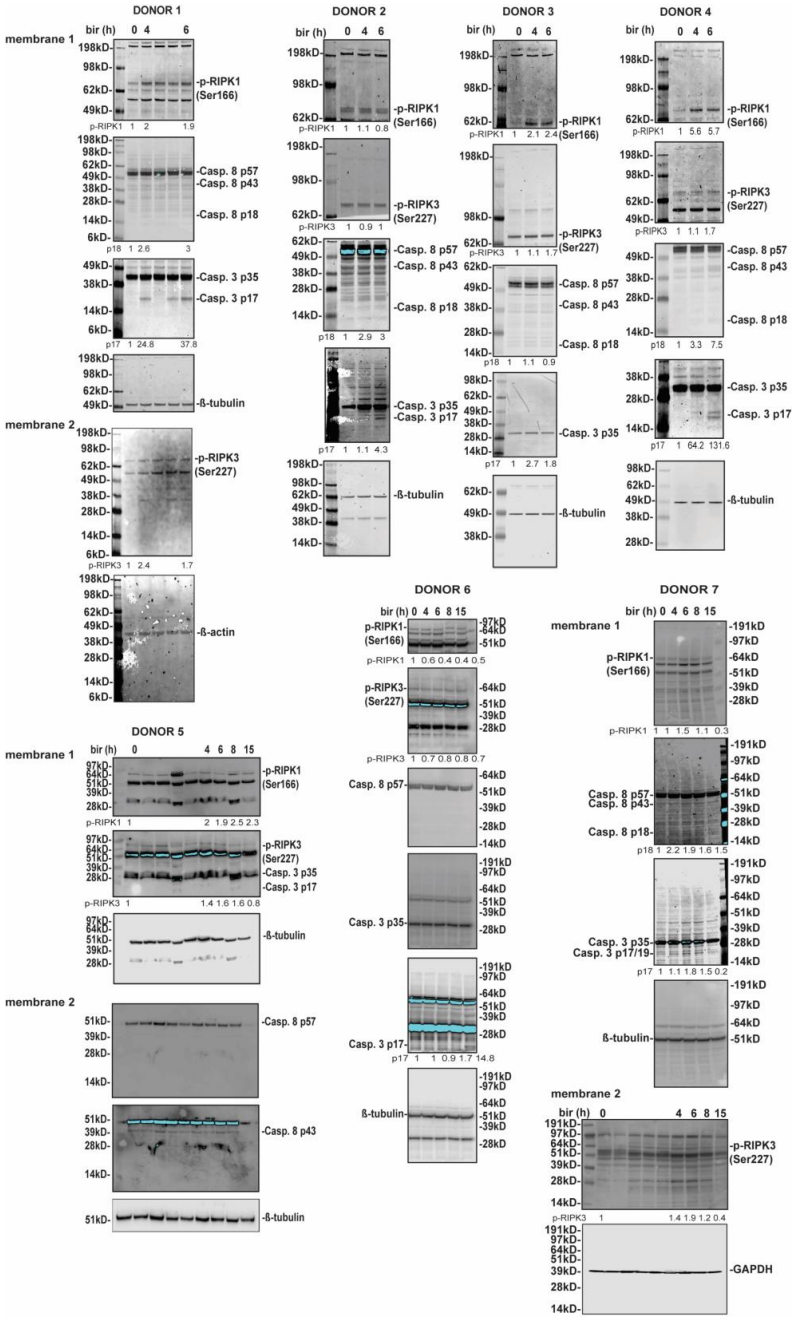

Supplementary Figure S7. Donors and full immunoblots for birinapant activation of apoptosis and necroptosis. β-actin as loading control for donor 1, membrane 2 and GAPDH as loading control for donor 7, membrane 2. Individual membranes are shown. Donor 1 is same as in Figure 3C. Quantification of p-RIPK1, p-RIPK3, caspase 3 p17 and caspase 8 p18 levels normalized to the loading control is indicated below the respective blots.

Paper II

PRO- AND ANTI-INFLAMMATORY TREATMENT DICTATES SMAC-MIMETIC CYTOTOXICITY IN HUMAN MACROPHAGES

Ingrid Nyhus Moen[1,2], Merisa Klaharn[1,2], Marie Holter-Sørensen[1,2], Animesh Sharma[1,3], Kristian K. Starheim[1,2,*]

1) Centre of Molecular Inflammation Research (CEMIR), Department of Clinical and Molecular Medicine (IKOM), Norwegian University of Science and Technology (NTNU), Trondheim, Norway, 2) Department of Hematology, St. Olavs University Hospital, Trondheim, Norway, 3) Proteomics and Modomics Experimental Core Facility (PROMEC), NTNU, Trondheim, Norway.

* Corresponding author: Kristian.starheim@ntnu.no

Paper III

TAK1-INHIBITORS ARE CYTOTOXIC FOR MULTIPLE MYELOMA CELLS ALONE AND IN COMBINATION WITH MELPHALAN

Short title: TAK1-inhibitors are cytotoxic to multiple myeloma.

Erling Håland,[1,2] Ingrid Nyhus Moen,[1-3] Elias Veidal,[1,2] Hanne Hella,[2] Kristine Misund,[2] Tobias S. Slørdahl,[2,3] and Kristian K. Starheim[1-3]

[1] CEMIR Centre of Molecular Inflammation Research, IKOM, NTNU, Trondheim, Norway; [2] Department of Clinical and Molecular medicine, NTNU, Trondheim, Norway; [3] Department of Hematology, St. Olavs University Hospital, Trondheim, Norway.

Correspondence: Kristian K. Starheim, Faculty of Medicine and Health Sciences, Department for Clinical and Molecular Medicine (IKOM), Norwegian University of Technology and Natural Sciences (NTNU), Pb. 8905, N-7491 Trondheim, NORWAY. E-mail: Kristian.starheim@ntnu.no, tel. +4790178148.

Abstract

Multiple myeloma (MM) is an incurable cancer caused by malignant transformation of plasma cells. Transforming growth factor-β activated kinase 1 (MAP3K7, TAK1) is a major regulator of nuclear factor kappa-light-chain-enhancer of activated B cells (NF- κB) and mitogen-activated protein kinase (MAPK) signaling. Both NF-κB and MAPK control expression of genes with vital roles for drug resistance in MM. TAK1 is an attractive drug target as it switches these survival pathways to cell death. Our analysis showed that patients with high *MAP3K7* expression in the tumor had shorter overall and progression free survival. The TAK1-inhibitors NG25 and 5Z-7-oxozeaenol (5Z-7) were cytotoxic to MM cell lines and patient cells. NG25 reduced expression of MYC and E2F controlled genes, involved in tumor cell growth, cell cycle progression and drug resilience. TAK1 can be activated by genotoxic stress. NG25 and 5Z-7 induced both synergistic and additive cytotoxicity in combination with the alkylating agent melphalan. Melphalan activated TAK1, NF-κB, and the MAPKs p38 and c-Jun N-terminal kinase (JNK), as well as a transcriptional UV-response. This was blocked by NG25, and instead apoptosis was activated. MM induce elevated bone-degradation resulting in myeloma bone disease (MBD), which is the main cause of disability and morbidity in MM patients. NG25 and 5Z-7 reduced differentiation and viability of human bone degrading osteoclasts, suggesting that TAK1-inhibition can have a double beneficial effect for patients. In sum, TAK1 is a promising drug target for MM treatment.

Key points

- TAK1-inhibitors reduce viability of myeloma cells alone and in combination with melphalan.

- TAK1-inhibitors block shift oncogenic transcription programs to cell death.

Introduction

Multiple myeloma (MM) is the second most common hematological malignancy worldwide. It is characterized by malignant transformation of clonal plasma cells in the bone marrow accompanied by secretion of monoclonal immunoglobulins, and cancer-induced bone degradation (myeloma bone disease, MBD). The overall survival time of multiple myeloma has improved in the later years due to novel therapeutic strategies.[1] However, the disease is still incurable due to minimal residual disease (MRD), development of drug resistance and relapse. A common treatment strategy in multiple myeloma is induction of DNA damage in the MM cells caused by DNA-damaging agents, such as melphalan. However, they are associated with side effects for the patients and they eventually develop of drug resistance.[2]

Transforming growth factor-β activated kinase 1 (MAP3K7, TAK1) is a serine/threonine kinase that is activated by a variety of immune receptors, as well as genotoxic stress such as DNA-damage. TAK1 plays an important role in development of chemo resistance in a magnitude of different types of cancer.[3] It induces expression of survival factors through nuclear factor kappa-light-chain-enhancer of activated B cells (NF-κB) and mitogen activated protein kinases (MAPK). MAPK consist of three major families - extracellular-signal-regulated-kinases (ERKs), p38 MAP kinases, and cJun NH_2-terminal kinases (JNKs).[4] NF-κB and MAPK regulate a wide range of immune- and oncological survival programs, and constitutive NF-κB activation is an important pro-tumor mechanism in MM.[5] Several p38-inhibitors have been tested in clinical trials for several types of cancer, but they have failed due to limited efficiency.[6] Targeting the kinases upstream in the signaling pathway, such as TAK1, has been proposed.[7] TAK1 restrains receptor-interacting serine/threonine-protein kinase 1 (RIPK1) dependent cell death, and inhibition of activated TAK1 shifts cells from pro-survival programs to cell death, making it an attractive drug target.[8] TAK1-inhibition has shown promising results in MM, but with limited investigation.[9,10]

Here, we show that the TAK1-inhibitors NG25 and 5Z-7 reduce viability of MM cell lines and primary cells. The combination of TAK1 inhibitors with melphalan or other DNA-damaging agents increases the cytotoxicity in a synergistic or additive manner. TAK1-inhibitors also reduced number and viability of osteoclasts, suggesting that they have an additional positive effect on MBD. Our findings suggest that TAK1-inhibitors in combination with DNA-damaging agents represent a potential treatment strategy in MM patients.

Methods

Cell culture

The myeloma cell lines used in this study were ANBL-6 (a kind gift from Dr. Diane Jelinek, Mayo Clinic, Rochester, MN, USA), INA-6 (a kind gift from Dr. Martin Gramatzki, Erlangen, Germany), JJN-3 (a kind gift from Dr. Jennifer Ball, University of Birmingham, UK), and RPMI-8226 (from ATCC, Rockville, MD, USA). ANBL-6 and INA-6 cells were grown in 10% heat-inactivated fetal calf serum (FCS) in RPMI-1640 (hereafter described as RPMI, Sigma-Aldrich, St. Louis, MO, USA, R8758) supplemented with recombinant human interleukin-6 (IL-6, 1 ng/ml) (Gibco, Life Technologies/Thermo Fisher Scientific, Waltham, MA, USA). JJN-3 cells were maintained in 10% heat-inactivated FCS in RPMI-1640. RPMI-8226 cells were maintained in 20% heat-inactivated FCS in RPMI-1640. All cells were cultured at 37° C in a humidified atmosphere containing 5% CO_2.

To obtain primary myeloma cells, $CD138^+$ cells were isolated from bone marrow specimens obtained through the Norwegian Myeloma Biobank (Biobank1) using RoboSep automated cell separator and Human CD138 Positive Selection Kit (StemCell Technologies, Grenoble, France). Informed consent was obtained from participating patients, and the regional ethics committee approved the study (REK Midt 2011/2029). Experiments with primary myeloma cells, were performed in 2 % heat-inactivated human serum (Blood Bank, St Olav's University Hospital, Trondheim, Norway) supplemented with recombinant human IL-6 (1 ng/ml).

To generate primary human osteoclasts, peripheral blood mononuclear cells were isolated from healthy donors by density centrifugation. Buffy coats were provided by the Blood Bank (St. Olavs Hospital, Trondheim) with approval by the Regional Committee for Medical and Health Research Ethics (REK Midt 2011/2029). Osteoclasts (OC) and pre-osteoclasts (pre-OC) was generated from PBMCs as described previously.[11] In brief, monocytes were isolated using $CD14^+$ magnetic bead separation according to the manufacturer's instructions (Miltenyi Biotec, Bergisch Gladbach, Germany, 130-050-201). $CD14^+$ monocytes were plated in α minimum essential medium (αMEM, Thermo Fisher Scientific, 41061-029) supplemented with 10% heat-inactivated human serum according to blood type, 30 ng/ml CSF-1 (216-MC), 10 ng/ml RANKL (390-TN-010), and 1 ng/ml TGF-β (240-B-002) (R&D systems, Minneapolis, MN, USA).[11,12] The cells were differentiated for 6-7 days to obtain osteoclast precursors (pre-OC), and until visible multinuclear cells for osteoclasts, typically 10-15 days.

The following compounds were used in cell culture: 5Z-7 (Sigma-Aldrich, O9890), doxorubicine (Sigma-Aldrich, D1515), etoposide (Sigma-Aldrich, E1383), NG25 (MedChemExpress, Monmouth Junction, NJ, USA, HY-15434), melphalan (Sigma-Aldrich, St. Louis, MO, USA, M2011), recombinant human TNF (R&D Systems, 410-MT-025).

Assessment of osteoclast differentiation

The number of mature osteoclasts was assessed by scoring the number of multinucleated cells (≥3 nuclei) that were positive for tartrate resistant acid phosphatase (TRAP). When multinucleated cells were visible by light microscopy, cells were fixed and stained for TRAP using the Leukocyte Acid Phosphatase Kit (Sigma-Aldrich, 387A-1KT) according to the manufacturer's instructions.

Cell lysis and western blotting

Cells were sedimented and washed in PBS before in lysis 15 minutes on ice (50 mM tris-HCl, TritonX-100 (1%), 150 mM NaCl, 5 mM EDTA, protease inhibitor cocktail (Roche, Basel, Switzerland, 1187358001), 1 mM Na_3VO_4 and 50 mM NaF. The samples were separated on NuPAGE Bis-Tris gels with MOPS or MES running buffer (Invitrogen, Thermo Fisher Scientific). Proteins were transferred from the gel onto a 0.2 µm nitrocellulose membrane using the iBlot gel transfer system (Life Technologies, Thermo Fisher Scientific). The membrane was blocked with 5% BSA in tris-buffered saline with 0.1% Tween 20 (TBS-T) and incubated with primary antibodies. Blots were washed with TBS-T before incubation with horse-radish peroxidase- or fluorophore-conjugated secondary antibodies (Dako, Agilent, Santa Clara, CA, USA and LiCor Biosciences, Lincoln, NE, USA). Membranes were analyzed on a LiCor Fc or xCT (LiCor Biosciences). For luminescence, a SuperSignal West Femto luminescence substrate was used (Thermo Fisher Scientific, 34096).

The following antigens were analyzed (antibodies in parenthesis): ATM phospho-Ser1981 (Cell Signaling Technologies (CST), Danvers, MA, USA, 5883), Bad phospho-Ser112 (CST, 5284), Bad (CST, 9239), Bak (CST, 12105), Bax (CST, 5023), BID (CST, 2002), Bim (CST, 2933), β-tubulin (Abcam, Cambridge, UK, Ab6046), Caspase 3 (CST, 9662), Caspase 8 (Enzo, ALX-804-242-C100), Caspase 8 (CST 9748), Caspase 9 (CST, 9502), c-myc (CST, 5605), ERK1/2 phospho-Thr202/Tyr204 (CST, 4370), ERK1/2 (CST, 9107), GAPDH (CST, 2118), JNK phospho-Thr183/185 (CST, 4668), JNK, PARP (CST, 9532), p38 phospho-Thr180/Tyr182 (CST, 9215), p38 (CST, 9212), p65 phospho-Ser536 (CST, 3033), p65 (CST, 6956), TAK1 phospho-Thr184/187 (4508), TAK1 (CST, 4505).

Cytotoxicity and viability assays

For viability assessment of MM cells, CellTiter-Glo® 2.0 Cell Viability Assay (Promega Madison, WI, USA G358C) was used to measure the levels of ATP in the wells according to the manufacturer's instructions. 5 000 cells of MM cell lines and 10 000 cells of $CD138^+$ primary MM cells were seeded in 96-well plates and stimulated as indicated and then incubated for 18 hours at 37 °C in humidified atmosphere containing 5 % CO_2. Luminescence was measured with a Victor 1420 multilabel counter (Perkin Elmer Inc., Waltham, MA, USA). All conditions were done in triplicates, and all experiments were performed at least three times.

For cell death assessment of pre-OC, cells were stimulated in Opti-MEM serum free medium (Thermo Fisher Scientific, 11058-021), and cell death was calculated by measuring lactate dehydrogenase-release (LDH) in medium using a colorimetric assay according to the

manufacturer's instructions (TaKaRa Bio, Saint-Germain-en-Laye, France, MK401). Cell viability of OC and pre-OC was measured using the colorimetric Cell titer 96® AQueous One Solution Cell Proliferation Assay (Promega, G358C) or the luminescent CellTiter-Glo® 2.0 Cell Viability Assay.

Cell cycle analysis.

INA-6 and RPMI-8225 cells were treated with TAK1-inhibitors or vehicle for 18 hours. Cells were then washed in PBS and fixated in ice cold methanol. Methanol was removed, cells were washed in PBS, and incubated in RNAse for 30 minutes at 37°C to remove RNA, before propidium iodide was added and cells incubated for 30 minutes at 37°C. Cells were then filtered with a 40 μM filter. Data were acquired using a LSRII flow cytometer (BD Biosciences, San Jose, CA, USA) and analyzed in FlowJo (Tree Star, Inc., OR, USA) using the Watson pragmatic model.

Survival and progression-free survival analysis of CoMMpass gene expression data.

RNA sequencing data of $CD138^+$ cells from 773 patients were available from the Multiple Myeloma Research Foundation CoMMpass Researcher Portal (IA15-release). Patient samples were divided into high and low *MAP3K7* expression based on the upper 20^{th} percentile (n= 154 patients) and lower 80^{th} percentile (n= 619 patients), and the CoMMpass researcher portal analysis tool was used to generate Kaplan-Meyer plots and hazard-ratio of progression-free survival and survival.

Transcriptome sequencing

INA-6 cells were treated with 2 μM NG25 or 10 μM melphalan or both for 6 hours. Total RNA was then extracted using RNeasy Mini kits including DNAse digestion with Qiacube (QIAGEN, Hilden, Germany, 74104). RNA quantity, quality/integrity and purity were evaluated using Qubit (Thermo Fisher Scientific, MA, USA), Bioanalyzer (Agilent, CA, USA) and NanoDrop (Thermo Fisher Scientific, MA, USA).

RNA sequencing libraries were generated for 12 RNA samples, using SENSE mRNA-Seq library prep kit V2, according to manufacturer's instructions (Lexogen GmbH, Vienna, Austria). In brief, 800 ng of total RNA was prepared and incubated with magnetic beads coated with oligo-dT, then all other RNAs except mRNA were removed by washing. Library preparation was then initiated by random hybridization of starter/stopper heterodimers to the poly(A) RNA still bound to the magnetic beads. These starter/stopper heterodimers contain Illumina-compatible linker sequences. A single-tube reverse transcription and ligation reaction extends the starter to the next hybridized heterodimer, where the newly synthesized cDNA insert was ligated to the stopper. Second-strand synthesis was performed to release the library from the beads. The resulting double-stranded library was purified and amplified (12 PCR cycles) after adding the adaptors and indexes. Finally, libraries were quantitated by qPCR using KAPA Library Quantification Kit (Kapa Biosystems, Inc., MA, USA) and validated using Agilent High Sensitivity DNA Kit on a Bioanalyzer (Agilent Technologies, CA, USA). The size range of the DNA fragments were measured to be in the range of 200-450 bp with average library size 240 bp.

Prior to sequencing, the libraries were quantitated by quantitative polymerase chain reaction using the KAPA Library Quantification Kit–Illumina/ABI Prism® (Kapa Biosystems, Wilmington, MA, USA) and validated using the Agilent High Sensitivity DNA Kit on a bioanalyzer. Libraries were normalized to 2.7 pM subjected to clustering. Single read sequencing was performed for 75 cycles on a NextSeq500 HO flowcell (Illumina, San Diego, CA, USA), according to the manufacturer's instructions. Base calling was done on the NextSeq500 instrument by RTA 2.4.6. FASTQ files were generated using bcl2fastq2 Conversion Software v2.20.0.422 (Illumina, Inc.).

FASTQ files were filtered and trimmed (fastp v0.20.0) and transcript counts were generated using quasi alignment (Salmon v1.3.0) to the transcriptome reference sequence (Ensembl, GRCh38 release100). Transcript sequences were imported into the R statistical software and aggregated to gene counts using the tximport (v1.14.0) bioconductor package. Data are available in the GEO Repository under accession number GSE178292.

For differential expression analysis, a DESeq2 unpaired analysis were performed in R studio to find differentially expressed genes. Gene Set Enrichment Analysis (GSEA; Broad Institute) was used to identify enriched pathways.

Statistical analysis

Statistical analysis was performed using the GraphPad Prism 6 software (GraphPad Software Inc., La Jolla, CA, USA). The tests used were one-way ANOVA with Turkey´s multiple comparison test, Kruskal-Wallis test with Dunn´s multiple comparison test, or two-way ANOVA with Tukey´s multiple comparison test. For dose-response curves, significant differences in response were calculated as follows: data were normalized within groups and IC50 was calculated by linear regression (non-linear regression, log(inhibitor) vs response, variable slope). Level of statistical significance was set at 0.05 (5%) for all experiments.

Results

TAK1-inhibitors are cytotoxic to MM cell lines alone and in combination with melphalan

Analysis of data from the MMRF CoMMpass study showed that MM patients with high expression of *MAP3K7* had lower overall and progression free survival (Supplementary Figure S1A, B). On the basis of this we tested whether the TAK1-inhibitors NG25 and 5Z-7 affected viability of MM cell lines. Both NG25 and 5Z-7 decreased viability of the cell lines INA-6, ANBL-6, JJN-3, and RPMI-8266 (Figure 1A, B). This is in accordance with previous works.[10] Sensitivity of cell lines varied, but IC50 was generally lower than in PBMCs from healthy donors (Supplementary Figure S1C, D, Supplementary Table 1).

As TAK1 can activate survival mechanisms after DNA-damage we hypothesized TAK1-inhibitors would render MM-cells more sensitive to melphalan.[3] Both NG25 and 5Z-7 decreased IC50 of melphalan in all tested cell lines (Figure 1C, D, Supplementary Table 2). Similar but less pronounced effects were seen in combination with the DNA-damaging drugs doxorubicin and etoposide (Supplementary Figure S1E, F and Supplementary Table 3, 4).

NG25-treatment induced cleavage of activator caspases 8 and 9, as well as the effector caspase 3 and PARP in INA-6 cells. This was further activated in melphalan + NG25-treated cells (Figure 1E, Supplementary Figure S4). This shows that TAK1-inhibition activates apoptosis, and that this is partly through caspase 8.

NG25 blocks melphalan-induced p38, ERK and NF-κB signaling

Melphalan is an alkylating agent that leads to DNA-damage and apoptosis.[2] However, DNA-damage can also activate survival programs to manage the genotoxic stress, including NF-κB and MAPK.[3] Melphalan induced phosphorylation of TAK1, p38, JNK, ERK and the NF-κB transcription factor p65, and increased total p65-levels, indicative of MAPK and NF-κB activation. NG25 blocked melphalan-induced TAK1, p38, JNK and p65-phosphorylation, and blocked the increase in p65 levels, but induced further ERK-phosphorylation (Figure 2A). In addition, we observed a decrease in total TAK1 protein levels in melphalan+NG25 treated cells. In sum, NG25 blocks melphalan-induced p38, JNK and NF-κB signaling.

The serine-protein kinase ATM (ATM) is recruited to double-stranded DNA-breaks, and coordinates cell cycle arrest, survival pathways as well as initiation of intrinsic apoptosis.[3] Melphalan induced ATM-phosphorylation in INA-6 cells (Figure 2B, Supplementary Figure S6). We did not observe activation of mitochondrial apoptosis under these circumstances, as tested by BCL2 associated agonist of cell death (BAD) dephosphorylation or BH3 interacting domain death agonist (BID) and BCL2-like protein 11 (BIM) cleavage (Supplementary Figure S2, S7). Thus, melphalan trigger ATM, and this might be responsible for TAK1-activation.

NG25 reduce transcription of oncogenic transcription programs

MAP kinases and NF-κB regulate transcription of a multitude of genes. To determine which genes are affected by NG25 and melphalan, we performed an RNA-seq on INA-6 cells treated with NG25, melphalan or a combination of the two. GSEA focusing on the hallmark pathways showed that melphalan-treatment upregulated genes involved in UV-response, DNA-repair, p53-pathway and TNF-signaling via NF-κB (Supplementary Figure S3A). NG25 induced expression of genes involved in cholesterol homeostasis and mTORC1-signaling and down-regulated MYC- and E2F-targets (Figure 3A, B). MYC is a central driver of MM pathology, and regulate survival as well as cell cycle control through E2F.[14,15] NG25 reversed the melphalan-induced UV-response (Figure 3C).

Consistent with the observation that NG25 decreased MYC-targets, NG25 also decreased MYC protein levels in MM cell lines, although not consistently in INA-6 (Figure 3D, Supplementary Figure S8). Of note, also melphalan reduced MYC protein levels (Supplementary Figure S8). We also performed a FACS-experiment to investigate whether the decreased MYC-activity had consequences for cell cycle progression in INA-6 and RPMI-8226 cells. NG25 did not affect cell cycle progression at the tested dose, whereas 5Z-7 treatment arrested cells in the G0/G1 phase (Figure 3E, Supplementary Figure S3B).

In sum, melphalan treatment induce pathways involved the DNA-damage response, and NG25 at least partly reverse these changes. In addition, NG25 down-regulates MYC which can render cancer cells less resilient to genotoxic stress.

TAK1-inhibitors reduce numbers and viability of osteoclasts.

Osteoclasts (OC) are specialized macrophages that degrade bone, and MM patients display elevated OC activity, leading to myeloma bone disease. We recently showed that inhibitors of the cellular inhibitor of apoptosis protein cIAP1/2, which acts upstream of TAK1 in several inflammatory pathways, reduced numbers and viability of human OC.[11] TAK1 was necessary for osteoclastogenesis in mouse.[16] On the basis of this we reasoned that TAK1-inhibitors also could block human osteoclastogenesis and have a double beneficial effect for MM patients. We found that treatment with NG25 and 5Z-7 during OC differentiation reduced both numbers and viability of human OC (Figure 4A-C). We also tested whether TAK1-inhibitors induced a more rapid cytotoxicity on differentiated pre-OC. Here, TAK1-inhibitors were only cytotoxic in combination of a TAK1-activating agent such as TNF (Figure 4D-G). In sum, TAK1-inhibitors can reduce osteoclast numbers through blocking the formation of new OC.

NG25 reduce viability of myeloma patient samples alone and in combination with melphalan.

To investigate whether the observed cytotoxic effects of NG25 and melphalan also was evident in patient samples, we took advantage of our access to blood banked $CD138^+$ plasma cells from myeloma patients. NG25 was cytotoxic to MM patient cells (Figure 5A, Supplementary Table 5). It also reduced the IC50 of melphalan, but the combined cytotoxicity was additive rather than synergistic (Figure 5B, Supplementary Table 6).

Discussion

In this study, we present findings showing that TAK1-inhibitors are cytotoxic to multiple myeloma cells and OC. Further, TAK1-inhibitors potentiated the cytotoxicity of melphalan and blocked melphalan-induced NF-κB and MAPK activation. NG25 reversed the melphalan-induced UV-response. On the basis of this we suggest that combining TAK1-inhibitors with alkylating agents such as melphalan and cyclophosphamide can be a beneficial combination for MM treatment.

NG25 reduced activity of oncogenic drivers such as MYC and E2F, but up-regulated genes involved in mTORC1-signaling and cholesterol homeostasis. The latter is consistent with previous findings that TAK1 knockout induce increased mTORC1-activity and hepatosteatosis in mice.[17] NG25 also neutralized the melphalan-induced transcriptional UV-response. In sum, TAK1-inhibitors can target MM cells in several manners: i) directly shifting constitutively- or melphalan-activated TAK1 from NF-κB/MAPK activation to cell death, ii) reducing activity of survival factors such as MYC and E2F, and iii) neutralizing the melphalan-induced UV-response.

Bone disease is a severe complication of MM. It causes pain for the patients and promotes tumor growth. The TAK1/RIPK1 pathway is central in regulation of inflammatory activation and death of macrophages, and we recently showed that Smac-mimetics, which work directly upstream of TAK1, blocked osteoclastogenesis and shifted OC to cell death.[11] Here we show that TAK1-inhibitors blocked osteoclastogenesis and was cytotoxic to differentiating OC at higher doses. This is consistent with previous findings in mouse genetic models.[16] TAK1-inhibitors thus have an additional antitumorigenic effect through blocking osteoclastogenesis and potentially limiting MBD.

In sum, TAK1-inhibitors reduce MM cell viability through and induce apoptosis through several mechanisms. They potently induce cell death in combination with melphalan and reduce OC numbers and viability. TAK1 is an interesting candidate for further clinical testing as a drug target in MM.

Acknowledgements

This work was supported by grants from The Norwegian Cancer Society (project ID 6799133), The Liaison Committee for education, research and innovation in Central Norway, the Joint Research Committee between St. Olavs Hospital and Faculty of Medicine and Health Science, NTNU, and the Research Council of Norway through its Center of Excellence funding scheme (project number 2223255/F50). The library prep, sequencing and parts of the bioinformatics analysis were performed in close collaboration with the Genomics Core Facility (GCF), Norwegian University of Science and Technology (NTNU). GCF is funded by the Faculty of Medicine and Health Sciences at NTNU and Central Norway Regional Health Authority. We thank Lill-Anny Grønseth (Biobank1) for assistance with patient samples, and professors Geir Bjørkøy and Anders Sundan for input on the manuscript. We would also thank our user panel of myeloma patients for inspiring discussions.

Authorship Contributions

K.K.S., E.H., I.N.M., and T.S.S. designed experiments; E.H., I.N.M., E.V., H.H., and K.K.S. conducted experiments, acquired and analyzed data; T.S.S. provided patient samples; K.M. analyzed RNA-sequencing data; E.H. and K.K.S. wrote the paper; all authors revised the paper and approved the final version of the manuscript.

Disclosure of Conflicts of Interest

The authors declare no competing interests.

References

1. Kumar SK, Rajkumar V, Kyle RA, et al. Multiple myeloma. *Nat Rev Dis Prim.* 2017;3:17046.
2. Chabner BA, Roberts Jr. TG. Timeline: Chemotherapy and the war on cancer. *Nat Rev Cancer*. 2005;5(1):65–72.
3. Mukhopadhyay H, Lee NY. Multifaceted roles of TAK1 signaling in cancer. *Oncogene*. 2019;3:.
4. Sabio G, Davis RJ. TNF and MAP kinase signalling pathways. *Semin Immunol*. 2014;26(3):237–245.
5. Demchenko YN, Kuehl WM. A critical role for the NFkB pathway in multiple myeloma. *Oncotarget*. 2010;1(1):59–68.
6. Cicenas J, Zalyte E, Rimkus A, et al. JNK, p38, ERK, and SGK1 Inhibitors in Cancer. *Cancers (Basel)*. 2017;10(1):.
7. Hammaker D, Firestein GS. "Go upstream, young man": lessons learned from the p38 saga. *Ann. Rheum. Dis.* 2010;69(Suppl 1):i77–i82.
8. Mihaly SR, Ninomiya-Tsuji J, Morioka S. TAK1 control of cell death. *Cell Death Differ.* 2014;21(11):1667–1676.
9. Tenshin H, Teramachi J, Oda A, et al. TAK1 inhibition subverts the osteoclastogenic action of TRAIL while potentiating its antimyeloma effects. *Blood Adv*. 2017;1(24):2124–2137.
10. Teramachi J, Tenshin H, Hiasa M, et al. TAK1 is a pivotal therapeutic target for tumor progression and bone destruction in myeloma. *Haematologica*. 2020;haematol.2019.234476.
11. Moen IN, Westhrin M, Håland E, et al. Smac-mimetics reduce numbers and viability of human osteoclasts. *Cell Death Discov.* 2021;7(1):36.
12. Harre U, Lang SC, Pfeifle R, et al. Glycosylation of immunoglobulin G determines osteoclast differentiation and bone loss. *Nat. Commun.* 2015;6(1):6651.
13. Holien T, Olsen OE, Misund K, et al. Lymphoma and myeloma cells are highly sensitive to growth arrest and apoptosis induced by artesunate. *Eur. J. Haematol.* 2013;91(4):339–346.
14. Manier S, Salem KZ, Park J, et al. Genomic complexity of multiple myeloma and its clinical implications. *Nat. Rev. Clin. Oncol.* 2017;14(2):100–113.
15. Bretones G, Delgado MD, León J. Myc and cell cycle control. *Biochim. Biophys. Acta - Gene Regul. Mech.* 2015;1849(5):506–516.
16. Lamothe B, Lai Y, Xie M, Schneider MD, Darnay BG. TAK1 is essential for osteoclast differentiation and is an important modulator of cell death by apoptosis and necroptosis. *Mol. Cell. Biol.* 2013;33(3):582–95.
17. Inokuchi-Shimizu S, Park EJ, Roh YS, et al. TAK1-mediated autophagy and fatty acid oxidation prevent hepatosteatosis and tumorigenesis. *J. Clin. Invest.* 2014;124(8):3566–3578.

Figure legends.

Figure 1. TAK1-inhibitors are cytotoxic to MM cell lines alone and in combination with melphalan. MM cell lines treated with NG25 or 5Z-7 at indicated concentrations for 18 hours before measuring the viability with CellTiter-Glo. (**A**) Mean and SD from three independent experiments are shown. Asterisks indicate statistically significant differences (One-way ANOVA, Turkey´s multiple comparison test, P<0,05) compared with untreated. (**B**) IC50-values of NG25 and 5Z-7 in MM cell lines. (**C**) MM cell lines treated with NG25 in combination with melphalan. Asterisks indicate statistically significant differences (two-way ANOVA, Tukey´s multiple comparison test, P<0,05) compared with the control not treated with NG25. Single asterisk denotes statistical significance as compared to the NG25-untreated for the lowest dose of NG25, double asterisk denotes statistical significance as compared to the untreated control for the highest dose of NG25. (**D**) MM cell lines treated with 5Z-7 in combination with melphalan. Asterisks indicate statistically significant differences (two-way ANOVA, Tukey´s multiple comparison test, P<0,05) compared with the control not treated with 5Z-7. Single asterisk denotes statistical significance as compared to the control not treated with 5Z-7 for the lowest dose of 5Z-7, double asterisk denotes statistical significance as compared to the untreated control for the highest dose of 5Z-7. (**E**) MM cells from the INA-6 cell line were treated with 2 μM NG25 or 10 μM melphalan or both at the indicated time points, and cell lysates were analyzed for full length and cleaved caspase 3, caspase 8, caspase 9, and PARP protein levels by immunoblotting. GAPDH is loading control, shown for corresponding membranes. One representative of three independent experiments is shown, and full membranes of all experiments are given in Supplementary Figure S4.

Figure 2. NG25 blocks melphalan-induced p38, ERK- and NF-κB signaling. (**A**) MM cells from the INA-6 cell line were treated with 2 μM NG25 or 10 μM melphalan or both for the indicated time, and cell lysates were analyzed for protein levels of the indicated antigens by immunoblotting. β-Tubulin is loading control, shown for corresponding membranes. One representative of three independent experiments is shown, and full membranes from all experiments are given in Supplementary Figure S5. (**B**) MM cells from the INA-6 cell line were treated with 10 μM melphalan at the indicated time points, and cell lysates were analyzed for p-ATM protein levels by immunoblotting. β-Tubulin is loading control. One representative of three independent experiments is shown, and full membranes from all experiments are given in Supplementary Figure S6.

Figure 3. NG25 reduce transcription of oncogenic survival programs. (**A-C**) MM cells from the INA-6 cell line were treated with 2 μM NG25 or 10 μM melphalan or both for 6 hours. Then RNA was isolated, and the transcriptome was analyzed by RNA-sequencing. **(A)** Significantly changed pathways (FDR q-value<0.02, NES>1.3) in NG25-treated cells (n=3) as compared to control (n=3), analyzed by GSEA on hallmark gene sets. **(B)** Heatmap showing gene expression levels (z-score of log2 TPM) of genes included in the gene sets in (A). **(C)** Heatmap showing gene expression levels (z-score log2 TPM) of genes included in the UV-response gene sets, in cells treated with melphalan (n=3) and/or NG25 (n=3). (**D**) MM cell lines treated with 2 μM NG25 for 4 hours. Cell lysates were then analyzed for protein levels by immunoblotting. β-Tubulin is loading control. One representative of three

independent experiments is shown, and full membranes from all experiments is given in Supplementary Figure S8. (**E**) INA-6 and RPMI-8226 MM cell lines were treated with 2 μM NG25 or 5Z-7 for 18 hours before fixation, PI-staining and flow cytometry analysis of cell cycle stage. The graph shows mean and SD from three independent experiments. Asterisks indicate significant differences (two-way ANOVA, Turkey´s multiple comparison test, P<0,05) compared with DMSO. Histograms from one representative experiment is given in Supplementary Figure S3B

Figure 4. **NG25 and 5Z-7 reduce viability and number of differentiating osteoclasts and trigger TNF-dependent cell death in pre-osteoclasts.** (**A-C**) Human $CD14^+$-monocytes were differentiated to OC, and treated with NG25 or 5Z-7 at indicated concentrations throughout differentiation, typically 10-15 days. (**A**) Representative phase-contrast images of TRAP-stained human osteoclasts, with arrowheads indicating multinuclear $TRAP^+$ cells. Frame in first column indicates cutout for detailed view. Bar is 150 μM. (**B**) Fold change of $TRAP^+$ multinuclear cells after NG25 or 5Z-7 treatment at indicated concentrations. 10 donors, mean, and SD are shown. (**C**) Viability at the time of $TRAP^+$ quantification measured with the CellTiter-Glo assay. 6 donors, mean and SD are shown. (**D-G**) Pre-osteoclasts were treated with indicated concentrations of NG25 (**D, E**) or 5Z-7 (**F, G**) with or without 25 ng/ml TNF for 18 h and analyzed for cell death. Cell death was measured by LDH-release (**D, F**). Cell viability was measures with the CellTiter-Glo assay (**E, G**). 5 donors, mean and SD are shown. Asterisk denotes statistical significance between controls or indicated groups (**B-G**) ($P < 0.05$, two-way ANOVA).

Figure 5. NG25 reduce viability of $CD138^+$ cells from patients, alone and in combination with melphalan. (**A**) $CD138^+$ cells from 10 individual donors were treated with NG25 before cell viability was measured. Individual donors, mean and SD are shown. Asterisks indicate statistically significant differences (Kruskal-Wallis test, Dunn´s multiple comparison test, P<0,05). (**B**) $CD138^+$ cells from 10 individual donors were treated with melphalan, NG25 or both in technical triplicates. Mean and SD of triplicates from each donor are shown. Single asterisk denotes statistical significance as compared to the control not treated with NG25 for the lowest dose of NG25, double asterisk denotes statistical significance as compared to the untreated control for the highest dose of NG25. Asterisks indicate statistically significant differences (two-way ANOVA, Tukey´s multiple comparison test, P<0,05). All treatments were for 18 hours, and viability was measured by CellTiter-Glo.

Figure 1

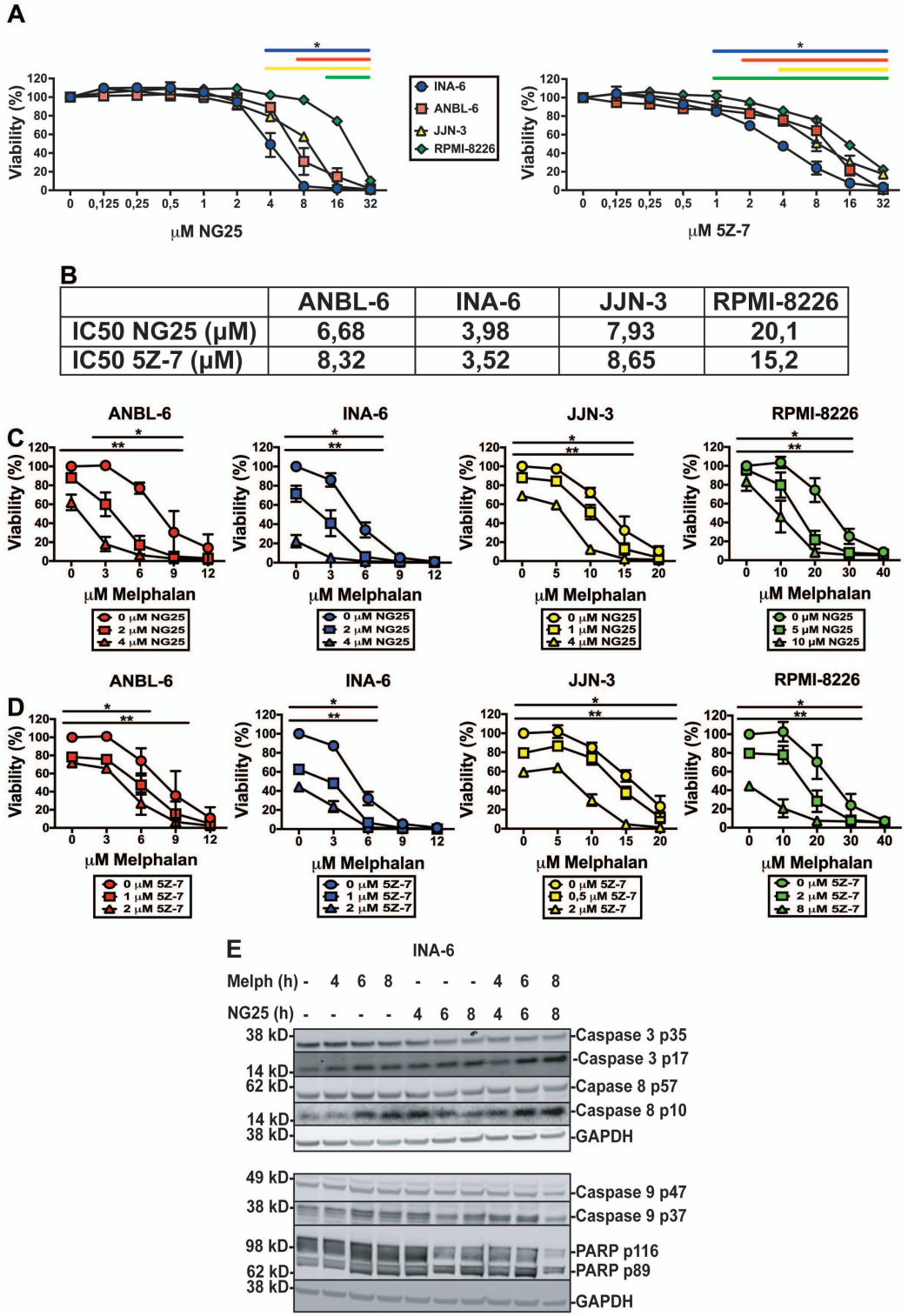

	ANBL-6	INA-6	JJN-3	RPMI-8226
IC50 NG25 (μM)	6,68	3,98	7,93	20,1
IC50 5Z-7 (μM)	8,32	3,52	8,65	15,2

Figure 2

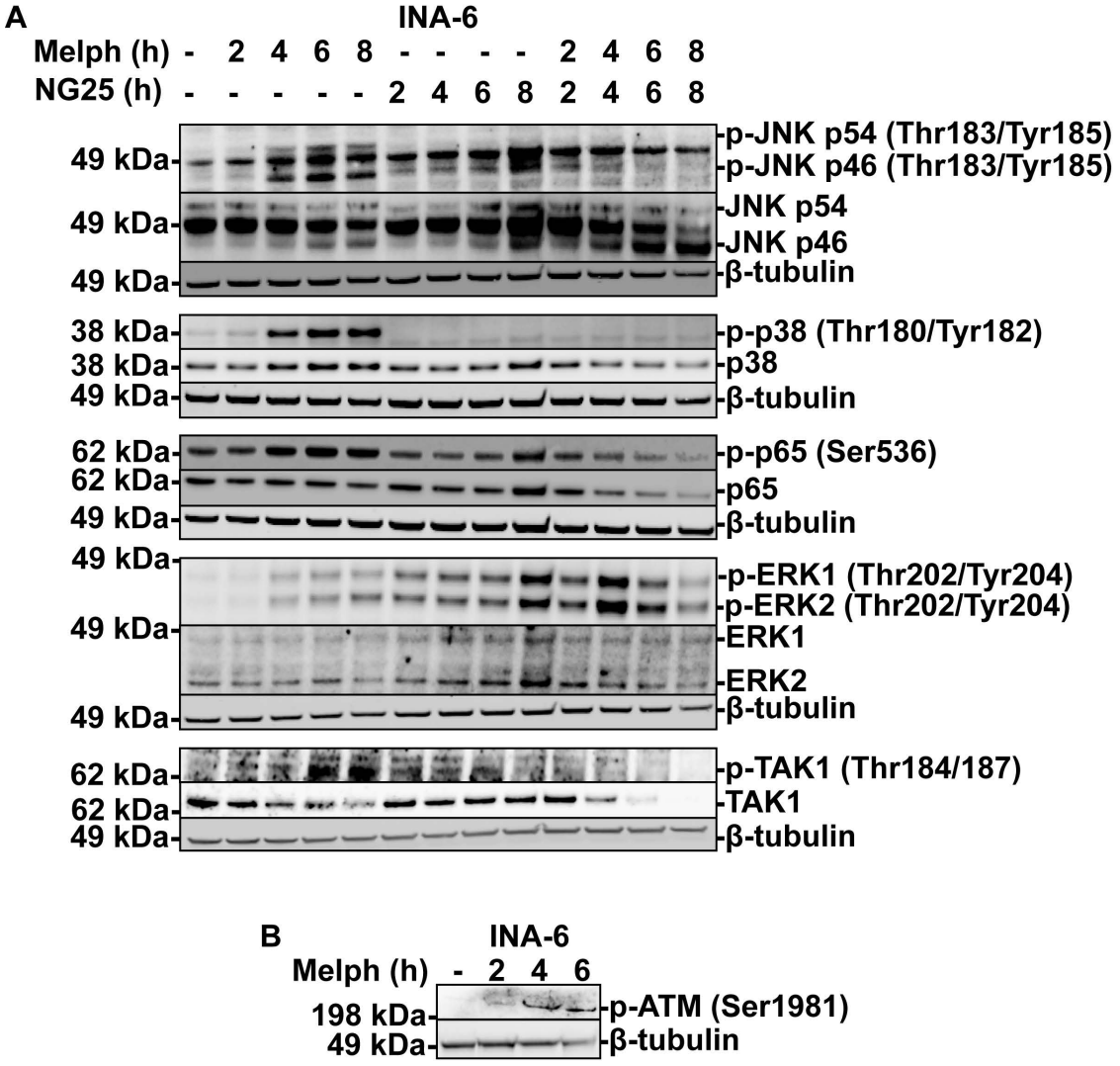
A
INA-6
Melph (h) - 2 4 6 8 - - - - 2 4 6 8
NG25 (h) - - - - - 2 4 6 8 2 4 6 8
49 kDa
p-JNK p54 (Thr183/Tyr185)
p-JNK p46 (Thr183/Tyr185)
49 kDa
JNK p54
JNK p46
49 kDa
β-tubulin
38 kDa
p-p38 (Thr180/Tyr182)
38 kDa
p38
49 kDa
β-tubulin
62 kDa
p-p65 (Ser536)
62 kDa
p65
49 kDa
β-tubulin
49 kDa
p-ERK1 (Thr202/Tyr204)
p-ERK2 (Thr202/Tyr204)
49 kDa
ERK1
ERK2
49 kDa
β-tubulin
62 kDa
p-TAK1 (Thr184/187)
62 kDa
TAK1
49 kDa
β-tubulin
B
INA-6
Melph (h) - 2 4 6
198 kDa
p-ATM (Ser1981)
49 kDa
β-tubulin

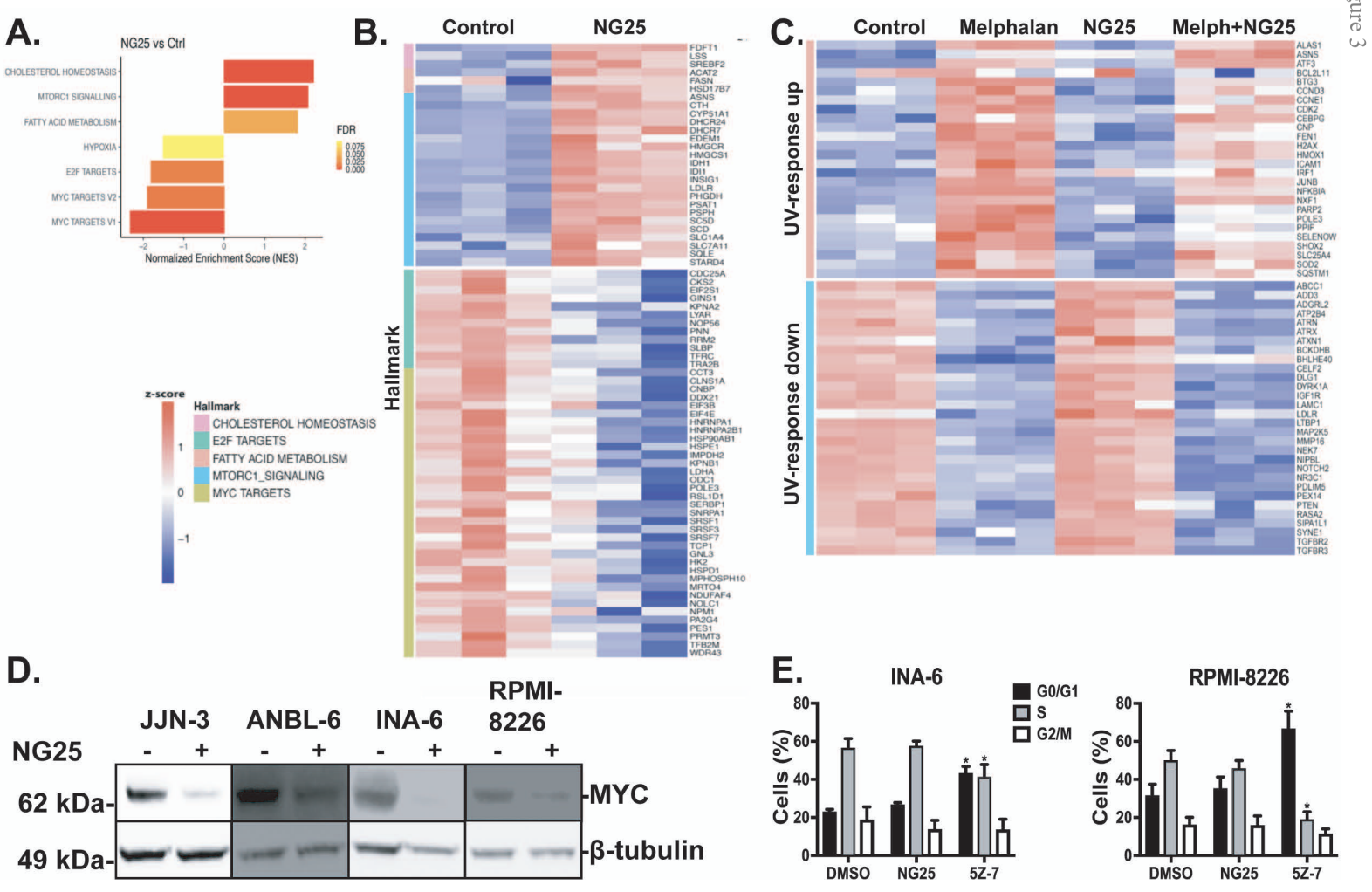
A.
NG25 vs Ctrl
CHOLESTEROL HOMEOSTASIS
MTORC1 SIGNALLING
FATTY ACID METABOLISM
HYPOXIA
E2F TARGETS
MYC TARGETS V2
MYC TARGETS V1
FDR
0.075
0.050
0.025
0.000
−2
−1
0
1
2
Normalized Enrichment Score (NES)
z-score
Hallmark
CHOLESTEROL HOMEOSTASIS
E2F TARGETS
FATTY ACID METABOLISM
MTORC1_SIGNALING
MYC TARGETS
B.
Control
NG25
Hallmark
FDFT1
LSS
SREBF2
ACAT2
FASN
HSD17B7
ASNS
CTH
CYP51A1
DHCR24
DHCR7
EDEM1
HMGCR
HMGCS1
IDH1
IDI1
INSIG1
LDLR
PHGDH
PSAT1
PSPH
SCD5
SCD
SLC1A4
SLC7A11
SQLE
STARD4
CDC25A
CKS2
EIF2S1
GINS1
KPNA2
LYAR
NOP56
PNN
RRM2
SLBP
TFRC
TRA2B
CCT3
CLNS1A
CNBP
DDX21
EIF3B
EIF4E
HNRNPA1
HNRNPA2B1
HSP90AB1
HSPE1
IMPDH2
KPNB1
LDHA
ODC1
POLE3
RSL1D1
SERBP1
SNRPA1
SRSF1
SRSF3
SRSF7
TCP1
GNL3
HK2
HSPD1
MPHOSPH10
MRTO4
NDUFAF4
NOLC1
NPM1
PA2G4
PES1
PRMT3
TFB2M
WDR43
C.
Control
Melphalan
NG25
Melph+NG25
UV-response up
UV-response down
ALAS1
ASNS
ATF3
BCL2L11
BTG3
CCND3
CCNE1
CDK2
CEBPG
CNP
FEN1
H2AX
HMOX1
ICAM1
IRF1
JUNB
NFKBIA
NXF1
PARP2
POLE3
PPIF
SELENOW
SHOX2
SLC25A4
SOD2
SQSTM1
ABCC1
ADD3
ADGRL2
ATP2B4
ATRN
ATRX
ATXN1
BCKDHB
BHLHE40
CELF2
DLG1
DYRK1A
IGF1R
LAMC1
LDLR
LTBP1
MAP2K5
MMP16
NEK7
NIPBL
NOTCH2
NR3C1
PDLIM5
PEX14
PTEN
RASA2
SPATL1
SYNE1
TGFBR2
TGFBR3
D.
JJN-3
ANBL-6
INA-6
RPMI-8226
NG25
- + - + - + - +
62 kDa-
49 kDa-
MYC
β-tubulin
E.
INA-6
RPMI-8226
G0/G1
S
G2/M
Cells (%)
0
20
40
60
80
DMSO
NG25
5Z-7
*

Figure 4

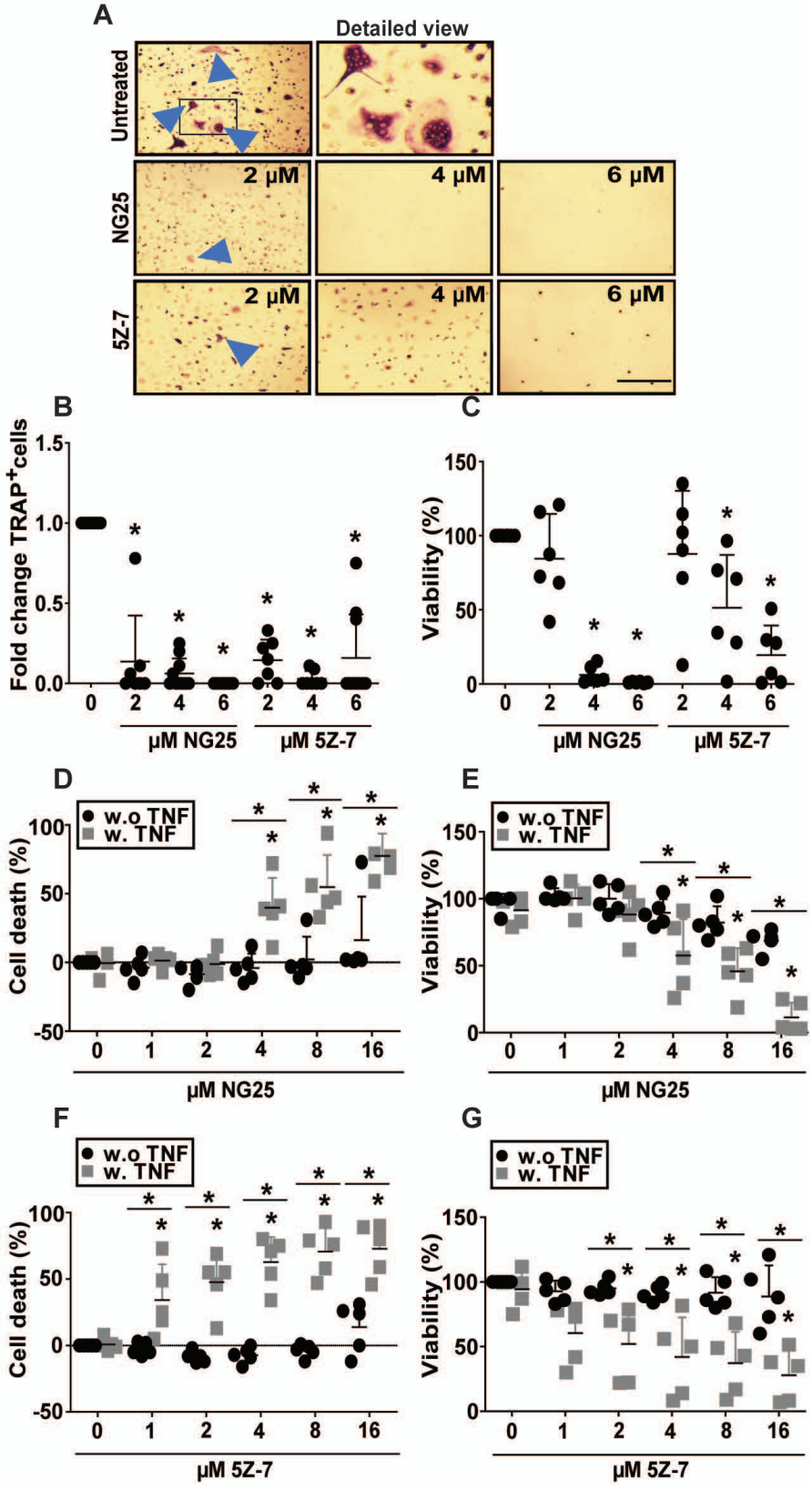
A
Detailed view
Untreated
NG25
5Z-7
2 μM
4 μM
6 μM
2 μM
4 μM
6 μM
B
Fold change TRAP+cells
μM NG25
μM 5Z-7
C
Viability (%)
μM NG25
μM 5Z-7
D
w.o TNF
w. TNF
Cell death (%)
μM NG25
E
w.o TNF
w. TNF
Viability (%)
μM NG25
F
w.o TNF
w. TNF
Cell death (%)
μM 5Z-7
G
w.o TNF
w. TNF
Viability (%)
μM 5Z-7

Figure 5

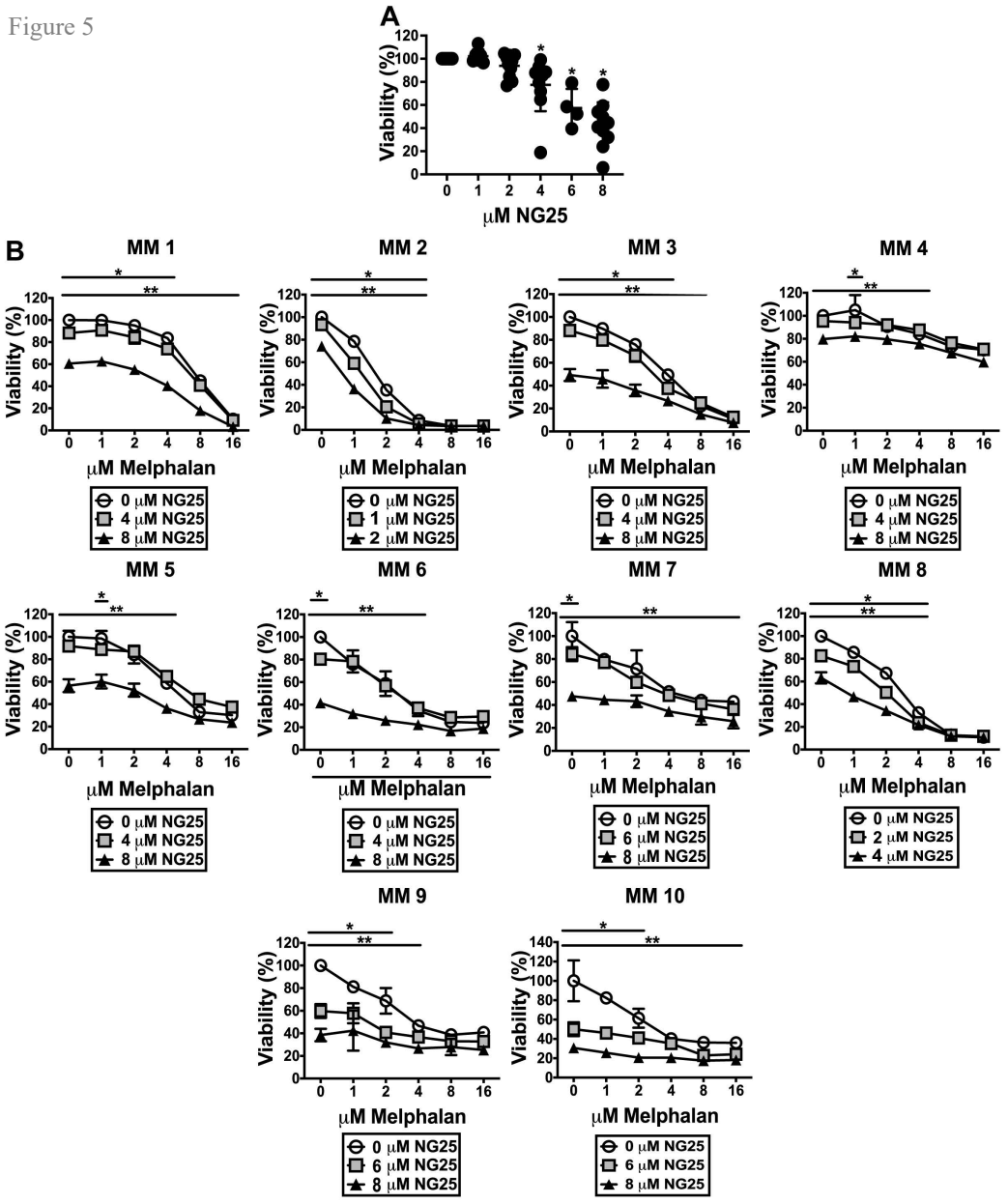
A
Viability (%)
μM NG25
B
MM 1
MM 2
MM 3
MM 4
MM 5
MM 6
MM 7
MM 8
MM 9
MM 10
μM Melphalan
0 μM NG25
4 μM NG25
8 μM NG25
1 μM NG25
2 μM NG25
6 μM NG25

SUPPLEMENTARY MATERIAL FOR

TAK1-INHIBITORS ARE CYTOTOXIC FOR MULTIPLE MYELOMA CELLS ALONE AND IN COMBINATION WITH MELPHALAN

Erling Håland,[1,2] Ingrid Nyhus Moen,[1-3] Elias Veidal,[1,2] Hanne Hella,[2] Kristine Misund,[2] Tobias S. Slørdahl,[2,3] and Kristian K. Starheim[1-3]

[1] CEMIR Centre of Molecular Inflammation Research, IKOM, NTNU, Trondheim, Norway; [2] Department of Clinical and Molecular medicine, NTNU, Trondheim, Norway; [3] Department of Hematology, St. Olavs University Hospital, Trondheim, Norway.

Correspondence: Kristian K. Starheim, Faculty of Medicine and Health Sciences, Department for Clinical and Molecular Medicine (IKOM), Norwegian University of Technology and Natural Sciences (NTNU), Pb. 8905, N-7491 Trondheim, NORWAY. E-mail: Kristian.starheim@ntnu.no, tel. +4790178148.

SUPPLEMENTARY FIGURES.

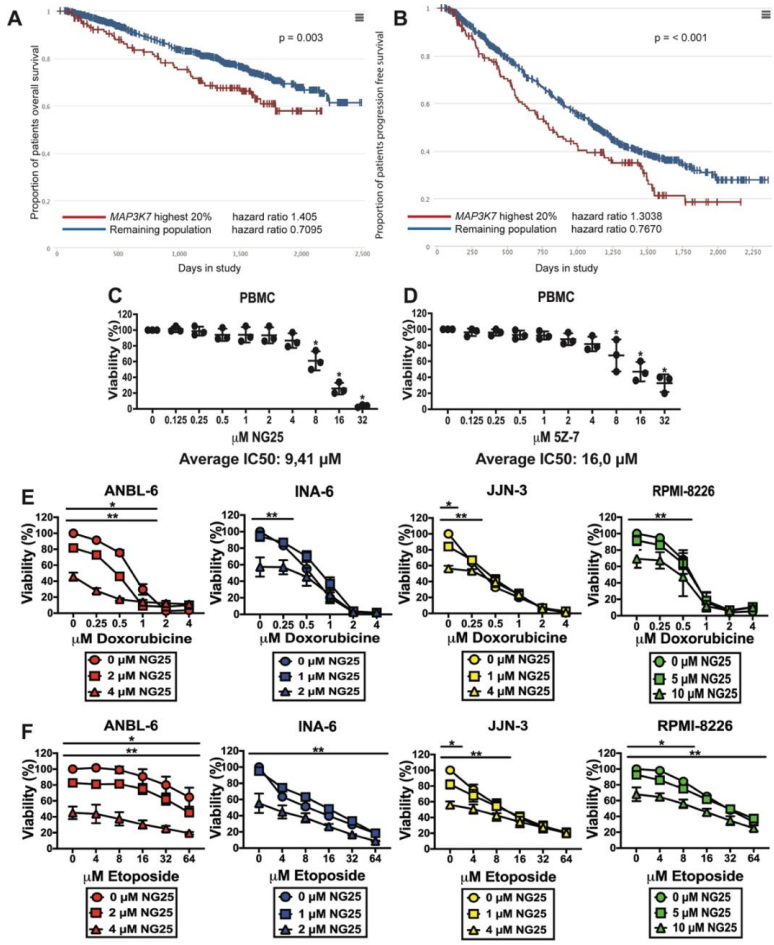

Supplementary Figure S1. NG25 is cytotoxic in PBMCs and in combination with DNA-damaging drugs in MM cell lines. (A) Survival and **(B)** progression-free survival curves generated from the CoMMpass data (IA15 Release) by comparing the upper 20th percentile *MAPK3K* expressing patients with the lower 85th percentile. Log-rank P is 0.003 (A) and <0.001 (B). (**C**) Three PBMC donors treated with NG25 in triplicates at indicated concentrations for 18 hours before measuring the viability with CellTiter-Glo. Asterisks indicate statistically significant differences (One-way ANOVA, Turkey´s multiple comparison test, P<0,05) compared with untreated. **(D)** Three PBMC donors treated with 5Z-7 in triplicates at indicated concentrations for 18 hours before measuring the viability with CellTiter-Glo. Asterisks indicate statistically significant differences (One-way ANOVA, Turkey´s multiple comparison test, P<0,05) compared with untreated. (**E**) MM cell lines treated with NG25 in combination with doxorubicine. Asterisks indicate statistically significant differences (two-way ANOVA, Tukey´s multiple comparison test, P<0,05) compared with the control not treated with NG25. Single asterisk denotes statistical significance as compared to the control not treated with NG25 for the lowest dose of NG25, double asterisk denotes statistical significance as compared to the untreated control for the highest dose of NG25. **(F)** MM cell lines treated with NG25 in combination with etoposide. Asterisks indicate statistically significant differences (two-way ANOVA, Tukey´s multiple comparison test, P<0,05) compared with the control not treated with NG25. Single asterisk denotes statistical significance as compared to the control not treated with NG25 for the lowest dose of NG25, double asterisk denotes statistical significance as compared to the untreated control for the highest dose of NG25.

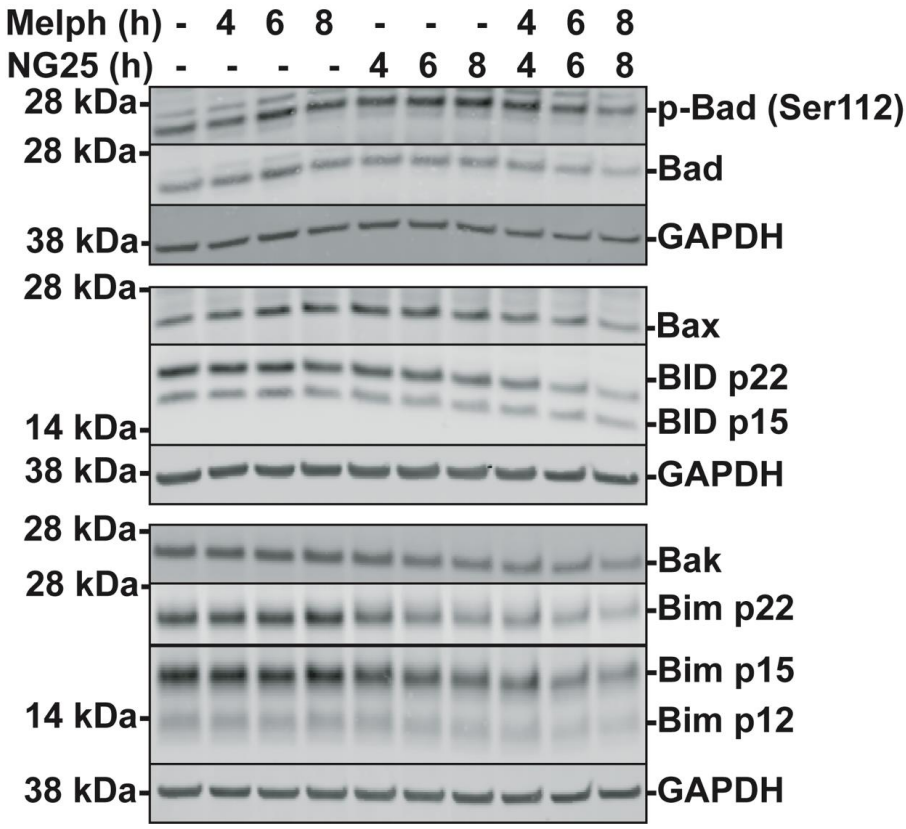

Supplementary Figure S2. Mitochondrial directed apoptosis is not activated during these experimental conditions. MM cells from the INA-6 cell line were treated with 2 μM NG25, 10 μM melphalan or both for the indicated time points (hours, h), and cell lysates were analyzed for protein levels by immunoblotting. GAPDH is loading control, shown for corresponding membranes. One representative of two independent experiments is shown. Full membranes for both experiments are given in Supplementary Figure S7.

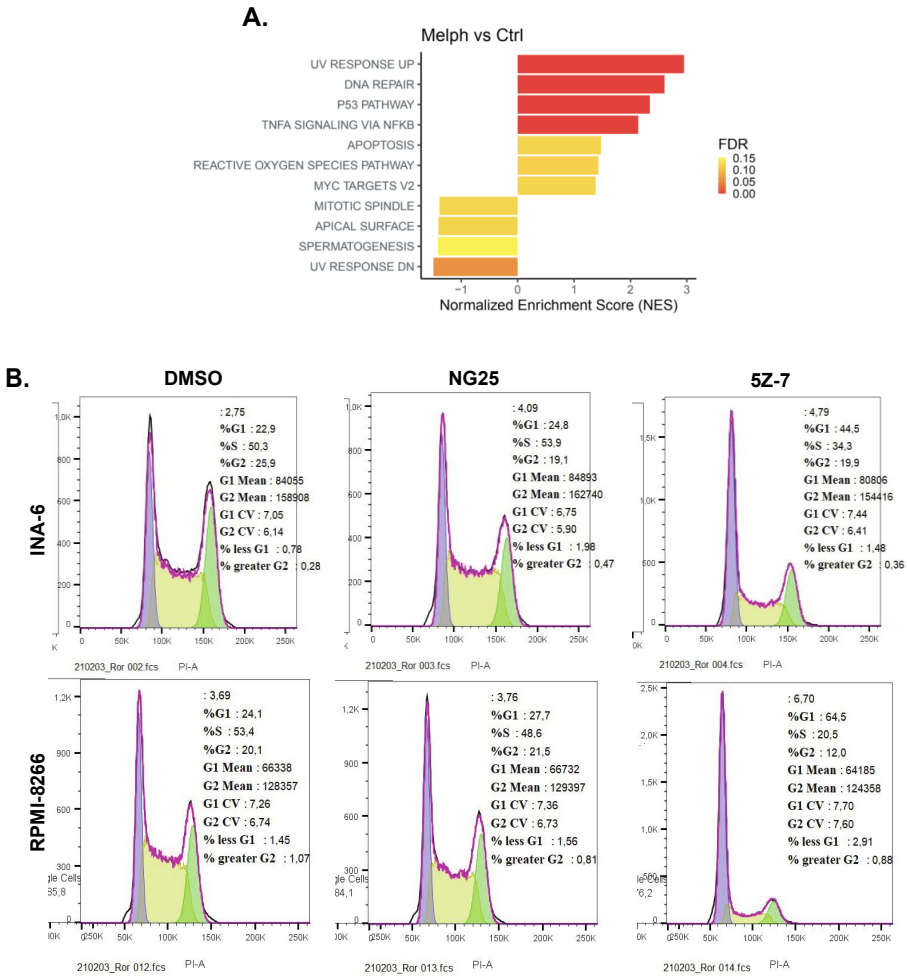

Supplementary Figure S3. Melphalan-induced gene expression patterns and flow-histograms from cell cycle analysis- (A) GO-enrichment plot of INA-6 cells treated with 10 µM melphalan as compared to untreated controls. (B) FlowJo printout of histograms and cell cycle stage population gating using the Watson pragmatic model. One representative donor is shown.

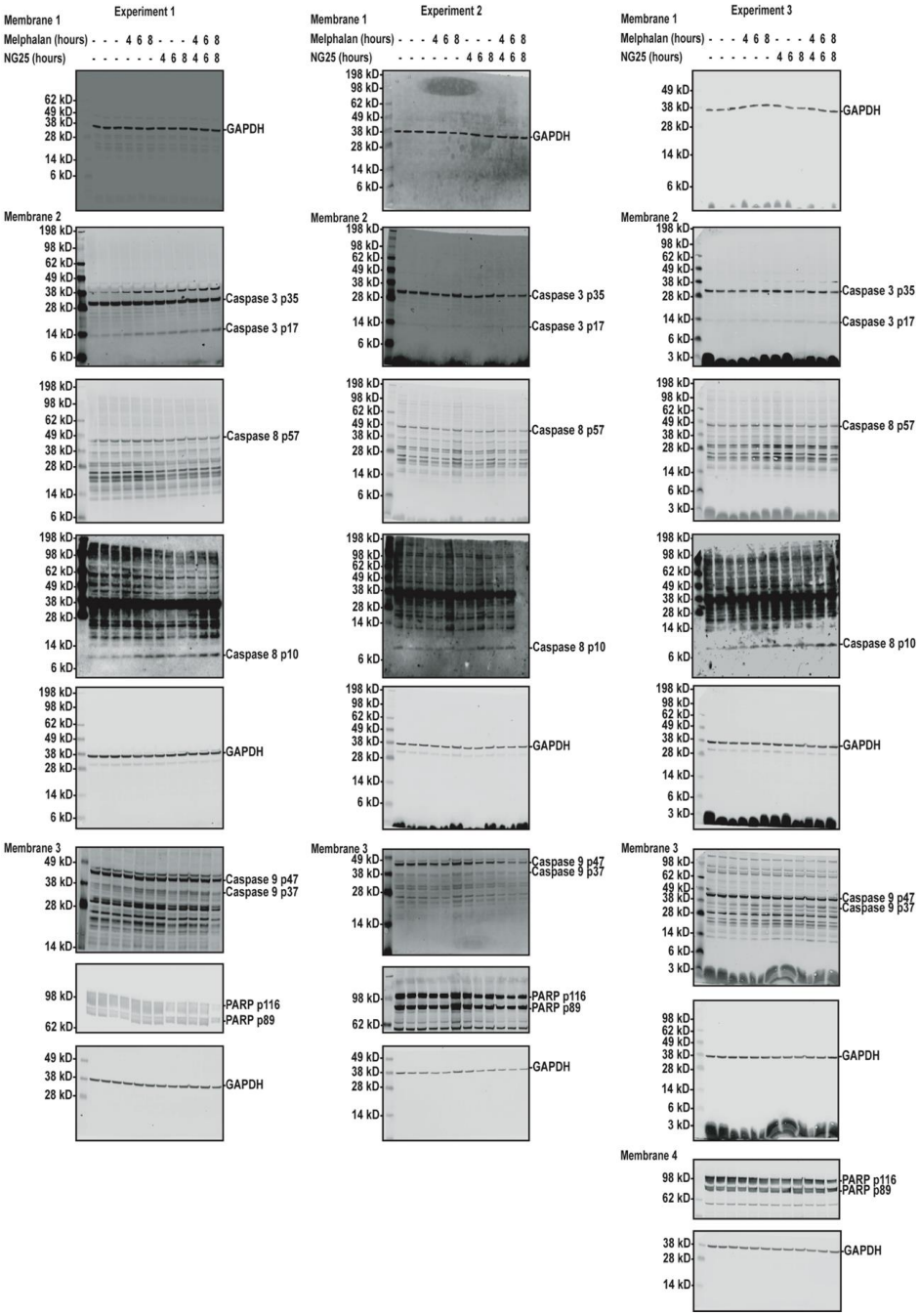

Supplementary Figure S4. Total experiments and full immunoblots for NG25 and melphalan effect on cell death signaling. INA-6 cells were treated with 2 μM NG25, 10 μM melphalan or both for the indicated time points (hours) and cell lysates were analyzed for caspase 3, caspase 8, caspase 9, and PARP protein levels by immunoblotting. GAPDH is loading control. Experiment 1 is same is in Figure 1E.

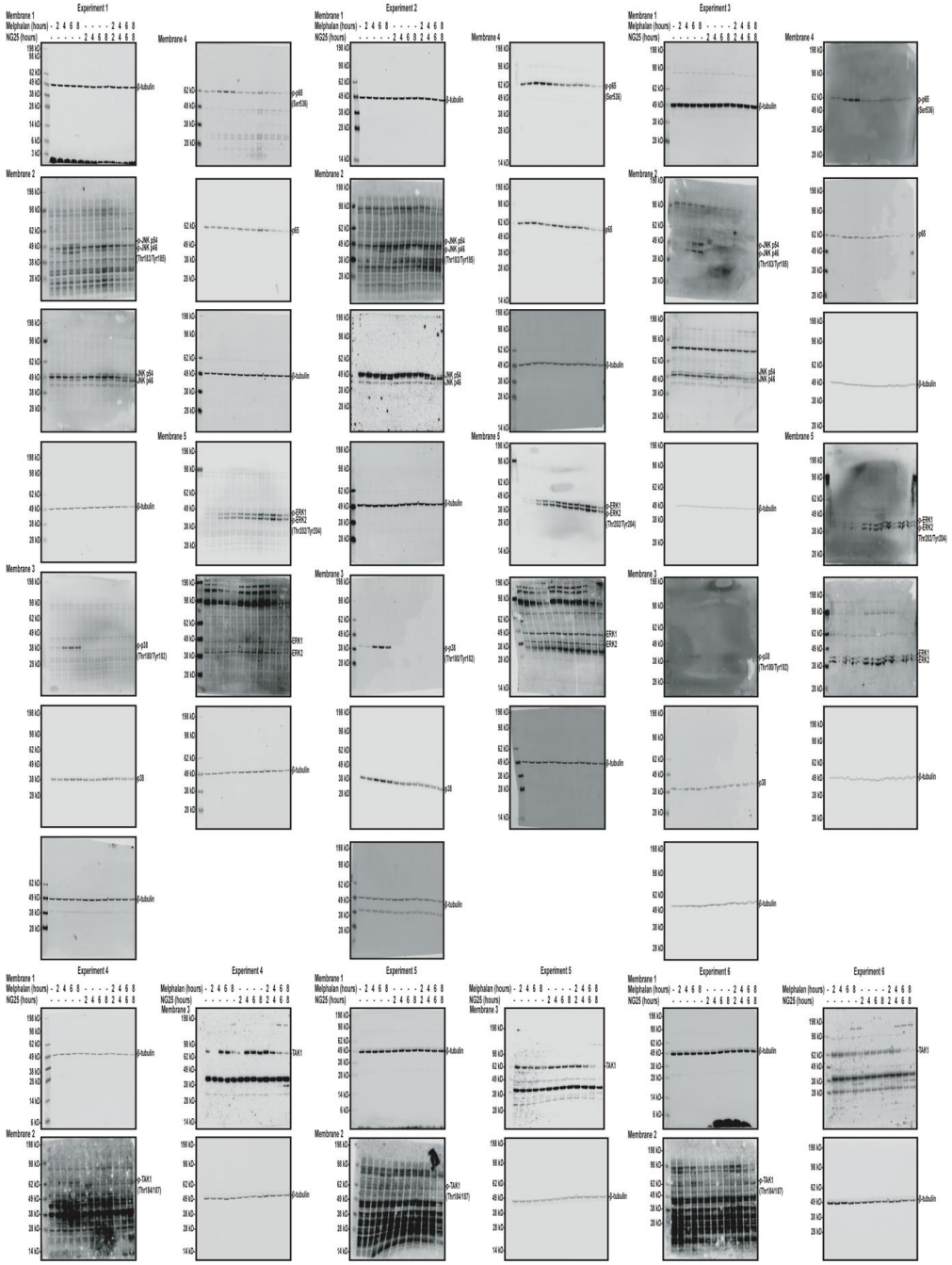

Supplementary Figure S5. Experiments and full immunoblots for NG25 and melphalan effect on MAPK and NF-κB. INA-6 cells were treated with 2 μM NG25 or 10 μM melphalan or both at the indicated time points, and cell lysates were analyzed for the indicated antigen levels by immunoblotting. β-Tubulin is loading control. Experiment 1 and 5 is same as in Figure 2A.

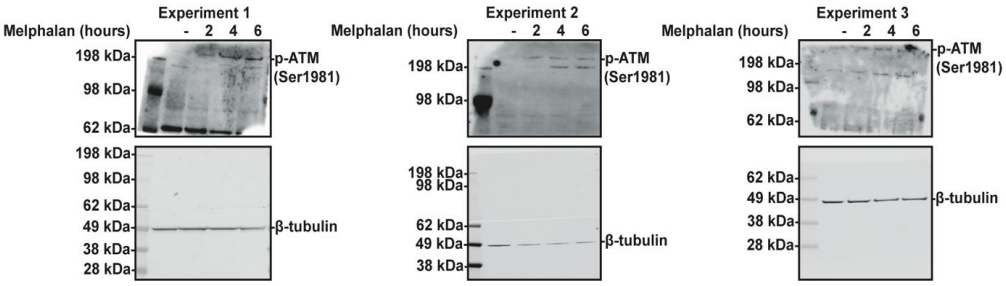

Supplementary Figure S6. Experiments and full immunoblots for NG25 and melphalan effect on ATM phosphorylation and activation. INA-6 cells line were treated with 10 μM melphalan at the indicated time points, and cell lysates were analyzed for phospho-Ser1981-ATM protein levels by immunoblotting. β-Tubulin is loading control. Experiment 1 is same as in Figure 2B.

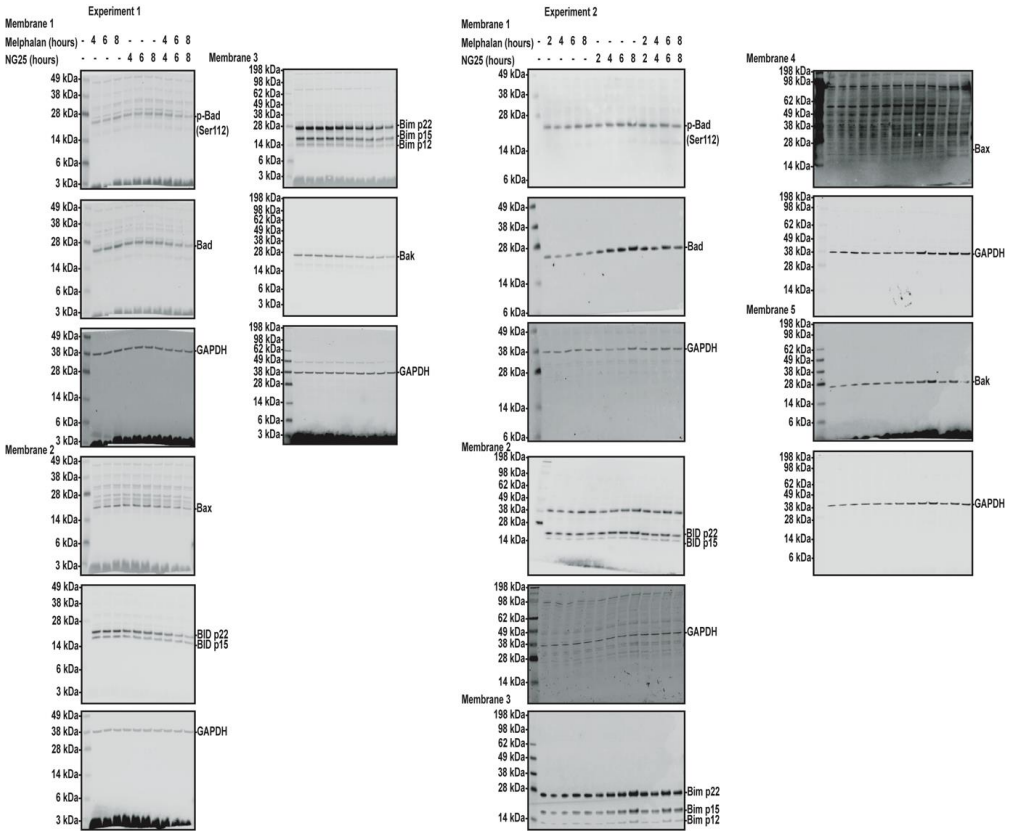

Supplementary Figure S7. Total experiments and full immunoblots for NG25 and melphalan effect on Bcl-2 family proteins. INA-6 cells were treated with 2 μM NG25 or 10 μM melphalan or both at the indicated time points, and cell lysates were analyzed protein levels of the indicated antigens by immunoblotting. GAPDH is loading control. Experiment 1 is same as in Figure S2.

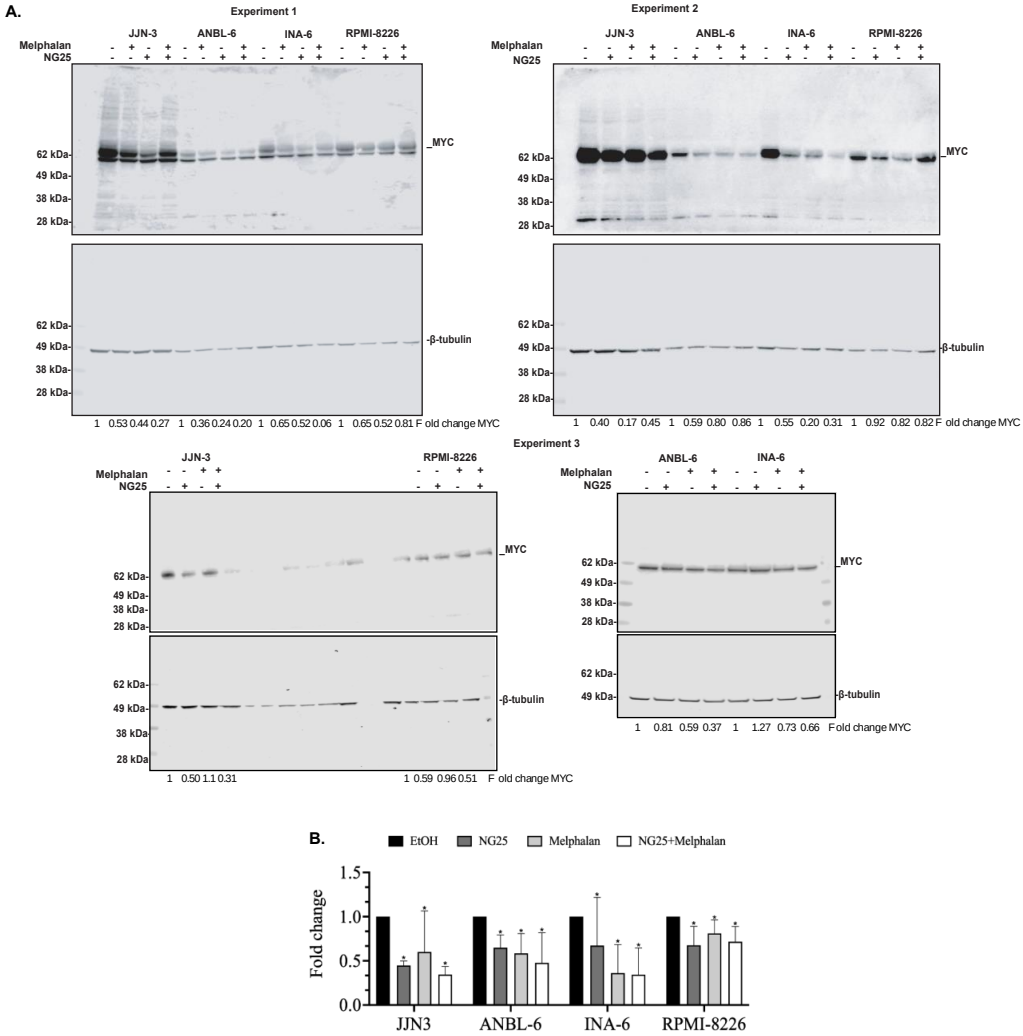

Supplementary Figure S8. MYC all membranes. **(A)** MM cells from the JJJN-3, ANBL-6, INA-6 and RPMI-8226 cell lines were treated with 2 μM NG25 for 4 hours, and cell lysates were analyzed for MYC protein levels by immunoblotting. β-Tubulin is loading control. Relative MYC protein levels (adjusted for loading) are given as fold change from untreated control. Experiment 2 is same as is Figure 3D. **(B)** Average fold change of MYC protein levels; average and standard deviation is shown. Asterisk indicate statistical difference as compared to the untreated control ($P<0.05$, one-way ANOVA, Tukeys Multiple Comparison test).

SUPPLEMENTARY TABLES.

Supplementary Table 1. IC50 TAK1-inhibitors PBMC. PBMCs were treated with TAK1-inhibitors for 18 hours, and cell viability was assessed by Cell Titer viability assay. Results are average of technical triplicates for each donor.

	Donor 1	**Donor 2**	**Donor 3**	**Average**
IC50 (µM NG25)	11,1	9,11	8,02	9,41
IC50 (µM 5Z-7)	23,1	16,4	8,55	16,0

Supplementary Table 2. IC50 melphalan + TAK1-inhibitors in MM cell lines. The indicated MM cell lines were treated with melphalan and the indicated doses of NG25 for 18 hours, before cell viability was assessed by Cell Titer viability assay. Results are average of three independent experiments.

Cell line	**Treatment**	**IC50 (µM melphalan)**
INA-6	0 µM NG25	4,94
	2 µM NG25	2,70
	4 µM NG25	0,66
ANBL-6	0 µM NG25	7,69
	2 µM NG25	3,45
	4 µM NG25	1,29
JJN-3	0 µM NG25	12,5
	1 µM NG25	9,59
	4 µM NG25	5,59
RPMI-8226	0 µM NG25	24,5
	5 µM NG25	14,4
	10 µM NG25	9,44
INA-6	0 µM 5Z-7	4,92
	1 µM 5Z-7	2,94
	2 µM 5Z-7	2,25
ANBL-6	0 µM 5Z-7	7,73
	1 µM 5Z-7	5,16
	2 µM 5Z-7	3,89
JJN-3	0 µM 5Z-7	15,5
	0,5 µM 5Z-7	12,9
	2 µM 5Z-7	6,44
RPMI-8226	0 µM 5Z-7	23,8
	2 µM 5Z-7	14,9
	8 µM 5Z-7	3,37

Supplementary Table 3. IC50 NG25 + doxorubicine in MM cell lines. The indicated MM cell lines were treated with doxorubicine and the indicated doses of NG25 for 18 hours, before cell viability was assessed by Cell Titer viability assay. Results are average of three independent experiments.

Cell line	**µM NG25**	**IC50 (µM doxorubicine)**
ANBL-6	0 µM NG25	0,73
	2 µM NG25	0,43
	4 µM NG25	0,02
INA-6	0 µM NG25	0,54
	1 µM NG25	0,73
	2 µM NG25	0,36
JJN-3	0 µM NG25	0,35
	1 µM NG25	0,41
	4 µM NG25	0,31
RPMI-8226	0 µM NG25	0,63
	5 µM NG25	0,59
	10 µM NG25	0,41

Supplementary Table 4. IC50 NG25 + etoposide in MM cell lines. The indicated MM cell lines were treated with etoposide and the indicated doses of NG25 for 18 hours, before cell viability was assessed by Cell Titer viability assay. Results are average of three independent experiments.

Cell line	**µM NG25**	**IC50 (µM etoposide)**
ANBL-6	0 µM NG25	97,9
	2 µM NG25	58,2
	4 µM NG25	2,24
INA-6	0 µM NG25	8,70
	1 µM NG25	14,2
	2 µM NG25	3,33
JJN-3	0 µM NG25	11,2
	1 µM NG25	10,2
	4 µM NG25	4,34
RPMI-8226	0 µM NG25	31,4
	5 µM NG25	31,6
	10 µM NG25	11,4

Supplementary Table 5. IC50 NG25 in primary myeloma cells. CD138+ cells from myeloma patients were treated with NG25 for 18 hours, and cell viability was determined by Cell Titer Viability assay. Results are average of technical triplicates for each donor.

Donor	**IC50 (µM NG25)**
MM1	9,37
MM2	2,74
MM3	8,01
MM4	13,8
MM5	8,57
MM6	6,92
MM7	7,68
MM8	4,96
MM9	6,79
MM10	5,92
Average IC50	**7,48**

Supplementary Table 6. IC50 for melphalan + NG25 in primary myeloma cells. CD138+ cells from myeloma patients were treated with melphalan and the indicated doses of NG25 for 18 hours, and cell viability was determined by Cell Titer Viability assay. Results are average of technical triplicates for each donor.

Donor	**Treatment**	**IC50 (μM melphalan)**
MM 1	0,0 μM NG25	7,36
	2,0 μM NG25	6,26
	4,0 μM NG25	2,12
MM 2	0,0 μM NG25	1,61
	1,0 μM NG25	1,16
	2,0 μM NG25	0,76
MM 3	0,0 μM NG25	3,92
	2,0 μM NG25	3,08
	4,0 μM NG25	0,87
MM 4	0,0 μM NG25	36,7
	2,0 μM NG25	50,7
	4,0 μM NG25	43,4
MM 5	0,0 μM NG25	5,88
	2,0 μM NG25	7,98
	4,0 μM NG25	1,96
MM 6	0,0 μM NG25	2,78
	2,0 μM NG25	3,07
	4,0 μM NG25	0,07
MM 7	0,0 μM NG25	6,48
	6,0 μM NG25	4,72
	8,0 μM NG25	0,61
MM 8	0,0 μM NG25	2,83
	2,0 μM NG25	1,98
	4,0 μM NG25	0,85
MM 9	0,0 μM NG25	5,40

	6,0 µM NG25	1,28
	8,0 µM NG25	0,20
MM 10	0,0 µM NG25	4,14
	6,0 µM NG25	0,74
	8,0 µM NG25	0,001

ISBN 978-82-326-5280-8 (printed ver.)
ISBN 978-82-326-6757-4 (electronic ver.)
ISSN 1503-8181 (printed ver.)
ISSN 2703-8084 (online ver.)

NTNU

Norwegian University of
Science and Technology